A NOVEL HSP90 INHIBITOR TO DISRUPT HSP90/p50CDC37 COMPLEX FOR PANCREATIC CANCER THERAPY

by

Tao Zhang

A dissertation submitted in partial fulfillment
of the requirements for the degree of
Doctor of Philosophy
(Pharmaceutical Sciences)
in The University of Michigan
2011

Doctoral Committee:

Associate Professor Duxin Sun, Chair
Professor David E. Smith
Professor Shaomeng Wang
Assistant Professor Wei Cheng

To my parents and my wife for their love, support and encouragement

To my son for the sweet smile and so much fun every day

ACKNOWLEDGEMENTS

I would like to express my deepest gratitude to my supervisor Dr. Duxin Sun for his guidance, inspiration, and support throughout the years. His positive attitude to science and open mind to new findings have greatly impressed me and will benefit my whole life. He is my best supervisor and friend. I sincerely appreciated his support both scientifically and personally.

I would like to thank my great dissertation committee, Dr. Wei Cheng, Dr. David E. Smith and Dr. Shaomeng Wang for the insightful comments on my research and career development.

I also thank all the professors, colleagues and students for their help in my research. Thanks to Dr. Shaomeng Wang for providing the AT-406 project and Donna McEachern for the animal surgery. Thanks to the professors in other universities, Dr. Chang-Guo Zhan, Dr. David Toft, Dr. Thomas Ratajczak, Dr. Wei Li, Dr. Dan Bolon, David Z. D'Argenio, most of whom I have not seen yet but they have helped me generously in my project by providing either technical support or materials. Thanks to the senior students in our lab, Dr. Xianhua Cao, Dr. Lanyan Fang and Dr. Seth Gibbs, who have given me a lot of help when I first joined in the group. I also thank other students and colleagues in our lab, and in the pharmaceutics department of both The Ohio State University and The University of Michigan, Dr. Hao Cheng, Dr. Ping Chen, Zhiliang Xie, Josephine Aimiuwu, Chien-Ming Li, Peng Zou, Yanke Yu, Bryan Newman, Wenjun Ni,

Dr. Huifei Cui, Shuwen Yu, Yanyan Li, Dr. Yiqun Jiang, Zhenkun Zhu, Hsui-Fang Lee, Dr. Wenpeng Zhang, Dr. Young Ho Seo, Dr. Xiaoqin Li, Yiling Liu, Xiaofei Zhang, Brunett Joseph, David John Maycock, Nan Zheng etc. The time I spent with those friends have made my graduate study so colorful and fulfilling.

I would like to give my special thanks to my wife, Yanyan Li, for her immeasurable love and support. She has given up her opportunity to stay in her lab in the Food Science and Technology Department and followed me from The Ohio State University to The University of Michigan without the least hesitation during our lab's transfer. For this I would also thank both my supervisor Dr. Duxin Sun and Yanyan's supervisor Dr. Steven J. Schwartz who decided to co-advise Yanyan, which makes us live together in Ann Arbor.

TABLE OF CONTENTS

LIST OF FIGURES

LIST OF TABLES

LIST OF APPENDICES

ABSTRACT

Pancreatic cancer is an aggressive disease with multiple biochemical and genetic alterations. In particular, Hsp90 has emerged as a promising target for pancreatic cancer therapeutics because it regulates the stabilization and conformational maturation of various oncogenic proteins simultaneously. Traditional Hsp90 inhibitors inhibit Hsp90 function through the blockage of nucleotide binding to Hsp90. In the present study, disruption of Hsp90/p50Cdc37 complex was revealed and confirmed as a novel and viable mechanism of Hsp90 inhibition. We reported that celastrol, a quinone methide triterpene purified from tripterygium wilfordii Hook F., could disrupt Hsp90/p50Cdc37 complex. A series of in silico, in vitro and in vivo assays were established to characterize the interaction between Hsp90 and p50Cdc37 and to investigate the underlying mechanism of the disruption by celastrol. In a reconstituted protein system, GST pull-down and ELISA demonstrated that p50Cdc37 was bound to ADP-bound/nucleotide-free Hsp90 but not to ATP-bound Hsp90, and that celastrol inhibited Hsp90/p50Cdc37 complex formation whereas the classical Hsp90 inhibitors had no effect. Celastrol inhibited Hsp90 ATPase activity without blocking ATP binding. Molecular docking and molecular dynamic simulations showed celastrol blocked the critical interaction between Hsp90 and p50Cdc37. Proteolytic fingerprinting indicated celastrol bound to the Hsp90 C-terminal domain to protect it from trypsin digestion. In pancreatic cancer cells, co-immunoprecipitation confirmed that celastrol inhibited the Hsp90 and p50Cdc37

interaction and induced Hsp90 client protein degradation. Celastrol resulted in pancreatic cancer cell apoptosis in vitro and significantly inhibited human pancreatic cancer xenograft growth in nude mice. Moreover, celastrol effectively suppressed tumor metastasis in a RIP-Tag2 transgenic mouse model with pancreatic islet cell carcinogenesis. These data suggest that celastrol represents a new class of Hsp90 inhibitors that can disrupt the Hsp90/p50Cdc37 complex to modulate chaperone activity. This alternative strategy of Hsp90 inhibition may offer more advantages than classical Hsp90 inhibition and further investigations are warranted to verify its therapeutic potential.

CHAPTER 1

Background and Introduction

1.1 Current Status of Pancreatic Cancer

Pancreatic cancer is the fourth leading cause of cancer death in the United States, causing 30 000 deaths per year [1]. It is an aggressive malignant disease, characterized by invasiveness, rapid progression and profound resistance to treatment [2]. Although it only accounts for 3% of all cancers, the survival rate is extremely low, with an overall 5-year survival <4% over the past 20 years [1]. The majority of patients are present with locally advanced or metastatic disease, and they have a grim median survival of 6–10 months and 3–6 months, respectively [3]. The high mortality rate results from the high incidence of metastatic disease at initial diagnosis, the aggressive clinical course and the failure of systemic therapies [4]. Despite the efforts in the last 3 decades, advances in screening, perioperative care, chemotherapy, and radiotherapy have had minimal impact on the course this aggressive disease [5]. Overall, 91% of patients with pancreatic cancer will die of it with our current therapeutic regimens [6].

1.2 Conventional Treatment Approaches for Pancreatic Cancer

Treatment options for pancreatic cancer vary with the disease stage (I – IV), which is defined by Joint Committee on Cancer depending on the extent of spreading [7]. In general, pancreatic tumors are classified as resectable, locally advanced or metastatic disease for different treatments.

1.2.1 Surgery

At the time of diagnosis, about 20% of pancreatic cancers are detected at the resectable stage [7]. These patients are considered eligible for surgery. Nonetheless, even after potentially curative resection, complete eradication of the disease is rarely achieved, because positive microscopic gross margins are found in up to 50% of patients [8]. After surgery, the patients are involved in adjuvant chemotherapy or chemoradiotherapy. They have a 5-year survival of only 4%–26% [9].

1.2.2 Adjuvant chemotherapy

After surgery, or at times when surgery is not possible, adjuvant chemotherapy or radiation therapy may be offered.

5-Fluorouracil (5-FU), a pyrimidine analogue, has been extensively studied in the treatment of pancreatic cancer since the1950s [10]. The active metabolite of 5-FU works at the S phase of cell division and inhibits RNA and DNA synthesis [10]. In patients present with metastatic or locally advanced tumors, single agent 5-FU has an overall survival of 6-10 months compared with 2-3.5 months in patients who received best supportive care without chemotherapy [11]. However, 5-FU-based combinations was found not be superior compared with use of 5-FU alone, and no statistical differences was noticed among various 5-FU-based combinations, either [12].

Gemcitabine is a deoxycytidine analogue. Similar to 5-FU, gemcitabine is also a cell-cycle specific agent, inhibiting DNA synthesis and function in the S phase [10]. The results from a Phase III study with 126 patients lead to the approval of gemcitabine in 1997 [13]. An improvement in clinical response ($P = 0.0022$) was noticed in gemcitabine-treated patients(23.85%) compared with 5-FU treated patients (4.8%) [13]. Gemcitabine-

treated patients had medican overall survival durations of 5.65 months and 1-year survival rate of 18%, while 5-FU-treated patients had those of 4.41 months and 2%, respectively (P = 0.0025) [13]. Since then, gemcitabine has been the reference regimen for pancreatic cancer chemotherapy.

1.2.3 Radiation therapy

Radiotherapy (intraoperative or external) has been given to improve the unsatisfactory results of surgery alone, however, it has exhibited limited effect. One study showed that intraoperative radiotherapy reduced the local recurrence rate after surgery (27.0% vs 56.4%, respectively; P < 0.01), but it did not significantly improve the survival rate, with 3-year survival rate of 7% for patients treated with radiotherapy vs 3% for those without radiotherapy treatment [14].

1.2.4 Combination of gemcitabine with cytotoxic agents

After gemcitabine became the standard chemotherapy drug for pancreatic cancer, various agents were combined with it for potential better impact. Although many phase II studies demonstrated the efficacy of combining gemcitabine with cytotoxic agents, which provided a potential clinical benefit, unfortunately, none of the randomized phase III trials have showed statistically significant improvement in overall survival.

The combination of gemcitabine and 5-FU was evaluated in many phase I and phase II trials, which suggested a clinical benefit [15]. However, results from phase III trials of gemcitabine plus 5-FU compared with single agent gemcitabine in patients with advanced disease have not shown any superiority in any clinical response and overall survival [15, 16].

Two phase III trials were conducted to compare gemcitabine with the combination therapy of gemcitabine and irinotecan in patients with advanced pancreatic cancer. Report from one trial showed that the combination group had an overall response rate of 15% while gemcitabine alone was 10% [17]. The median survival duration was 6.4 and 6.5 months for combination and single agent treatment group, respectively [17]. Therefore, no significant clinical benefit was achieved from the combination.

Two phase III randomized trials evaluated the effect of addition of oxaliplatin to gemcitabine [10]. One trial reported that the median survival time was 4.9 months for standard gemcitabine treatment, 6.2 months for fixed dose rate infusion gemcitabine treatment, and 5.7 months for the standard gemcitabine treatment combined with oxaliplatin [18]. There were no statistically significant differences among them. Another study in patients with metastatic pancreatic cancer resulted in median survival of 9.0 months for combination and 7.1 months for gemcitabine alone treatment group [10]. Similarly, the trend toward improvement was not statistically significant.

A phase III trial compared gemcitabline alone and in combination with cisplatin, and the results demonstrated a significant improvement in response rate (9.2% vs 26.4%, $P = 0.02$) without significant increase in overall survival (20 weeks vs 30 weeks, $P = 0.43$) [19].

The conclusion from the data of combining gemcitabine and capecitabine remains controversial. One phase III trial in 319 patients demonstrated an improvement in median survival in combination group (8.4 months) compared with gemcitabine alone (7.3 months), which was not statistically significant [20]. Another study showed a

statistically significant clinical benefit with median overall survival of 7.4 months upon combination treatment versus 6.0 months for gemcitabine alone [10].

Phase III trial comparing gemcitabine alone with gemcitabine and pemetrexed also failed to significant clinical benefit [21].

1.3 Targeted Therapy

Despite efforts in the past several decades, conventional treatment approaches such as surgery, radiation, chemotherapy, or the combination of these have had little impact on the progression of this disease [22]. Thus, there is a critical requirement for improved treatments capable of inhibiting and reversing the aggression of pancreatic tumor, which would be based on a detailed understanding of the pathogenesis of the disease.

The advances in molecular biology have dramatically improved our knowledge of pancreatic cancer pathogenesis. Although the clinical course of pancreatic cancer patients may indicate that pancreatic cancer springs up suddenly, the development of pancreatic adenocarcinomas from non-invasive precursor lesions in fact requires a prolonged series of stepwise progressions [23]. Based on Huslst's definition of pancreatic intraepithelial neoplasia (PanINs) from the transition between normal pancreatic ductal epithelium to invasive cancer, a widely adapted international system for classifying PanINs histologically has been established [23]. Histologically, PanIN-1 is characterized with elongated cells, mucin production and papillary architecture; PanIN-2 is characterized with nuclear abnormalities such as enlargement, some loss of polarity and crowding; PanIN-3 is characterized with budding into lumen, severe nuclear atypia and abnormal mitosis [24]. PanINs have represented graded stages of increasingly dysplastic growth. A

consistent set of genetic alterations in simultaneous lesions has been identified and provided supportive evidence of the relationship between PanINs and the pathogenesis of pancreatic adenocarcinoma. The first genetic changes detected in the progression are the activating K-ras mutations, which occur in about 30% of the earliest stage lesions of histological disturbance [2]. The frequency of K-ras mutations increase with disease progression, and in pancreatic adenocarcinomas the occurrence of mutations is nearly 100% [2]. The PanIN-1 stage is marked by additional changes including the appearance of numerous p16 abnormalities and shortening of telomeres. The *p16* tumor-suppressor gene is inactivated in around 955 of pancreatic cancers [22]. Almost all of the lowest grade PanINs (PanIN-1) have a very dramatic shortening of telomeres, which is likely to set up the chromosomal instability throughout all stages of pancreatic ductal tumorigenesis and in the carcinomas [24]. TP53 is the second most frequently inactivated tumor-suppressor gene, appearing in the more advanced PanINs [22]. The severely dysplastic PanIN-3 lesions have loss of SMAD4/DPC4 protein expression and BRCA2 mutations [2]. In addition, over-expression of growth factors and their receptors, such as TGF-beta, VEGF, and EGFR [25], have also been linked to pancreatic cancer. This knowledge has provided the foundation for targeted therapy. This knowledge has provided the foundation for targeted therapy.

1.3.1 The Ras pathway

K-ras is a member of the Ras family genes. It activates the downstream signaling pathways including Raf, MAPK and PI3K-AKT cascades when activated by signaling partners such as epidermal growth factor receptor (EGFR) [3]. The mutation of K-ras is the first notable genetic alteration identified in pancreatic cancer. Oncogenic K-ras is

involved in the initiation or early phase of pancreatic tumorigenesis, and more than 85% of the pancreatic cancer patients have K-ras gene mutation at the early stage of cancer development [22].

Ras must be activated via post-translational modifications to function, requiring an important enzyme, farnesyltransferase [3]. Tipifarnib, a arnesyltransferase inhibitor (FKI), was combined with gemcitabine in a phase III trial [26]. However, the results were disappointing. Other Ras related inhibitors under investigation include romidepsin, a histone deacetylase inhibitor which inhibits Ras-mediated signal transduction, and fanesylthiosalicylic acid (salirasib) which dissociates Ras from membrane-binding site [3].

An alternative strategy of targeting Ras signaling pathway is to block protein translation using the RNA-directed gene silencing technologies. In a phase II trial using the antisense inhibitor ISIS 2503 combined with gemcitabine demonstrated a response rate of 10.4% and median survival of 6.6 months. However, further efforts on this approach diminished due to the failure antisense inhibitor in lung cancer and melanoma [3]. Another technique using small interfering RNAs (siRNAs) has showed promising results but has not entered clinical trial yet [3].

1.3.2 The epidermal growth factor receptor (EGFR) pathway

EGFR is a transmembrane receptor tyrosine kinase of the ErbB family, which has four different members: EGFR (HER-1 or ErbB1), HER-2 (ErbB2), HER-3 (ErbB3), and HER-4 (ErbB4) [3]. Upon binding to its ligands, such as EGF (epidermal growth factor) or TGF-α (trasforming growth factor α), EGFR is activated and forms homo- or heterodimeric complexes with another member of the ErbB receptor family, leading to

phosphorylation of tyrosine residues and activation of downstream signalling pathways [3]. Overexpression of EGFR and its ligands EGF and TGF-α (43, 46 and 54%, respectively) is frequently observed in pancreatic cancer, which seems to be correlated with increased tumor aggressiveness and poor prognosis [27].

Two possible therapeutic approaches, small-molecule tyrosine kinase inhibitors (TKIs) and monoclonal anti-bodies directed against the extracellular ligand binding domain, have been investigated clinically to achieve an antitumor effect.

Erlotinib is an orally active small molecule TKI that binds to the ATP-binding site of EGFR. Preliminary studies of erlotinib alone and in combination with gemcitabine showed antitumor activity and minor side effects [15]. In a phase III trial involving 569 patients, erlotinib in combination with gemcitabine demonstrated a small but statistically significant increase in the survival, which led to the approval of erlotinib by the FDA as the first targeted therapy for patients with advanced pancreatic cancer [28]. In a phase II trial, erlotinib was investigated in combination with capecitabine in gemcitabine refractory patients and demonstrated an increase in overall survival (3.4 vs 6.5 months) [29]. Other EGFR tyrosine kinase inhibitors which have been under evaluation in early phase clinical trials include gefitinib and lapatinib [3].

The strategy of inhibiting EGFR with monoclonal antibody has also been investigated in clinical trials. Cetuximab is a chimeric IgG1 monoclonal anti-body specifically binding to the extracellular domain of EGFR to block downstream signaling proteins, such as vascular endothelial growth factor (VEGF) and interleukin 8 (IL-8) [15]. A phase II trial designed to determine the efficacy and tolerability of cetuximab combined with gemcitabine demonstrated well-tolerated toxicity and longer survival [15].

However, cetuximab did not show encouraging results in a phase III trial in patients with locally advanced and metastatic pancreatic cancers [3].

1.3.3 Vascular endothelial growth factor (VEGF)

VEGF is an important mediator of tumor angiogenesis, and it is also known to stimulate cell survival and proliferation. Expression of VEGF can be stimulated by hypoxia, growth factors and oncogenic proteins. VEGF has been found to be overexpressed in more than 90% of pancreatic cancers [30]. VEGF inhibitors are therefore been investigated for inhibit angiogenesis for pancreatic cancer therapy.

Currently, one of the most commonly used VEGF inhibitors is bevacizumab (Avastin), a humanized monoclonal immunoglobulin G antibody which is approved for use in patients with colorectal cancer [10]. To date, there are two phase III trials comparing the use of bevaciumab with and without gemcitabine, and a phase III trial evaluating emcitabine plus erlotinib with or without bevacizumab [10]. However, none of these have shown any survival benefit yet. For example, in the phase III trial using gemcitabine plus erlotinib, addition of bevacizumab increased the median survival from 6 months to 7.1 months, which was statistically significant [31]. Other VEGF inhibitors such as sorafenib, axitinib and sunitinib have been investigated in phase I and II trial [3, 10]. Phase III trials are warranted to claim for any clinical benefit.

1.3.4 Matrix metalloproteinases (MMPs)

Matrix metalloproteinases (MMPs) are a family of zinc-dependent proteolytic enzymes. They are responsible for the degradation of extracellular matrix, contributing to the invasive growth and spread ofa variety of solid malignancies including pancreatic cancer[3]. Despite the promising preclinical results, MMP inhibitor marimastat have

failed to show significant improvement in terms of clinical benefit in phase III clinical trials [3].

1.3.5 P13K-Akt mTOR pathway

Upon activation by Ras or EGFR, PI3K activates Akt, which targets multiple downstream proteins including the mammalian target of rapamycin (mTOR) [3]. Increased activation of the P13K/Akt/mTOR pathway have been found in more than 59% of pancreatic cancers [32].

Everolimus is an oral administered mTOR inhibitor which has been evaluated in metastatic pancreatic cancer in a phase II tiral [33]. It failed to show any statistically significant activity. Temsirolimus is another mTOR inhibitor approved for the treatment of renal-cell carcinoma, similar to everolimus, the attempt to use this agent in pancreatic cancer was not successful either [34].

1.3.6 The cyclo-oxygenase (COX) pathway

The COX enzymes play an essential role in converting arachidonic acid into prostaglandins [3]. COX1 is constitutively expressed while COX2 is inducible [3]. The upregulation of COX2 was found in 90% of pancreatic cancers [35]. The COX enzymes involve in multiple molecular events in pancreatic cancer, including cell migration, invasion, angiogenesis, immunosuppression, resistance to apoptosis, the production of free radicals and peroxidation of procarcinogens to carcinogens [3, 36]. Celecoxib is a highly selective COX-2 inhibitor, which has been used in combination with gemcitabine in phase II trials against advanced pancreatic cancer [3, 37, 38]. One study showed overall clinical response of 54.7% and median survival of 9.1 months, while another

study demonstrated that the addition of celecoxib had no significant benefit. A conclusion about the clinical benefit of celecoxib needs more results from clinical trials.

1.3.7 Other potential therapeutic targets

Besides the above mentioned signaling pathway or proteins, many other targets are under investigation in early clinical stage or preclinical settings for antipancreatic cancer activity. These include: The TGF-β and SMAD4 pathway, the hepatocyte growth factor receptor pathway, the insulin-like growth factor pathway, the focal adhesion kinase pathway, the Src pathway, the hedgehog pathway, the Notch pathway, the Wnt pathway, telomerase, microRNAs and cancer stem cells [3].

1.4 Heat Shock Protein 90 (Hsp90)

Although the above mentioned targeted therapies have yielded encouraging results in preclinical settings, the application in clinical trials has not translated into statically significant improvements. Considering the development and progression of pancreatic cancer are driven by multiple genetic and epigenetic changes, targeting a single pathway is unlikely to be effective. Thus, discovery of molecular targets that modulate multiple signaling pathways, such as molecular chaperone Hsp90, is likely to be a promising strategy.

1.4.1 Introduction of Hsp90

The molecular chaperone Hsp90 was initially identified as one of the highly conserved heat shock proteins involved in the stress response [39, 40]. Hsp90 is a highly abundant protein, constituting about 1-2% of total proteins under non-stress conditions in most tissues [41, 42]. It possesses common molecular chaperone functions and controls

the confirmation, stability, activation, intracellular disposition, and proteolytic turnover of many important proteins, including transmembrane tyrosine kinases (Her-2, EGFR), metastable signaling proteins (Akt, Raf-1 and IKK), mutated signaling proteins (p53, v-Src), chimeric signaling proteins (Bcr-Abl), cell cycle regulators (Cdk4, Cdk6), and steroid receptors (androgen, estrogen, and progesterone receptors) [43, 44]. Over the past several years, the application of global analysis has extended Hsp90 clientele to more than 200 proteins, covering almost all the cellular processes [45-47].

1.4.2 Hsp90 structure and protein folding mechanism

The crystal structures of yeast Hsp90 and Grp94 (Hsp90 isoform in mammalian endoplasmic reticulum) have been resolved [48, 49]. Hsp90 exists as a homodimer, and each monomer consists of three highly conserved domains: an N-terminal ATP-binding domain (25 kDa), a middle domain (35 kDa) and a C-terminal dimerization domain (12 kDa) [50]. In eukaryotes, the N-terminal and middle domains are connected by a charged linker [51]. The N-terminus of Hsp90 contains a specific ATP binding pocket [52]. The major role of the middle domain is to discriminate various types of client proteins to adjust the molecular chaperone for proper substrate activation [53]. The C-terminal dimerization domain strengthens the weak association between the two N-terminal domains of the Hsp90 dimer [51]. The C-terminal domain of eukaryotic Hsp90 has a conserved pentapeptide (MEEVD) implicated in binding to the tetratricopeptide repeat (TPR) domain of cochaperones, such as Hop (Hsp organizing protein) and Sti1 (stress-inducible protein 1, yeast homologue of Hop) [51, 54]. The C-terminal domain also contains a putative nucleotide binding site that exhibits allosteric control over N-terminal domain [55].

The ATPase activity of Hsp90 leads to the conformational changes of Hsp90 and drives the chaperone cycle [43].The “open” state of the Hsp90 dimer, with its two N-termini separated, can capture client proteins [56]. ATP binding causes the rotation of the “lid” segment, which flaps over the mouth of the ATP binding pocket [56, 57]. This change triggers the N-terminal β-strand swapping, brings the N-terminal domains together and results in the formation of a compacted, ring-shaped Hsp90 dimer [56, 57]. In the closed stage, the middle domain catalytic loop interacts with lid segment, which prepares conformation for hydrolysis [48]. Upon ATP hydrolysis, Hsp90 returns to an open conformation with dissociated N-terminal domains and lid segment released [58].

The chaperone cycle driven by ATPase activity is composed by the formation and dissociation of a series of multichaperone complexes between Hsp90 and various cochaperones. The Hsp90 multi-chaperone system has been extensively studied using yeast Hsp90 for steroid receptor maturation [59]. It starts from a newly synthesized or misfolded steroid receptor binding to Hsp70/Hsp40 complex. This three protein complex associates with the “open” state Hsp90 via the bridging cochaperone Hop that interacts simultaneously with Hsp90 and Hsp70 [54]. Hop not only binds to the C-terminal MEEVD motif of Hsp90, but also connect with the N-terminal region of Hsp90, preventing the association of Hsp90 N-terminal domain. Thus, ATPase activity is inhibited, promoting client transfer from Hsp70 to Hsp90 [51, 60, 61]. Upon ATP binding to Hsp90, Hop is replaced by p23 and immunophilins, converting the intermediate chaperone complex into the mature complex [62]. Another cochaperone, Aha1 (activator of Hsp90 ATPase), associates with the middle domain of Hsp90, facilitating conformational adjustments to favor ATP binding to the N-terminal

nucleotide binding domain [63]. Both Aha1 and immunophilins stimulate the ATPase activity of Hsp90 [63-65]. Upon ATP hydrolysis, the correctly-folded client protein is released from Hsp90 [51]. Recent studies have shown that the mechanistic basis of the Hsp90 chaperone cycle are conserved in yeast and human, although a slower turnover rate was observed with human Hsp90 [56].

Protein kinases are the largest class of Hsp90 clients, matured via a similar chaperone cycle with different cochaperones involved, such as p50Cdc37 [51, 66, 67]. p50Cdc37 was originally discovered in yeast as an essential cell cycle protein [68], and later it was proved to be a kinase-specific cochaperone of Hsp90 [66]. The Hsp70/Hsp40 complex first prepares a newly synthesized or misfolded protein kinase for interaction with the N-terminal domain of p50Cdc37, followed by recruitment of Hsp90 to the complex with the help of Hop [69, 70]. The C-terminal side chain of p50Cdc37 associates with the "lid" of Hsp90, which closes the N-terminal ATP binding pocket [71]. Crystallographic studies reveal that the insertion of Cdc37 C-terminus to the Hsp90 N-terminal ATP pocket inhibits the ATPase activity of Hsp90 and prevents its N-terminal dimerization [72]. This holds Hsp90 in an "open" conformation in the intermediate complex for client loading [71]. Although the release of p50Cdc37 C-terminus from Hsp90 N-terminal clamp is required for the transition from "open" to the "closed" conformation, p50Cdc37 may stay in the complex by interacting with client protein [71]. Other cochaperones, such as p23 and Aha1, may be required as well [57]. More details of kinase maturation in the complex remain to be understood.

Because early studies have shown that the function of cytoplasmic Hsp90 is essential for normal cell viability and growth [73], it was difficult, if not impossible, to

consider Hsp90 as a potential therapeutic target. However, since geldanamycin (GA) was demonstrated to possess potent anti-cancer effects through inhibiting Hsp90 [74, 75], a great deal of efforts have been devoted to this area and a diversity of Hsp90 inhibitors have either been identified or synthesized [74, 76].

1.4.3 Hsp90 N-terminal ATP binding site inhibitors

Benzoquinone ansamycins, represented by geldanamycin (Figure 1.1) [77], were the first class of natural Hsp90 inhibitors discovered. Geldanamycin, a natural occurring antibiotic, was originally isolated from Streptomyces hygroscopicus as early as 1970s [78]. Structural and biochemical studies have demonstrated that GA is a competitive inhibitor of ATP binding to Hsp90 [79]. Binding of GA in the N-terminal ATP pocket restrains Hsp90 in its ADP-bound conformation and prevents the subsequent "clamping" of Hsp90 around a client protein [80, 81], resulting in ubiquitination and proteasomal degradation of the client [82]. This N-terminal ATP pocket has distinctive characteristics in comparison with most other nucleotide-binding proteins [83], which explains the selectivity of GA.

Although GA exhibited potent anti-cancer activities in preclinical studies, it had little clinical potential mostly due to the high hepatotoxicity observed in animal models [84]. As a result, GA derivatives that maintain similar anti-cancer activities but with better toxicological properties were synthesized, such as 17-AAG (17-allylamino-17-desmethoxygeldanamycin; tanespimycin, KOS-953) (Figure 1.1) [77, 85], 17-DMAG (17-dimethylaminoethylamino-17-demethoxygeldanamycin) (Figure 1.1) [77, 86], and IPI-504 (17-allylamino-17-demethoxygeldanamycin hydroquinone hydrochloride) (Figure 1.1) [77, 87].

The clinical results of 17-AAG has greatly improved our understanding of Hsp90 inhibitors. 17-AAG entered Phase I trials in 1999 [88, 89] and several intravenous formulations have completed Phase I testing [90, 91]. Early signs of therapeutic activity have been seen in melanoma, breast cancer, prostate cancer, and multiple myeloma [89, 92-95]. Phase II clinical trials for 17-AAG are currently ongoing [90, 91], which mainly focus on tumor types hallmarked by specific Hsp90 chaperoning targets, such as leukemia expressing Bcr-Abl and Her-2 positive breast cancer [89, 96]. 17-AAG was recently administered in combination with trastuzumab in patients whose disease progressed following trastuzumab treatment; this trial has demonstrated promising anti-tumor activity and acceptable toxicity [93]. However, several drawbacks of 17-AAG, including low water-solubility, instability in solution, and low oral bioavailability may be the major obstacle to further clinical application [78, 97].

In addition to 17-AAG, other GA derivatives have been developed for clinical use as well. Currently 17-DMAG, a more water-soluble analogue of 17-AAG, has entered Phase I and Phase II clinical testing, and displayed higher oral bioavailability, lower toxicity, and increased stability compared with 17-AAG [90, 98]. Another water soluble hydroquinone hydrochloride analogue of 17-AAG is IPI-504 [99]. IPI-504 is in Phase I and Phase II clinical trials to evaluate its potential for treating cancer that has become resistant to therapy with tyrosine kinase inhibitors, such as Philadelphia chromosome-positive chronic myelogenous leukemia (CML) [100].

Radicicol (Figure 1.1) [77] is a macrocyclic natural antibiotic initially isolated from the fungus Monocillium nordinii and Monosporium bonorden [101]. Like GA, radicicol was also shown to compete with nucleotide for binding to N-terminal ATP

pocket of Hsp90 [79]. Radicicol displayed anti-cancer activity *in vitro* but not *in vivo* due to its chemical and metabolic instability [54, 102]. Hence, synthetic efforts have been directed to generate radicicol derivatives with improved stability and *in vivo* efficacy [103]. Several oxime derivatives and cycloproparadicicol have been developed and shown anti-tumor activity in preclinical animal models with tolerable toxicity [102, 104, 105].

The search for natural Hsp90 inhibitors has been accompanied with the synthesis of small molecule inhibitors with higher specificity and better pharmacological profiles. The availability of crystal structures of the Hsp90 N-domain and the development of structure-based design and high-throughput screening (HTS) assays have prompted successful exploration of a range of new synthetic scaffolds that have Hsp90 inhibitory capacity [78, 106, 107].

The first group of these was empirically designed based on the purine scaffold (Figure 1.1) [108, 109], which mimics the unique shape adopted by natural nucleotide ligand inside of the N-terminal pocket of Hsp90 [108, 110]. The favorable interaction between PU3 and the ATP pocket of Hsp90 was visualized in crystal structure, and PU3 showed similar biological effects to geldanamycin [111]. PU3 thus became a lead compound for synthesis of clinically applicable purine-scaffold Hsp90 inhibitors, which were primarily modified on either position C8 or C9 of purine [108]. These synthetic derivatives could be roughly categorized to 8-benzyl [112, 113], 8-phenylsylfanyl [113, 114], 8-(7'-substituted benzothiazolothio) [115], and 9-benzyl purine derivatives [116]. Major improvements of purine-scaffold Hsp90 inhibitors include insensitivity to multi-drug resistance [117], favorable water solubility, oral bioavailability, and metabolic

stability [113, 115, 116, 118]. For instance, PU-H71 and PU-DZ8 are currently under advanced preclinical investigation [119]. CNF-2024, an orally available 9-benzyl purine derivative with low nanomolar potency, has entered Phase I clinical trials, tested in chronic lymphocytic leukemia, advanced solid tumors, lymphomas, and more recently in advanced breast cancer [108].

Pyrazole (Figure 1.1) [109, 120] is another important class of synthetic small molecules that has been identified [121, 122]. A molecule of 3, 4-diaryl pyrazole (CCT018159) binds deeply into the N-terminal ATP pocket of Hsp90, as shown in crystallographic studies [121]. Similar with GA, a decrease in Hsp90 client protein levels (Raf-1 and Cdk4) and an increase in Hsp70 expression were observed in CCT018159-treated cancer cells [121]. Structure-based design generated more potent pyrazole amide CCT0129397 and isoxazole CCT0130024 [123]; and an optimized analogue NVP-AUY922 has just entered clinical trials [124].

Finally, a novel family of short peptide derivatives composed of the three core amino acids, Phe-D-Trp-Leu, at the center of the molecule was recently reported to inhibit ATP binding to Hsp90 [125]. They killed various cancer cell lines, but not normal cells *in vitro* and did not show toxicity *in vivo* [125]. A few of these peptide derivatives were reported to cause a marked inhibition of multidrug resistance in human *MDR1* gene-transfected mouse lymphoma cells [126].

1.4.4 Hsp90 C-terminal binding inhibitors

An allosteric regulation between the C-terminal and N-terminal domains of Hsp90 suggests that the ATP binding site located at the Hsp90 C-terminus can modulate Hsp90's N-terminal ATPase activity [127-129]. Several Hsp90 C-terminal inhibitors,

such as novobiocin [129], epigallocatechin-3-gallate (EGCG) [130], cisplatin [131], molybdate [132], and taxol [133], have been identified.

Novobiocin (Figure 1.1) [77], a coumarin antibiotic isolated from Streptomyces species, reprents the originally identified Hsp90 C-terminal inhibitors [129]. Inhibition of Hsp90 by novobiocin induced similar cellular responses as N-terminal inhibitors, i.e., destabilization of a range of Hsp90 client proteins such as Her-2, Raf-1 and p53 mutant via the ubiquitin-proteasome pathway [128, 134]. Two related coumarin antibiotics, chlorobiocin and coumermycin A1, also bind to the C-terminus of Hsp90 and have improved activity compared with novobiocin [128, 135].

Due to the lack of co-crystal structure of a C-terminal inhibitor bound to Hsp90, the exploration of C-terminal inhibitors was largely based on the molecular characteristic of Hsp90 and structure of identified inhibitors like novobiocin. A lead compound DHN2 was transformed from novobiocin [136], and the optimization of DHN2 generated the indole derivative 46, which remains to be the most potent novobiocin analogue [136].

1.4.5 Inhibitors disrupting cochaperone/Hsp90 interactions

An alternative strategy of Hsp90 modulation is to disrupt Hsp90 and cochaperone interactions. Since the Hsp90 chaperoning process is a dynamic cycle requiring so many cochaperones and accessory proteins, targeting the chaperone machinery at any stage is likely to achieve Hsp90 inhibition and pharmacologic effect.

HOP is essential for facilitating client protein loading onto the Hsp90. Assembly of Hsp70/Hsp40/client complex and Hsp90 is achieved by associations of their C-terminal tails with two independent TPR domains of Hop, TPR1 and TPR2A, respectively [137]. These interactions, especially the one between TPR2A of Hop and the

C-terminal MEEVD motif of Hsp90, are essential for function of this multi-molecular complex [138, 139]. Recently, a designed TPR module, CTPR390+, which binds to the Hsp90 C-terminus with higher affinity and more specificity than TPR2A, was shown to be capable of competing with endogenous TPR2A for Hsp90 binding and thereby to prevent the formation of Hsp70/Hsp90 complex, triggering Her-2 degradation with consequent inhibition of breast cancer cell proliferation [140]. Furthermore, a high-throughput AlphaScreen assay was developed to identify novel small molecules that hinder the Hsp90/TPR2A interaction and the identified compounds were shown to inhibit the growth of breast cancer cells, which was correlated with a reduced level of Her-2 [137]. Remarkably, inhibition of Hsp90 through this way did not induce Hsp70 expression [137, 140]. However, it is evident that these novel compounds will have modest selectivity for tumor versus non-tumor cells.

1.4.6 Inhibitors targeting client/Hsp90 associations

Inhibition of client/Hsp90 interactions offers the ultimate selectivity, but little is known about the molecular basis for these interactions [54]. The key to targeting the client/Hsp90 interaction is to study the structure and biochemistry of the molecular complexes. The three dimensional structure of an Hsp90/p50Cdc37/Cdk4 complex has been determined by electron microscopy [141], providing the first structural view of the interaction between a client protein and Hsp90 [48, 54, 141]. However, many details of the client/chaperone interactions are still unclear, making the targeting of these associations more challenging.

Shepherdin, a peptidomimetic, has been designed to specifically block the interaction between Hsp90 and the anti-apoptotic client survivin [142]. Shepherdin has

exhibited exhibit anti-leukemia activity in animal models [143]. However, besides the Hsp90 and survivin complex, shepherdin also interacts with the ATP pocket of Hsp90, and affects a range of Hsp90 clients in addition to survivin [54]. Therefore, the real mechanism that is responsible for the anti-cancer activity of shepherdin remains to be determined.

1.4.7 Post-translational modifications of Hsp90

Post-translational modifications, such as hyperphorphorylation, S-nitrosylation and reversible hyperacetylation, have been found to regulate chaperoning function of Hsp90 [144].

Several studies have revealed the mechanism of Hsp90 hyperacetylation by histone deacetylases (HDACs). HDACs and acetyltransferases (HATs) regulate Hsp90 activity by manipulating the reversible acetylation of lysine residues on Hsp90 [145]. One key acetylation site identified is lysine K294 in the middle domain of Hsp90 [146, 147]. A recent study identified p300 as one of the HATs involved in acetylating Hsp90 [148]. Hyperacetylation of Hsp90 has been observed after treating with a variety of pan-HDAC inhibitors, such as LAQ824 and LBH589 [147, 149]. HDAC6 is unique among the 18 HDAC family members identified so far because it deacetylates non-histone proteins, such as Hsp90 and α-tubulin [149]. Hyperacetylation of Hsp90 by either HDAC6 knockdown or pan-HDAC inhibitors has been associated with decreased binding of ATP and/or co-chaperones to Hsp90, promoting Hsp90 client proteins degradation [150]. HDAC1 may also contribute to Hsp90 deacetylation [151]. MS-275 is a synthetic selective inhibitor of HDAC1 (and not HDAC6) [145]. It induces hyperacetylation of Hsp90 in leukemia cells expressing mutant fms-like tyrosine kinase 3 (FLT3), inhibiting

the direct interaction between Hsp90 and FLT3, and leading to its proteasome-dependent degradation [151]. The hyperacetylation of Hsp90 by MS-275 has been shown to inhibit ATP, co-chaperone p23 and client proteins binding to Hsp90 [149]. Therefore, inhibition of either one of the two HDAC family members is associated with Hsp90 hyperacetylation and impairment of chaperoning function. In addition, siRNA-mediated depletion of HDAC6 improved the affinity of 17-AAG for Hsp90 through enhancing the degree of Hsp90 acetylation [150].

Hsp90 thiol oxidation was discovered from the study of the anticancer activity of tubocapsenolide A (TA) [152], a compound isolated from Tubocapsicum anomalum [153]. TA rapidly and selectively induced thiol oxidation of Hsp90 and Hsp70 respectively, thereby inhibiting the chaperone activity of the Hsp90/Hsp70 complex. TA-induced effects could be prevented by N-acetylcysteine, a thiol anti-oxidant.

1.5 Limitations of Classical Hsp90 Inhibitors

Hsp90 mediates the folding, assembly, and maturation of many client proteins implicated in pancreatic cancer, and it is also expressed 6 to 7-folds higher in human pancreatic cancer than in normal tissues [154], which makes it an attractive target. As summarized above, there are different types of Hsp90 modulation. However, so far, all Hsp90 inhibitors in the clinic act via competitive binding to the N-terminal ATP binding site [55], which has obvious limitations:

Firstly, using ATP binding sites as drug targets may have a risk of identifying compounds that non-specifically block the ATP binding sites of other GHL ATPases (Table 1.1). The GHL ATPases family members (such as Hsp90, DNA gyrase B, PMS2, and MutL) have closely related ATP binding cavities [155]. Therefore, classical Hsp90

inhibitors (geldanamycin, radicicol, novobiocin) not only block the ATP binding site of Hsp90, but may inhibit other proteins. For instance, geldanamycin inhibits ATP binding of both Hsp90 and the mitochondrial Hsp90 homolog, tumor necrosis factor receptor-associated protein 1 (TRAP1) [156]; radicicol inhibits the ATP binding of Hsp90, histidine kinase Sln1 [157], pyruvate dehydrogenase kinase (PDK) [158], and topoisomerase VI (Topo VI) [159]; novobiocin inhibits the C-terminal ATP binding site of Hsp90, DNA gyrase B [155, 160], and topoisomerase VI (Topo VI) [161].

Secondly, while the clinical efficacy of these classical Hsp90 inhibitors remains uncertain, side effects such as hepatotoxicity and occurrence of multidrug resistance via Pgp have been observed. A phase I trial with 17-AAG (450 mg/m^2/week) downregulated Cdk4 and Raf-1 in 9 melanoma patients (Cancer Research UK), but only two patients showed stable disease [162]. Dose-limiting toxicity included grade 3-4 heptotoxicity and grade 3 diarrhea. Another phase I trial of 17-AAG (Maximal Tolerated Dose, MTD, 295 mg/m2) in 6 patients with refractory advanced cancer (University of Pittsburg) did not produce objective response [163], but rather showed dose-limiting toxicities (fatigue, anorexia, diarrhea, nausea, vomiting, and elevation of liver enzymes). A Clinical trial of 17-AAG (MTD 431 mg/m2) in 21 patients in Mayo clinic did not show an anticancer response. But dose-limiting toxicity was noticed at the MTD [108, 119].

Thirdly, all the N-terminal ATP site binding Hsp90 inhibitors induce the heat shock response, exhibiting as the overexpression of Hsps including Hsp27, Hsp40, Hsp70 and Hsp90 [55]. This phenomenon occurs because the N-terminal inhibitors disassemble the Hsp90/HSF1 complex, and HSF1 translocates to the nucleus and initiates transcription of the heat shock response [55]. Therefore, the anti-cancer activity of Hsp90

inhibitors may be jeopardized due to the anti-apoptotic and pro-survival effects manifested by overexpression of Hsps.

Finally, the application of classical Hsp90 inhibitors for Hsp90 inhibition may be a double-edged sword. Their effect on signaling pathways have not been fully examined, which could be much more complicated than expected. In contrast to the antitumor activity, Price et al have reported that 17-AAG and other Hsp90 inhibitors can enhance osteoclast formation and potentiate bone metastasis of a human breast cancer cell line [164]. In consistence with this, recent studies have shown that Hsp90 inhibition by 17-AAG promotes growth of prostate carcinoma cells in bone in the xenograft model, which is likely due to the transient activation of Erk, Akt and Src kinase [165]. Thus, the short-lived kinase activation induced by classical Hsp90 inhibitors favors bone metastasis, which could dramatically affect the clinical potential of these compounds.

1.6 Evidence to Support Identifying Novel Hsp90 Inhibitors That Disrupt the Hsp90 and p50Cdc37 Interaction

The wide-ranging functions of Hsp90 result from its ability to chaperone many client proteins through an ordered formation of multichaperone complexes with cochaperones [43, 166]. With the increasing understanding of the Hsp90 function cycle and the promising results of ATP binding blockers of Hsp90, interest in Hsp90 inhibition has expanded from the central component Hsp90 to various modulators in the chaperone machinery. Inhibition of cochaperones (Aha1, p50Cdc37, CHIP, Hop, Hsp70, and PP5) has exhibited therapeutic anticancer potentials as well [166]. Silencing of Aha1, the only known Hsp90 ATPase activator, decreases client protein activation and increases cellular sensitivity to the Hsp90 inhibitor 17-AAG [167]. Simultaneous knockdown both Hsc70

and Hsp72 induces proteasome-dependent degradation of Hsp90 client proteins, G1 cell-cycle arrest, and extensive tumor-specific apoptosis [168]. p50Cdc37 silencing promotes the proteasome-mediated degradation of kinase clients via a degradation pathway independent of Hsp90 binding, and enhances apoptosis in combination with 17-AAG [169]. Not only targeting cochaperones has exhibited pharmacological benefits, the interference of Hsp90/cochaperone complex has shown therapeutic potential as well. The compounds disrupting Hsp90 and Hop interaction have been identified and shown activity in human breast cancer cells [137, 140]. The appearance of Hsp90/Hop inhibitors has demonstrated proof-of-concept for successfully targeting protein-protein interactions in Hsp90 multichaperone complex.

We aim to target the Hsp90/p50Cdc37 complex based on the following evidence:

Hsp90 may exist in "altered and heightened" superchaperone complexes with co-chaperones in cancer cells, while Hsp90 is largely uncomplexed in normal cells (Figure 1.2) [170, 171]. This is supported by the selective sensitivity of Hsp90 inhibitors against cancer cells vs. normal cells in vitro and in vivo [142, 170, 172]. For instance, the binding affinity of 17-AAG to Hsp90 in cancer cells is 100-fold higher than its binding to Hsp90 in normal cells [170]. The peptimimetic shepherdin pulled down more Hsp90 from cancer cells than normal cells.

Because the Hsp90 chaperoning process involves the formation of protein complexes with cochaperones, halting Hsp90-cochaperone interaction at various stages is likely to also inhibit Hsp90 activity. In this context, inhibitors that block the Hsp90-cochaperone interaction may offer much more specificity against cancer cells. p50Cdc37 was originally discovered in yeast as an essential cell cycle protein [68]. Later studies

proved it to be an Hsp90 cochaperone, acting as an adaptor to load protein kinase to Hsp90 complex [66, 166]. Most of the Hsp90 clients that p50Cdc37 is associated with are crucial elements implicated in signal transduction, cell proliferation and survival [166]. The important role of p50Cdc37 in the Hsp90 chaperoning cycle may indicate its involvement in malignancy. Indeed, p50Cdc37 overexpression is found in prostate cancer cells and tissues [173], and its upregulation during hepatocarcinogenesis can protect cancer development from inhibitory compounds and promote tumorigenesis [174]. In addition, p50Cdc37 is highly expressed in proliferative tissues [175] and can function as an oncogene to induce hyperproliferative disorders and tumor formation in a genetically engineered mouse model [173, 176]. All these findings suggest that p50Cdc37 can be exploited as a therapeutic target.

1.7 Specific Aims

Our goal is to identify novel Hsp90 inhibitors to disrupt Hsp90 and p50Cdc37 interaction for use in pancreatic cancer therapy. We hypothesize that disruption of Hsp90/p50Cdc37 complex, without affecting ATP binding to Hsp90, will block client protein loading to the superchaperone complex and induce premature client protein degradation (Figure 1.3). These novel inhibitors will exhibit more specific inhibition of Hsp90 activity in pancreatic cancer cells.

Aim 1: To identify new compounds which disrupt the Hsp90/p50Cdc37 complex

Aim 2: To evaluate Hsp90 and p50Cdc37 interactions and to confirm the selected compounds to inhibit Hsp90 by disassembling the Hsp90/p50Cdc37 complex

Aim 3: To study the anti-pancreatic cancer efficacy of the selected compounds *in vitro* and *in vivo*

Aim 4: To examine whether classical Hsp90 inhibitors will induce the transient activation of MEK/ERK signaling cascade in pancreatic cancer cells, and to investigate the mechanism and consequence and possible treatments via combination treatment.

1.8 References

1. *Cancer Facts & Figures 2009.* America Cancer Society
2. Bardeesy, N. and R.A. DePinho, *Pancreatic cancer biology and genetics.* Nat Rev Cancer, 2002. **2**(12): p. 897-909.
3. Wong, H.H. and N.R. Lemoine, *Pancreatic cancer: molecular pathogenesis and new therapeutic targets.* Nat Rev Gastroenterol Hepatol, 2009. **6**(7): p. 412-22.
4. Pliarchopoulou, K. and D. Pectasides, *Pancreatic cancer: current and future treatment strategies.* Cancer Treat Rev, 2009. **35**(5): p. 431-6.
5. Borja-Cacho, D., et al., *Molecular targeted therapies for pancreatic cancer.* Am J Surg, 2008. **196**(3): p. 430-41.
6. Shah, A.P., J.B. Strauss, and R.A. Abrams, *Review and commentary on the role of radiation therapy in the adjuvant management of pancreatic cancer.* Am J Clin Oncol. **33**(1): p. 101-6.
7. Li, J., M.G. Wientjes, and J.L. Au, *Pancreatic cancer: pathobiology, treatment options, and drug delivery.* AAPS J. **12**(2): p. 223-32.
8. Yokoyama, Y., Y. Nimura, and M. Nagino, *Advances in the treatment of pancreatic cancer: limitations of surgery and evaluation of new therapeutic strategies.* Surg Today, 2009. **39**(6): p. 466-75.
9. Duffy, M.J., et al., *Tumor markers in pancreatic cancer: a European Group on Tumor Markers (EGTM) status report.* Ann Oncol. **21**(3): p. 441-7.
10. Mehta, S.P., *Palliative chemotherapy for pancreatic malignancies.* Surg Clin North Am. **90**(2): p. 365-75.
11. Palmer, K.R., et al., *Chemotherapy prolongs survival in inoperable pancreatic carcinoma.* Br J Surg, 1994. **81**(6): p. 882-5.
12. Sultana, A., et al., *Meta-analyses of chemotherapy for locally advanced and metastatic pancreatic cancer.* J Clin Oncol, 2007. **25**(18): p. 2607-15.
13. Burris, H.A., 3rd, et al., *Improvements in survival and clinical benefit with gemcitabine as first-line therapy for patients with advanced pancreas cancer: a randomized trial.* J Clin Oncol, 1997. **15**(6): p. 2403-13.
14. Zerbi, A., et al., *Intraoperative radiation therapy adjuvant to resection in the treatment of pancreatic cancer.* Cancer, 1994. **73**(12): p. 2930-5.
15. Di Marco, M., et al., *Metastatic pancreatic cancer: is gemcitabine still the best standard treatment? (Review).* Oncol Rep. **23**(5): p. 1183-92.
16. Berlin, J.D., et al., *Phase III study of gemcitabine in combination with fluorouracil versus gemcitabine alone in patients with advanced pancreatic carcinoma: Eastern Cooperative Oncology Group Trial E2297.* J Clin Oncol, 2002. **20**(15): p. 3270-5.
17. Stathopoulos, G.P., et al., *A multicenter phase III trial comparing irinotecan-gemcitabine (IG) with gemcitabine (G) monotherapy as first-line treatment in*

patients with locally advanced or metastatic pancreatic cancer. Br J Cancer, 2006. **95**(5): p. 587-92.
18. Poplin, E., et al., *Phase III, randomized study of gemcitabine and oxaliplatin versus gemcitabine (fixed-dose rate infusion) compared with gemcitabine (30-minute infusion) in patients with pancreatic carcinoma E6201: a trial of the Eastern Cooperative Oncology Group.* J Clin Oncol, 2009. **27**(23): p. 3778-85.
19. Colucci, G., et al., *Gemcitabine alone or with cisplatin for the treatment of patients with locally advanced and/or metastatic pancreatic carcinoma: a prospective, randomized phase III study of the Gruppo Oncologia dell'Italia Meridionale.* Cancer, 2002. **94**(4): p. 902-10.
20. Herrmann, R., et al., *Gemcitabine plus capecitabine compared with gemcitabine alone in advanced pancreatic cancer: a randomized, multicenter, phase III trial of the Swiss Group for Clinical Cancer Research and the Central European Cooperative Oncology Group.* J Clin Oncol, 2007. **25**(16): p. 2212-7.
21. Oettle, H., et al., *A phase III trial of pemetrexed plus gemcitabine versus gemcitabine in patients with unresectable or metastatic pancreatic cancer.* Ann Oncol, 2005. **16**(10): p. 1639-45.
22. Li, D., et al., *Pancreatic cancer.* Lancet, 2004. **363**(9414): p. 1049-57.
23. Kern, S.E., et al., *An introduction to pancreatic adenocarcinoma genetics, pathology and therapy.* Cancer Biol Ther, 2002. **1**(6): p. 607-13.
24. Hruban, R.H., et al., *Pancreatic intraepithelial neoplasia: a new nomenclature and classification system for pancreatic duct lesions.* Am J Surg Pathol, 2001. **25**(5): p. 579-86.
25. Buchler, P., et al., *Hypoxia-inducible factor 1 regulates vascular endothelial growth factor expression in human pancreatic cancer.* Pancreas, 2003. **26**(1): p. 56-64.
26. Van Cutsem, E., et al., *Phase III trial of gemcitabine plus tipifarnib compared with gemcitabine plus placebo in advanced pancreatic cancer.* J Clin Oncol, 2004. **22**(8): p. 1430-8.
27. Yamanaka, Y., et al., *Coexpression of epidermal growth factor receptor and ligands in human pancreatic cancer is associated with enhanced tumor aggressiveness.* Anticancer Res, 1993. **13**(3): p. 565-9.
28. Moore, M.J., et al., *Erlotinib plus gemcitabine compared with gemcitabine alone in patients with advanced pancreatic cancer: a phase III trial of the National Cancer Institute of Canada Clinical Trials Group.* J Clin Oncol, 2007. **25**(15): p. 1960-6.
29. Kulke, M.H., et al., *Capecitabine plus erlotinib in gemcitabine-refractory advanced pancreatic cancer.* J Clin Oncol, 2007. **25**(30): p. 4787-92.
30. Seo, Y., et al., *High expression of vascular endothelial growth factor is associated with liver metastasis and a poor prognosis for patients with ductal pancreatic adenocarcinoma.* Cancer, 2000. **88**(10): p. 2239-45.
31. Van Cutsem, E., et al., *Phase III trial of bevacizumab in combination with gemcitabine and erlotinib in patients with metastatic pancreatic cancer.* J Clin Oncol, 2009. **27**(13): p. 2231-7.

32. Ruggeri, B.A., et al., *Amplification and overexpression of the AKT2 oncogene in a subset of human pancreatic ductal adenocarcinomas.* Mol Carcinog, 1998. **21**(2): p. 81-6.
33. Wolpin, B.M., et al., *Oral mTOR inhibitor everolimus in patients with gemcitabine-refractory metastatic pancreatic cancer.* J Clin Oncol, 2009. **27**(2): p. 193-8.
34. Ito, D., et al., *In vivo antitumor effect of the mTOR inhibitor CCI-779 and gemcitabine in xenograft models of human pancreatic cancer.* Int J Cancer, 2006. **118**(9): p. 2337-43.
35. Tucker, O.N., et al., *Cyclooxygenase-2 expression is up-regulated in human pancreatic cancer.* Cancer Res, 1999. **59**(5): p. 987-90.
36. Ding, X.Z., R. Hennig, and T.E. Adrian, *Lipoxygenase and cyclooxygenase metabolism: new insights in treatment and chemoprevention of pancreatic cancer.* Mol Cancer, 2003. **2**: p. 10.
37. Ferrari, V., et al., *Gemcitabine plus celecoxib (GECO) in advanced pancreatic cancer: a phase II trial.* Cancer Chemother Pharmacol, 2006. **57**(2): p. 185-90.
38. Dragovich, T., et al., *Gemcitabine plus celecoxib in patients with advanced or metastatic pancreatic adenocarcinoma: results of a phase II trial.* Am J Clin Oncol, 2008. **31**(2): p. 157-62.
39. Ritossa, F., *Discovery of the heat shock response.* Cell Stress Chaperones, 1996. **1**(2): p. 97-8.
40. Westerheide, S.D. and R.I. Morimoto, *Heat shock response modulators as therapeutic tools for diseases of protein conformation.* J Biol Chem, 2005. **280**(39): p. 33097-100.
41. Welch, W.J., *The role of heat-shock proteins as molecular chaperones.* Curr Opin Cell Biol, 1991. **3**(6): p. 1033-8.
42. Welch, W.J. and J.R. Feramisco, *Purification of the major mammalian heat shock proteins.* J Biol Chem, 1982. **257**(24): p. 14949-59.
43. Kamal, A., M.F. Boehm, and F.J. Burrows, *Therapeutic and diagnostic implications of Hsp90 activation.* Trends Mol Med, 2004. **10**(6): p. 283-90.
44. Wiech, H., et al., *Hsp90 chaperones protein folding in vitro.* Nature, 1992. **358**(6382): p. 169-70.
45. McClellan, A.J., et al., *Diverse cellular functions of the Hsp90 molecular chaperone uncovered using systems approaches.* Cell, 2007. **131**(1): p. 121-35.
46. Zhao, R., et al., *Navigating the chaperone network: an integrative map of physical and genetic interactions mediated by the hsp90 chaperone.* Cell, 2005. **120**(5): p. 715-27.
47. Falsone, S.F., et al., *A proteomic snapshot of the human heat shock protein 90 interactome.* FEBS Lett, 2005. **579**(28): p. 6350-4.
48. Ali, M.M., et al., *Crystal structure of an Hsp90-nucleotide-p23/Sba1 closed chaperone complex.* Nature, 2006. **440**(7087): p. 1013-7.
49. Dollins, D.E., et al., *Structures of GRP94-nucleotide complexes reveal mechanistic differences between the hsp90 chaperones.* Mol Cell, 2007. **28**(1): p. 41-56.
50. Pearl, L.H. and C. Prodromou, *Structure and mechanism of the Hsp90 molecular chaperone machinery.* Annu Rev Biochem, 2006. **75**: p. 271-94.

51. Terasawa, K., M. Minami, and Y. Minami, *Constantly updated knowledge of Hsp90.* J Biochem, 2005. **137**(4): p. 443-7.
52. Dutta, R. and M. Inouye, *GHKL, an emergent ATPase/kinase superfamily.* Trends Biochem Sci, 2000. **25**(1): p. 24-8.
53. Hawle, P., et al., *The middle domain of Hsp90 acts as a discriminator between different types of client proteins.* Mol Cell Biol, 2006. **26**(22): p. 8385-95.
54. Pearl, L.H., C. Prodromou, and P. Workman, *The Hsp90 molecular chaperone: an open and shut case for treatment.* Biochem J, 2008. **410**(3): p. 439-53.
55. Brandt, G.E. and B.S. Blagg, *Alternate strategies of Hsp90 modulation for the treatment of cancer and other diseases.* Curr Top Med Chem, 2009. **9**(15): p. 1447-61.
56. Richter, K., et al., *Conserved conformational changes in the ATPase cycle of human Hsp90.* J Biol Chem, 2008. **283**(26): p. 17757-65.
57. Wandinger, S.K., K. Richter, and J. Buchner, *The Hsp90 chaperone machinery.* J Biol Chem, 2008. **283**(27): p. 18473-7.
58. Hessling, M., K. Richter, and J. Buchner, *Dissection of the ATP-induced conformational cycle of the molecular chaperone Hsp90.* Nat Struct Mol Biol, 2009. **16**(3): p. 287-93.
59. Scheibel, T. and J. Buchner, *The Hsp90 complex--a super-chaperone machine as a novel drug target.* Biochem Pharmacol, 1998. **56**(6): p. 675-82.
60. Prodromou, C., et al., *Regulation of Hsp90 ATPase activity by tetratricopeptide repeat (TPR)-domain co-chaperones.* EMBO J, 1999. **18**(3): p. 754-62.
61. Richter, K., et al., *Sti1 is a non-competitive inhibitor of the Hsp90 ATPase. Binding prevents the N-terminal dimerization reaction during the atpase cycle.* J Biol Chem, 2003. **278**(12): p. 10328-33.
62. Neckers, L., *Development of small molecule Hsp90 Inhibitors: utilizing both forward and reverse chemical genomics for drug identification.* Current Medicinal Chemistry, 2003. **10**(9): p. 733-739.
63. Meyer, P., et al., *Structural basis for recruitment of the ATPase activator Aha1 to the Hsp90 chaperone machinery.* EMBO J, 2004. **23**(3): p. 511-9.
64. McLaughlin, S.H., H.W. Smith, and S.E. Jackson, *Stimulation of the weak ATPase activity of human hsp90 by a client protein.* J Mol Biol, 2002. **315**(4): p. 787-98.
65. Panaretou, B., et al., *Activation of the ATPase activity of hsp90 by the stress-regulated cochaperone aha1.* Mol Cell, 2002. **10**(6): p. 1307-18.
66. Pearl, L.H., *Hsp90 and Cdc37 -- a chaperone cancer conspiracy.* Curr Opin Genet Dev, 2005. **15**(1): p. 55-61.
67. Caplan, A.J., A.K. Mandal, and M.A. Theodoraki, *Molecular chaperones and protein kinase quality control.* Trends Cell Biol, 2007. **17**(2): p. 87-92.
68. Reed, S.I., *The selection of S. cerevisiae mutants defective in the start event of cell division.* Genetics, 1980. **95**(3): p. 561-77.
69. Arlander, S.J., et al., *Chaperoning checkpoint kinase 1 (Chk1), an Hsp90 client, with purified chaperones.* J Biol Chem, 2006. **281**(5): p. 2989-98.
70. Mandal, A.K., et al., *Cdc37 has distinct roles in protein kinase quality control that protect nascent chains from degradation and promote posttranslational maturation.* J. Cell Biol., 2007. **176**: p. 319-328.

71. Roe, S.M., et al., *The Mechanism of Hsp90 regulation by the protein kinase-specific cochaperone p50(cdc37).* Cell, 2004. **116**(1): p. 87-98.
72. Siligardi, G., et al., *Regulation of Hsp90 ATPase activity by the co-chaperone Cdc37p/p50cdc37.* J Biol Chem, 2002. **277**(23): p. 20151-9.
73. Borkovich, K.A., et al., *hsp82 is an essential protein that is required in higher concentrations for growth of cells at higher temperatures.* Mol Cell Biol, 1989. **9**(9): p. 3919-30.
74. Whitesell, L., et al., *Inhibition of heat shock protein HSP90-pp60v-src heteroprotein complex formation by benzoquinone ansamycins: essential role for stress proteins in oncogenic transformation.* Proc Natl Acad Sci U S A, 1994. **91**(18): p. 8324-8.
75. Supko, J.G., et al., *Preclinical pharmacologic evaluation of geldanamycin as an antitumor agent.* Cancer Chemother. Pharmacol., 1995. **36**: p. 305-315.
76. Schulte, T.W., Neckers, L.M., *The benzoquinone ansamycin 17-allylamino-17-demethoxygeldanamycin binds to HSP90 and shares important biologic activities with geldanamycin.* . Cancer Chemother. Pharmacol., 1998. **42**: p. 273-279.
77. Workman, P., et al., *Drugging the cancer chaperone HSP90: combinatorial therapeutic exploitation of oncogene addiction and tumor stress.* Ann N Y Acad Sci, 2007. **1113**: p. 202-16.
78. Messaoudi, S., et al., *Recent advances in Hsp90 inhibitors as antitumor agents.* Anticancer Agents Med Chem, 2008. **8**(7): p. 761-82.
79. Roe, S.M., et al., *Structural basis for inhibition of the Hsp90 molecular chaperone by the antitumor antibiotics radicicol and geldanamycin.* J Med Chem, 1999. **42**(2): p. 260-6.
80. Blagg, B.S. and T.D. Kerr, *Hsp90 inhibitors: small molecules that transform the Hsp90 protein folding machinery into a catalyst for protein degradation.* Med Res Rev, 2006. **26**(3): p. 310-38.
81. Neckers, L., *Chaperoning oncogenes: Hsp90 as a target of geldanamycin.* Handb Exp Pharmacol, 2006(172): p. 259-77.
82. Mimnaugh, E.G., C. Chavany, and L. Neckers, *Polyubiquitination and proteasomal degradation of the p185c-erbB-2 receptor protein-tyrosine kinase induced by geldanamycin.* J Biol Chem, 1996. **271**(37): p. 22796-801.
83. Prodromou, C., et al., *Identification and structural characterization of the ATP/ADP-binding site in the Hsp90 molecular chaperone.* Cell, 1997. **90**(1): p. 65-75.
84. Neckers, L., T.W. Schulte, and E. Mimnaugh, *Geldanamycin as a potential anti-cancer agent: its molecular target and biochemical activity.* Invest New Drugs, 1999. **17**(4): p. 361-73.
85. Solit, D.B., et al., *Phase I trial of 17-allylamino-17-demethoxygeldanamycin in patients with advanced cancer.* Clin Cancer Res, 2007. **13**(6): p. 1775-82.
86. Smith, V., et al., *Comparison of 17-dimethylaminoethylamino-17-demethoxy-geldanamycin (17DMAG) and 17-allylamino-17-demethoxygeldanamycin (17AAG) in vitro: effects on Hsp90 and client proteins in melanoma models.* Cancer Chemother Pharmacol, 2005. **56**(2): p. 126-37.

87. Sydor, J.R., et al., *Development of 17-allylamino-17-demethoxygeldanamycin hydroquinone hydrochloride (IPI-504), an anti-cancer agent directed against Hsp90.* Proc Natl Acad Sci U S A, 2006. **103**(46): p. 17408-13.
88. Banerji, U., et al., *Phase I pharmacokinetic and pharmacodynamic study of 17-allylamino, 17-demethoxygeldanamycin in patients with advanced malignancies.* J Clin Oncol, 2005. **23**(18): p. 4152-61.
89. Pacey, S., et al., *Hsp90 inhibitors in the clinic.* Handb Exp Pharmacol, 2006(172): p. 331-58.
90. Ronnen, E.A., et al., *A phase II trial of 17-(Allylamino)-17-demethoxygeldanamycin in patients with papillary and clear cell renal cell carcinoma.* Invest New Drugs, 2006. **24**(6): p. 543-6.
91. Heath, E.I., et al., *A phase II trial of 17-allylamino-17- demethoxygeldanamycin in patients with hormone-refractory metastatic prostate cancer.* Clin Prostate Cancer, 2005. **4**(2): p. 138-41.
92. Solit, D.B. and N. Rosen, *Hsp90: a novel target for cancer therapy.* Curr Top Med Chem, 2006. **6**(11): p. 1205-14.
93. Modi, S., et al., *Combination of trastuzumab and tanespimycin (17-AAG, KOS-953) is safe and active in trastuzumab-refractory HER-2 overexpressing breast cancer: a phase I dose-escalation study.* J Clin Oncol, 2007. **25**(34): p. 5410-7.
94. da Rocha Dias, S., et al., *Activated B-RAF is an Hsp90 client protein that is targeted by the anticancer drug 17-allylamino-17-demethoxygeldanamycin.* Cancer Res, 2005. **65**(23): p. 10686-91.
95. Grbovic, O.M., et al., *V600E B-Raf requires the Hsp90 chaperone for stability and is degraded in response to Hsp90 inhibitors.* Proc Natl Acad Sci U S A, 2006. **103**(1): p. 57-62.
96. Dai, C. and L. Whitesell, *HSP90: a rising star on the horizon of anticancer targets.* Future Oncol, 2005. **1**(4): p. 529-40.
97. McCollum, A.K., et al., *P-Glycoprotein-mediated resistance to Hsp90-directed therapy is eclipsed by the heat shock response.* Cancer Res, 2008. **68**(18): p. 7419-27.
98. Hollingshead, M., et al., *In vivo antitumor efficacy of 17-DMAG (17-dimethylaminoethylamino-17-demethoxygeldanamycin hydrochloride), a water-soluble geldanamycin derivative.* Cancer Chemother Pharmacol, 2005. **56**(2): p. 115-25.
99. Didelot, C., et al., *Anti-cancer therapeutic approaches based on intracellular and extracellular heat shock proteins.* Curr Med Chem, 2007. **14**(27): p. 2839-47.
100. Peng, C., et al., *Inhibition of heat shock protein 90 prolongs survival of mice with BCR-ABL-T315I-induced leukemia and suppresses leukemic stem cells.* Blood, 2007. **110**(2): p. 678-85.
101. Delmotte, P. and J. Delmotte-Plaque, *A new antifungal substance of fungal origin.* Nature, 1953. **171**(4347): p. 344.
102. Soga, S., et al., *Development of radicicol analogues.* Curr Cancer Drug Targets, 2003. **3**(5): p. 359-69.
103. Proisy, N., et al., *Inhibition of Hsp90 with synthetic macrolactones: synthesis and structural and biological evaluation of ring and conformational analogs of radicicol.* Chem Biol, 2006. **13**(11): p. 1203-15.

104. Shiotsu, Y., et al., *Novel oxime derivatives of radicicol induce erythroid differentiation associated with preferential G(1) phase accumulation against chronic myelogenous leukemia cells through destabilization of Bcr-Abl with Hsp90 complex.* Blood, 2000. **96**(6): p. 2284-91.
105. Yamamoto, K., et al., *Total synthesis as a resource in the discovery of potentially valuable antitumor agents: cycloproparadicicol.* Angew Chem Int Ed Engl, 2003. **42**(11): p. 1280-4.
106. Huth, J.R., et al., *Discovery and design of novel HSP90 inhibitors using multiple fragment-based design strategies.* Chem Biol Drug Des, 2007. **70**(1): p. 1-12.
107. Park, H., Y.J. Kim, and J.S. Hahn, *A novel class of Hsp90 inhibitors isolated by structure-based virtual screening.* Bioorg Med Chem Lett, 2007. **17**(22): p. 6345-9.
108. Chiosis, G., *Discovery and development of purine-scaffold Hsp90 inhibitors.* Curr Top Med Chem, 2006. **6**(11): p. 1183-91.
109. Solit, D.B. and G. Chiosis, *Development and application of Hsp90 inhibitors.* Drug Discov Today, 2008. **13**(1-2): p. 38-43.
110. Chiosis, G., et al., *A small molecule designed to bind to the adenine nucleotide pocket of Hsp90 causes Her2 degradation and the growth arrest and differentiation of breast cancer cells.* Chem Biol, 2001. **8**(3): p. 289-99.
111. Wright, L., et al., *Structure-activity relationships in purine-based inhibitor binding to HSP90 isoforms.* Chem Biol, 2004. **11**(6): p. 775-85.
112. Vilenchik, M., et al., *Targeting wide-range oncogenic transformation via PU24FCl, a specific inhibitor of tumor Hsp90.* Chem Biol, 2004. **11**(6): p. 787-97.
113. He, H., et al., *Identification of potent water soluble purine-scaffold inhibitors of the heat shock protein 90.* J Med Chem, 2006. **49**(1): p. 381-90.
114. Llauger, L., et al., *Evaluation of 8-arylsulfanyl, 8-arylsulfoxyl, and 8-arylsulfonyl adenine derivatives as inhibitors of the heat shock protein 90.* J Med Chem, 2005. **48**(8): p. 2892-905.
115. Zhang, L., et al., *7'-substituted benzothiazolothio- and pyridinothiazolothio-purines as potent heat shock protein 90 inhibitors.* J Med Chem, 2006. **49**(17): p. 5352-62.
116. Kasibhatla, S.R., et al., *Rationally designed high-affinity 2-amino-6-halopurine heat shock protein 90 inhibitors that exhibit potent antitumor activity.* J Med Chem, 2007. **50**(12): p. 2767-78.
117. Rodina, A., et al., *Selective compounds define Hsp90 as a major inhibitor of apoptosis in small-cell lung cancer.* Nat Chem Biol, 2007. **3**(8): p. 498-507.
118. Biamonte, M.A., et al., *Orally active purine-based inhibitors of the heat shock protein 90.* J Med Chem, 2006. **49**(2): p. 817-28.
119. Chiosis, G. and H. Tao, *Purine-scaffold Hsp90 inhibitors.* IDrugs, 2006. **9**(11): p. 778-82.
120. McDonald, E., et al., *Discovery and development of pyrazole-scaffold hsp90 inhibitors.* . Curr Top Med Chem, 2006. **6**: p. 1193-1203.
121. Cheung, K.M., et al., *The identification, synthesis, protein crystal structure and in vitro biochemical evaluation of a new 3,4-diarylpyrazole class of Hsp90 inhibitors.* Bioorg Med Chem Lett, 2005. **15**(14): p. 3338-43.

122. Sharp, S.Y., et al., *In vitro biological characterization of a novel, synthetic diaryl pyrazole resorcinol class of heat shock protein 90 inhibitors.* Cancer Res, 2007. **67**(5): p. 2206-16.
123. Sharp, S.Y., et al., *Inhibition of the heat shock protein 90 molecular chaperone in vitro and in vivo by novel, synthetic, potent resorcinylic pyrazole/isoxazole amide analogues.* Mol Cancer Ther, 2007. **6**(4): p. 1198-211.
124. Brough, P.A., et al., *4,5-diarylisoxazole Hsp90 chaperone inhibitors: potential therapeutic agents for the treatment of cancer.* J Med Chem, 2008. **51**(2): p. 196-218.
125. Orosz, A., et al., *Novel nontoxic heat shock protein 90 inhibitors having selective antiproliferative effect.* Int J Biochem Cell Biol, 2006. **38**(8): p. 1352-62.
126. Molnar, J., et al., *Effects of nontoxic heat shock protein 90 inhibitor peptide derivatives on reversal of MDR of tumor cells.* In Vivo, 2007. **21**(2): p. 429-33.
127. Garnier, C., et al., *Binding of ATP to heat shock protein 90: evidence for an ATP-binding site in the C-terminal domain.* J Biol Chem, 2002. **277**(14): p. 12208-14.
128. Marcu, M.G., T.W. Schulte, and L. Neckers, *Novobiocin and related coumarins and depletion of heat shock protein 90-dependent signaling proteins.* J Natl Cancer Inst, 2000. **92**(3): p. 242-8.
129. Marcu, M.G., et al., *The heat shock protein 90 antagonist novobiocin interacts with a previously unrecognized ATP-binding domain in the carboxyl terminus of the chaperone.* J Biol Chem, 2000. **275**(47): p. 37181-6.
130. Palermo, C.M., C.A. Westlake, and T.A. Gasiewicz, *Epigallocatechin gallate inhibits aryl hydrocarbon receptor gene transcription through an indirect mechanism involving binding to a 90 kDa heat shock protein.* Biochemistry, 2005. **44**(13): p. 5041-52.
131. Itoh, H., et al., *A novel chaperone-activity-reducing mechanism of the 90-kDa molecular chaperone HSP90.* Biochem J, 1999. **343 Pt 3**: p. 697-703.
132. Hartson, S.D., et al., *Molybdate inhibits hsp90, induces structural changes in its C-terminal domain, and alters its interactions with substrates.* Biochemistry, 1999. **38**(12): p. 3837-49.
133. Byrd, C.A., et al., *Heat shock protein 90 mediates macrophage activation by Taxol and bacterial lipopolysaccharide.* Proc Natl Acad Sci U S A, 1999. **96**(10): p. 5645-50.
134. Allan, R.K., et al., *Modulation of chaperone function and cochaperone interaction by novobiocin in the C-terminal domain of Hsp90: evidence that coumarin antibiotics disrupt Hsp90 dimerization.* J Biol Chem, 2006. **281**(11): p. 7161-71.
135. Burlison, J.A. and B.S. Blagg, *Synthesis and evaluation of coumermycin A1 analogues that inhibit the Hsp90 protein folding machinery.* Org Lett, 2006. **8**(21): p. 4855-8.
136. Burlison, J.A., et al., *Development of novobiocin analogues that manifest anti-proliferative activity against several cancer cell lines.* J Org Chem, 2008. **73**(6): p. 2130-7.
137. Yi, F. and L. Regan, *A novel class of small molecule inhibitors of Hsp90.* ACS Chem Biol, 2008. **3**(10): p. 645-54.

138. Chen, S. and D.F. Smith, *Hop as an adaptor in the heat shock protein 70 (Hsp70) and hsp90 chaperone machinery.* J Biol Chem, 1998. **273**(52): p. 35194-200.
139. Scheufler, C., et al., *Structure of TPR domain-peptide complexes: critical elements in the assembly of the Hsp70-Hsp90 multichaperone machine.* Cell, 2000. **101**(2): p. 199-210.
140. Cortajarena, A.L., F. Yi, and L. Regan, *Designed TPR modules as novel anticancer agents.* ACS Chem Biol, 2008. **3**(3): p. 161-6.
141. Vaughan, C.K., et al., *Structure of an Hsp90-Cdc37-Cdk4 complex.* Mol Cell, 2006. **23**(5): p. 697-707.
142. Plescia, J., et al., *Rational design of shepherdin, a novel anticancer agent.* Cancer Cell, 2005. **7**(5): p. 457-68.
143. Gyurkocza, B., et al., *Antileukemic activity of shepherdin and molecular diversity of hsp90 inhibitors.* J Natl Cancer Inst, 2006. **98**(15): p. 1068-77.
144. Neckers, L., *Heat shock protein 90: the cancer chaperone.* J Biosci, 2007. **32**(3): p. 517-30.
145. Minucci, S. and P.G. Pelicci, *Histone deacetylase inhibitors and the promise of epigenetic (and more) treatments for cancer.* Nat Rev Cancer, 2006. **6**(1): p. 38-51.
146. Scroggins, B.T., et al., *An acetylation site in the middle domain of Hsp90 regulates chaperone function.* Mol Cell, 2007. **25**(1): p. 151-9.
147. Kovacs, J.J., et al., *HDAC6 regulates Hsp90 acetylation and chaperone-dependent activation of glucocorticoid receptor.* Mol Cell, 2005. **18**(5): p. 601-7.
148. Yang, Y., et al., *Role of acetylation and extracellular location of heat shock protein 90alpha in tumor cell invasion.* Cancer Res, 2008. **68**(12): p. 4833-42.
149. Bali, P., et al., *Inhibition of histone deacetylase 6 acetylates and disrupts the chaperone function of heat shock protein 90: a novel basis for antileukemia activity of histone deacetylase inhibitors.* J Biol Chem, 2005. **280**(29): p. 26729-34.
150. Rao, R., et al., *HDAC6 inhibition enhances 17-AAG--mediated abrogation of hsp90 chaperone function in human leukemia cells.* Blood, 2008. **112**(5): p. 1886-93.
151. Nishioka, C., et al., *MS-275, a novel histone deacetylase inhibitor with selectivity against HDAC1, induces degradation of FLT3 via inhibition of chaperone function of heat shock protein 90 in AML cells.* Leuk Res, 2008. **32**(9): p. 1382-92.
152. Hsieh, P.W., et al., *Cytotoxic withanolides from Tubocapsicum anomalum.* J Nat Prod, 2007. **70**(5): p. 747-53.
153. Chen, W.Y., et al., *Tubocapsenolide A, a novel withanolide, inhibits proliferation and induces apoptosis in MDA-MB-231 cells by thiol oxidation of heat shock proteins.* J Biol Chem, 2008. **283**(25): p. 17184-93.
154. Ogata, M., et al., *Overexpression and localization of heat shock proteins mRNA in pancreatic carcinoma.* Journal of Nippon Medical School, 2000. **67**(3): p. 177-185.
155. Chene, P., *ATPases as drug targets: learning from their structure.* Nat Rev Drug Discov, 2002. **1**(9): p. 665-73.
156. Felts, S.J., et al., *The hsp90-related protein TRAP1 is a mitochondrial protein with distinct functional properties.* J Biol Chem, 2000. **275**(5): p. 3305-12.

157. Besant, P.G., et al., *Inhibition of branched-chain alpha-keto acid dehydrogenase kinase and Sln1 yeast histidine kinase by the antifungal antibiotic radicicol.* Mol Pharmacol, 2002. **62**(2): p. 289-96.
158. Kato, M., et al., *Distinct structural mechanisms for inhibition of pyruvate dehydrogenase kinase isoforms by AZD7545, dichloroacetate, and radicicol.* Structure, 2007. **15**(8): p. 992-1004.
159. Corbett, K.D. and J.M. Berger, *Structural basis for topoisomerase VI inhibition by the anti-Hsp90 drug radicicol.* Nucleic Acids Res, 2006. **34**(15): p. 4269-77.
160. Neckers, L. and S.P. Ivy, *Heat shock protein 90.* Curr Opin Oncol, 2003. **15**(6): p. 419-24.
161. Bellon, S., et al., *Crystal structures of Escherichia coli topoisomerase IV ParE subunit (24 and 43 kilodaltons): a single residue dictates differences in novobiocin potency against topoisomerase IV and DNA gyrase.* Antimicrob Agents Chemother, 2004. **48**(5): p. 1856-64.
162. Goetz, M.P., et al., *Phase I trial of 17-allylamino-17-demethoxygeldanamycin in patients with advanced cancer.* J Clin Oncol, 2005. **23**(6): p. 1078-87.
163. Ramanathan, R.K., et al., *Phase I Pharmacokinetic-Pharmacodynamic Study of 17-(Allylamino)-17-Demethoxygeldanamycin (17AAG, NSC 330507), a Novel Inhibitor of Heat Shock Protein 90, in Patients with Refractory Advanced Cancers.* Clin. Cancer Res., 2005. **11**(9): p. 3385-3391.
164. Price, J.T., et al., *The heat shock protein 90 inhibitor, 17-allylamino-17-demethoxygeldanamycin, enhances osteoclast formation and potentiates bone metastasis of a human breast cancer cell line.* Cancer Res, 2005. **65**(11): p. 4929-38.
165. Yano, A., et al., *Inhibition of Hsp90 activates osteoclast c-Src signaling and promotes growth of prostate carcinoma cells in bone.* Proc Natl Acad Sci U S A, 2008. **105**(40): p. 15541-6.
166. Smith, J.R. and P. Workman, *Targeting CDC37: an alternative, kinase-directed strategy for disruption of oncogenic chaperoning.* Cell Cycle, 2009. **8**(3): p. 362-72.
167. Holmes, J.L., et al., *Silencing of HSP90 cochaperone AHA1 expression decreases client protein activation and increases cellular sensitivity to the HSP90 inhibitor 17-allylamino-17-demethoxygeldanamycin.* Cancer Res, 2008. **68**(4): p. 1188-97.
168. Powers, M.V., P.A. Clarke, and P. Workman, *Dual targeting of HSC70 and HSP72 inhibits HSP90 function and induces tumor-specific apoptosis.* Cancer Cell, 2008. **14**(3): p. 250-62.
169. Smith, J.R., et al., *Silencing the cochaperone CDC37 destabilizes kinase clients and sensitizes cancer cells to HSP90 inhibitors.* Oncogene, 2008.
170. Kamal, A., et al., *A high-affinity conformation of Hsp90 confers tumour selectivity on Hsp90 inhibitors.* Nature, 2003. **425**(6956): p. 407-10.
171. Workman, P., *Altered states: selectively drugging the Hsp90 cancer chaperone.* Trends Mol Med, 2004. **10**(2): p. 47-51.
172. Le Brazidec, J.Y., et al., *Synthesis and biological evaluation of a new class of geldanamycin derivatives as potent inhibitors of Hsp90.* J Med Chem, 2004. **47**(15): p. 3865-73.

173. Stepanova, L., et al., *Induction of human Cdc37 in prostate cancer correlates with the ability of targeted Cdc37 expression to promote prostatic hyperplasia.* Oncogene, 2000. **19**(18): p. 2186-93.
174. Pascale, R.M., et al., *Role of HSP90, CDC37, and CRM1 as modulators of P16(INK4A) activity in rat liver carcinogenesis and human liver cancer.* Hepatology, 2005. **42**(6): p. 1310-9.
175. Stepanova, L., et al., *Mammalian p50(Cdc37) is a protein kinase-targeting subunit of Hsp90 that binds and stabilizes Cdk4.* Genes Dev., 1996. **10**: p. 1491-1502.
176. Stepanova, L., et al., *The oncoprotein kinase chaperone CDC37 functions as an oncogene in mice and collaborates with both c-myc and cyclin D1 in transformation of multiple tissues.* Mol Cell Biol, 2000. **20**(12): p. 4462-73.

Table 1.1 Hsp90 inhibitors block the ATP binding sites of Hsp90 and other ATPases

	Hsp90	TRAP1	Sln1	PDK	Topo VI	Gyrase B
Geldanamycin	Inhibit	Inhibit				
Radicicol	Inhibit		Inhibit	Inhibit	Inhibit	
Novobiocin	Inhibit				Inhibit	Inhibit

Figure 1.1 Chemical structures of Hsp90 N-terminal ATP binding site inhibitors

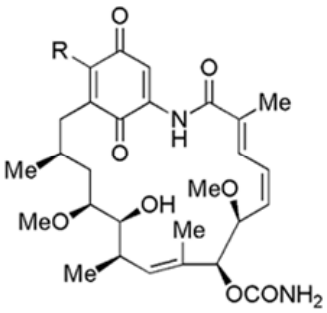

Geldanamycin R = OCH_3
17-AAG R = $NHCH_2CH{=}CH_2$
17-DMAG R = $NHCH_2CH_2N(CH_3)_2$

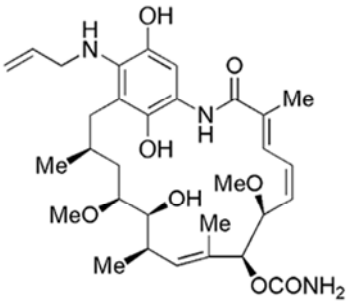

IPI-504

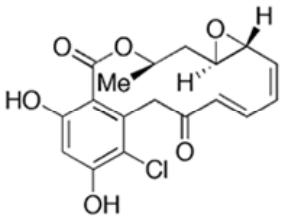

Radicicol

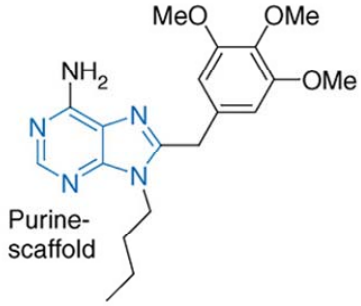

PU3

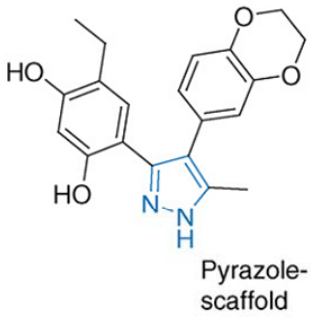

CCT018159

Figure 1.2 Hsp90 status in normal and cancer cells

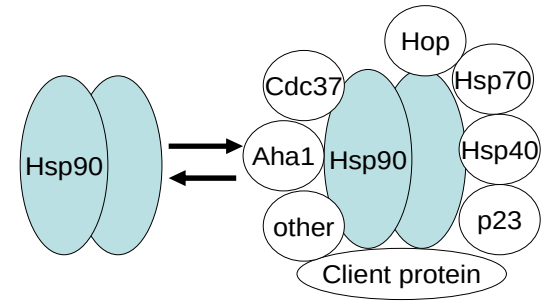

Native form	Super-chaperone complex
In normal cells	In cancer cells
Low 17-AAG affinity	High 17-AAG affinity
Low ATPase	High ATPase

Figure 1.3 Novel Hsp90 inhibitors to disrupt Hsp90/p50Cdc37 complex

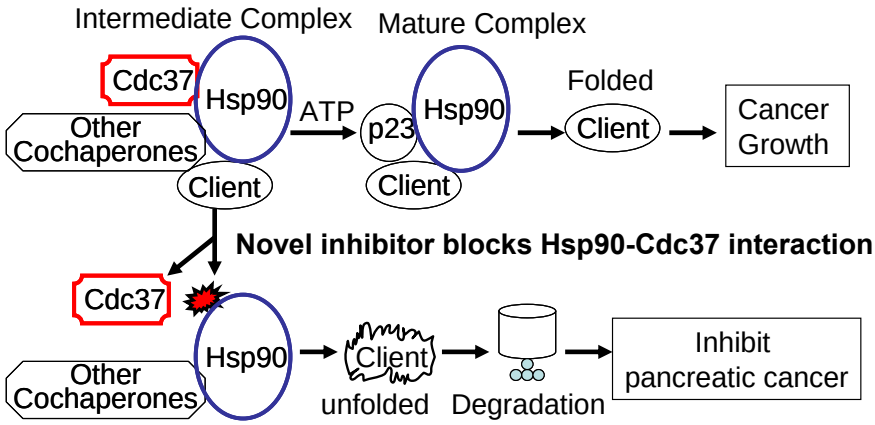

CHAPTER 2

A Novel Hsp90 Inhibitor to Disrupt Hsp90/p50Cdc37 Complex against Pancreatic Cancer Cells

2.1 Abstract

Pancreatic cancer is an aggressive disease with multiple biochemical and genetic alterations. Thus, a single agent targeting one molecule/signaling cascade may not be sufficient to treat this disease. The purpose of this study is to identify a novel Hsp90 inhibitor to disrupt protein-protein interactions in the Hsp90 multichaperone complex and, as a result, inhibit chaperoning function and exert antitumor effect against pancreatic cancer cells. Here, we reported that celastrol, a quinone methide triterpene purified from tripterygium wilfordii Hook F., disrupted the Hsp90/p50Cdc37 complex. Molecular docking and molecular dynamic simulations showed that celastrol blocked the critical interaction between Glu33 of Hsp90 and Arg167 of p50Cdc37. Immunoprecipitation confirmed that celastrol (10 μM) disrupted the Hsp90 and p50Cdc37 interaction in the pancreatic cancer cell line Panc-1. Different from a classical Hsp90 inhibitor (geldanamycin), celastrol (0.1-100 μM) did not interfere with ATP binding to Hsp90. Nevertheless, celastrol (1-5 μM) also induced Hsp90 client protein degradation. Celastrol resulted in cell apoptosis *in vitro* and significantly inhibited Panc-1 xenograft growth in nude mice. Moreover, celastrol (3 mg/kg) effectively suppressed tumor metastasis by more than 80% in a RIP-Tag2 transgenic mouse model with pancreatic islet cell

carcinogenesis. The data suggest that celastrol is a novel Hsp90 inhibitor that can disrupt the Hsp90/p50Cdc37 complex against pancreatic cancer cells.

2.2 Introduction

Pancreatic cancer is the fourth leading cause of cancer death in the United States [1]. The overall 5-year survival rate for pancreatic cancer patients is only 4% due to the lack of effective treatments [2]. Currently, targeted therapy against a malfunctioning molecule or pathway has produced promising results for various solid tumors, such as gefitinib® against lung cancer, avastin® and ebitux® against colon cancer, herceptin® against breast cancer, and SU-011248 against kidney cancer [3, 4]. However, clinical trials using antibodies against EGFR, VEGF, and HER2 in pancreatic cancer have had minimal benefits [5-7]. Considering that pancreatic cancer possesses multiple genetic abnormalities, targeting a single pathway is unlikely to be effective. Thus, identification of new targets that modulate multiple signaling pathways is anticipated for treating pancreatic cancer.

Targeting molecular chaperone Hsp90 may offer significant advantages due to its simultaneous regulation of various oncogenic proteins [8, 9]. Most of Hsp90 client proteins (eg, HER-2/neu, EGFR, Akt, Cdk4, Bcr-Abl, p53, Raf-1) are essential for cancer cell survival and proliferation [9]. These client proteins are chaperoned by Hsp90 through a dynamic cycle driven by ATP binding and subsequent hydrolysis [10]. Hsp90 requires various cochaperones, such as Cdc37, Hsp70, Hsp40, Hop, Hip, p23, pp5, and immunophilins, for its function. These cochaperones bind to and release from the multichaperone complex at various times to regulate the folding, assembly, and maturation of client proteins [10]. The well known Hsp90 inhibitors such as

geldanamycin (GA) and its derivative 17-allyamino-geldanamycin (17AAG) blocks ATP binding to Hsp90 [10]. This blockage causes the catalytic cycle of Hsp90 to arrest in the ADP-bound conformation, subsequently leads to premature release and degradation of client proteins [10]. This strategy has shown promising results and 17-AAG are now in clinical trial for different cancers [11].

However, all current Hsp90 inhibitors in the clinic work employ the same mechanism of ATP blockage to inhibit its function. Therapeutic limitations have been noticed, such as hepatotoxicity and development of multidrug resistance [12]. So far, none of these inhibitors has received the FDA approval. It would be premature to conclude that the strategy of blocking the ATP binding to Hsp90 is a viable approach for developing Hsp90 inhibitors. In addition, many compounds which can inhibit Hsp90 function would be excluded during drug screening simply because they could not bind to the ATP pocket. Since the Hsp90 chaperoning process involves the transient formation of multiprotein complexes with cochaperones, halting the chaperoning cycle at various stages is also likely to achieve Hsp90 inhibition. Thus, we hypothesize that disrupting the interaction of Hsp90 with its cochaperones will achieve Hsp90 inhibition against cancer cells.

One of the essential cochaperones is p50Cdc37, which loads client proteins to Hsp90 [13, 14]. In the present study, we intend to identify an Hsp90 inhibitor which disrupts the Hsp90 and p50Cdc37 interaction to treat pancreatic cancer. We hypothesize that disruption of Hsp90 and p50Cdc37 interaction, without affecting ATP binding to Hsp90, should exhibit similar anticancer effects with GA/17AAG treatment. Previous studies have shown that celastrol (Figure 2.1A), a quinone methide triterpene purified

from tripterygium wilfordii Hook F., modulates Hsp90 signaling pathway and induces heat shock response similar to other Hsp90 inhibitors [15, 16]. We find that celastrol did not affect ATP binding to Hsp90. Molecular docking results showed that celastrol blocked p50Cdc37 binding to Hsp90, which was confirmed by co-immunoprecipitation in pancreatic cancer cell line Panc-1 cells. Celastrol treatment resulted in Hsp90 client proteins degradation and induced apoptosis in Panc-1 *in vitro*. Moreover, celastrol exhibited anticancer activity in Panc-1 xenograft model and RIP1-Tag2 transgenic mice with islet tumors *in vivo*. These data provide a novel strategy of Hsp90 inhibition through disruption of Hsp90/cochaperone complex, providing an alternative strategy of developing Hsp90 inhibitors against cancers.

2.3 Materials and Methods

2.3.1 Drugs and reagents

Celastrol was purchased from Cayman Chemical (Ann Arbor, MI), proteasome inhibitor MG132 from Calbiochem, Inc. (San Diego, CA), and lactacystin from Sigma-Aldrich (St.Louis, MO). Geldanamycin (GA) was kindly provided by Dr George Wang from Department of Chemistry in the Ohio State University. The following antibodies were used for immunoblotting: Akt, Hsp90 (Cell Signaling, Beverly, MA), Hsp70, Hop (StressGen, Victoria, BC, Canada), Cdk4, Cdc37, IκB-α, p27, Hsp90 (Santa Cruz, Santa Cruz, CA), actin, and p23 (Abcam, Cambridge, MA). Monoclonal Hsp90 antibody H9010 and purified Hsp90β protein were kind gifts of Dr. David Toft (Mayo Clinic, Rochester, MN).

2.3.2 Molecular modeling

The initial coordinates of the human Hsp90 protein used in our computational studies came from the X-ray crystal structure (1US7.pdb) [17] deposited in the Protein Data Bank [18]. For comparison, the yeast Hsp90-p23/Sba1 X-ray structure 2CG9.pdb was also used [19]. Using these proteins, we carried out molecular docking, molecular dynamics (MD) simulations, and protein-ligand binding free energy calculations.

To explore the possible Hsp90-ligand binding mode, the first step is to identify the residues in the interface between Hsp90 and p50Cdc37 in the Hsp90/p50Cdc37 complex and to dock celastrol to the Hsp90 N-terminal domain. We aim to find the site dwhere celastrol could be most comfortably inserted. The molecular docking for each possible Hsp90-celastrol binding mode was carried out as previously described [20]. Briefly, a celastrol-binding site was defined within the residues at the interface of Hsp90/p50Cdc37 complex and centered on the lid segment of Hsp90. Celastrol was initially positioned ~10 Å in front of an attempted binding site. The initial docking calculations were performed on celastrol with the N-terminal Hsp90 binding site using the '*automatic docking*' Affinity module of the InsightII package (Accelrys, Inc., San Diego, CA). The Affinity methodology uses a combination of Monte Carlo type and Simulated Annealing (SA) procedure to dock the guest molecule (celastrol) to the host (Hsp90) [21]. The Hsp90-ligand binding structure obtained from the initial docking was further refined by performing a molecular dynamics (MD) simulation in water.

Each binding complex simulated in this study was neutralized by adding an appropriate number of sodium counterions and was solvated in a rectangular box of TIP3P water molecules with a minimum solute-wall distance of 10 Å [22]. The partial

atomic charges for celastrol were obtained after geometry optimizations at the HF/6-31G* level and subsequent single-point calculations of the electrostatic potential, to which the charges were fitted using the RESP procedure [23, 24]. Force field parameters of celastrol were assigned based on the atom types of the force field model developed by Cornell *et al*. [24]. Gaussian03 program was used to optimize the geometries and generate electrostatic potentials. The MD simulation was performed by using the Sander module of the Amber8 program (University of California, San Francisco) in a way similar to what we performed for other protein-ligand systems [20]. Each of the solvated systems was carefully equilibrated before a sufficiently long MD simulation in room temperature. The MD simulations were performed with a periodic boundary condition in the NPT ensemble at T = 298.15 K with Berendsen temperature coupling and constant pressure (P = 1 atm) with the isotropic molecule-based scaling. The SHAKE algorithm was applied to fix all covalent bonds containing a hydrogen atom, a time step of 2 fs was used, and the non-bond pair list was updated every 10 steps [25]. The particle mesh Ewald (PME) method was used to treat long-range electrostatic interactions. A residue-based cutoff of 10 Å was applied to the non-covalent interactions [26].

The obtained stable MD trajectory was used to estimate the binding free energy (ΔG_{bind}) by using the molecular mechanics/Poisson-Boltzmann surface area (MM-PBSA) free energy calculation method [27]. 100 snapshots were used to perform the MM-PBSA calculation. Our MM-PBSA calculation for each snapshot was carried out in the same way as we did for other protein-ligand systems [20]. The finally calculated binding free energy was taken as the average of the ΔG_{bind} values with the 100 snapshots.

Most of the MD simulations in water were performed on a HP supercomputer, Superdome, at the Center for Computational Sciences, University of Kentucky. The other computations were carried out on SGI Fuel workstations and a 34-processors IBM x335 Linux cluster in our own lab.

2.3.3 MTS assay

The human Panc-1 cells were seeded in 96-well plate at a density of 3000-5000 cells per well. Twenty-four hours later cells were treated with increasing concentrations of either celastrol or GA as indicated. The viable cells were assessed by MTS assay after 24 h. The IC_{50} values for cytotoxicity were calculated with WinNonlin software (Pharsight, Mountain View, CA).

2.3.4 Annexin V-EGFP assay

Control cells and cells treated with 5μM of celastrol were stained with Annexin V-EGFP for analysis of phosphoserine inversion. The Annexin V-EGFP Apoptosis Detection Kit was obtained from BioVision Research Products (Mountain View, CA). The staining was performed according to the manual from manufacturer.

2.3.5 ATP-Sepharose binding assay

The assay was performed as previously described [28]. Briefly, 5μg of human hsp90β protein was pre-incubated on ice in 200 μl incubation buffer (10 mM Tris-HCl, 50 mM KCl, 5 mM $MgCl_2$, 2 mM DTT, 20 mM Na_2MoO_4, 0.01% Nonidet P-40, pH 7.5) containing celastrol or GA. Following incubation, 25 μl of pre-equilibrated γ-phosphate-linked ATP-Sepharose (Jena Bioscience GmbH, Jena, Germany) was added and

incubated at 37 °C for 30 min with frequent agitation. Sepharose was subsequently washed and analyzed by SDS-PAGE.

2.3.6 Western blotting and immunoprecipitation

The procedure for the Western blot analysis was briefly described as follows. After drug treatment, cells were washed twice with ice-cold phosphate-buffered saline (PBS), collected in lysis buffer (20 mM Tris, pH 7.5, 1% Nonidet P-40, 150 mM NaCl, 5mM EDTA, 1 mM Na_3VO_4) supplemented with protease inhibitor mixture (Sigma, added at a 1:100 dilution), and incubated on ice for 20 min. The lysate was then centrifuged at 14,000 × *g* for 10 min. Equal amounts of protein were subjected to SDS-PAGE, transferred onto nitrocellulose membranes, and probed with appropriate antibodies. Immunoprecipitation was done as previously described [16].

2.3.7 Nude mice xenograft model

Four to six-week old nu/nu athymic female mice were obtained from Charles River Laboratories (Charles River, Wilmington, MA). The human Panc-1 cells ($5\text{-}10\times10^6$) were mixed with reconstituted basement membrane (Collaborative Research, Bedford, MA) and implanted s.c. to the right and left flanks of the mice. Tumor volumes were calculated with the formula: $\text{width}^2\times\text{length}/2$. When tumors reached 100 mm^3, animals were randomized into different groups for treatment (n= 6/group).

Celastrol and GA were dissolved in the vehicle (10% DMSO, 70% Cremophor/ethanol (3:1), and 20% PBS) [29], and administered at 3 mg/kg by i.p. injection for two continuous days. Then the dosing schedule was changed to one injection per three days. Tumor sizes and body weights were measured twice a week.

2.3.8 RIP1-Tag2 transgenic mice model

RIP1-Tag2 transgenic mice express the insulin promoter-driven SV40 T-antigen and produce spontaneous multifold and multistage pancreatic islet carcinomas. RIP1-Tag2 positive mice were identified by PCR analysis of genomic DNA from tail biopsy. Positive mice of 8-week age were randomly divided into 3 groups and injected with vehicle, 3mg/kg celastrol or GA once every three days. After 4 weeks of injection, some mice from each group were sacrificed and tumor tissues were collected. The remaining mice were monitored to calculate the survival rate.

2.4 Results

2.4.1 Molecular docking of celastrol for the interactions with Hsp90

To investigate whether celastrol disrupts Hsp90 and p50Cdc37 interaction, we first tested whether celastrol could bind Hsp90 residues located at the interface of the Hsp90/p50Cdc37 complex, or the ATP-binding pocket of Hsp90 (Figure 2.2B). *In silico* molecular modeling was used to reveal how celastrol binds to Hsp90 and predict the corresponding Hsp90-ligand binding energy.

To explore the best possible mode of celastrol binding with Hsp90, we first performed molecular docking. Then, simulated annealing (SA) and molecular dynamic (MD) simulations were carried out on a variety of possible protein-ligand binding structures. The simulated protein-ligand binding structures were used to for calculating binding free energy. The most favorable structure of the ligand binding with Hsp90 had a binding energy of -18.8 kcal/mol, excluding the entropic contribution [20]. The *in silico* model of the Hsp90-celastrol binding and the subsequent MD simulation showed that celastrol formed a favorable complex with Hsp90 in a binding site distinct from the ATP-

binding pocket (Figure 2.3C). MD trajectory of the optimum docking model revealed that the distances between celastrol and the key residues in the Hsp90 binding site were found to be stable after the first 0.5 ns of the MD simulation (Figure 2.4D). The cyclohexa dienone moiety of celastrol was bound to a polar groove of Hsp90 that was defined by several residues in the lid segment (residues #94 to #125) and the mouth of the nucleotide-binding pocket. Thus, the hydroxyl and carbonyl groups of celastrol protruded into a polar and charged pocket which was surrounded by the side chains Gln119, Glu33, Arg32, and Gly118 (Figure 2.5E&F). In addition, these groups occupied the positions suitable for the formation of an H-bond between Glu33 and the NH group of the Gly118 backbone, while the carboxyl moiety of celastrol formed two other H-bonds with the side chains of Arg32 and His197.

2.4.2 Molecular modeling of Hsp90/celastrol complex with p50Cdc37

We further examined whether the mode of celastrol binding to the new binding site of Hsp90 could disrupt Hsp90/p50Cdc37 complex. Hsp90/celastrol complex was superimposed on the Hsp90/p50Cdc37 crystal structure to replaced Hsp90. This new complex was submitted to a long MD simulation (~4 ns). The simulated (Hsp90/celastrol)/p50Cdc37 complex was depicted in Figure 2.6G. Celastrol was found in the mouth of the nucleotide binding pocket. The three strongest H-bonds stabilizing celastrol in this orientation were still formed by the side chain of Arg32, Glu33, and Gly118 residues. As mentioned above, celastrol filled the binding pocket by forming a π-π stacking interaction with Arg32. The carboxylate of celastrol was involved in a network of H-bonds with the Arg32 and His197 side chains. The results showed that celastrol induced a major conformational change in the binding pocket which disrupted an

essential H-bond interaction between Arg167 of p50Cdc37 and Glu33 of Hsp90. This should significantly decrease the binding affinity of p50Cdc37 cochaperone to its cognate Hsp90, and thus disrupt the Hsp90 and p50Cdc37 interaction.

In the Hsp90 superchaperone complex, the current understanding of the Hsp90/p23 interaction depicts p23 binding to the mature complex of Hsp90 [9]. To predict whether celastrol prevents the interaction of Hsp90 and p23 (Sba1) cochaperone, we superimposed the Hsp90/celastrol complex with the X-ray structure of the Hsp90/p23 interaction (Figure 2.7H). The results showed that the formation of the Hsp90/celastrol complex requires the lid segment residues being close to residues #26 to #33. Hsp90 protein existed in two remarkably different conformations in the available X-ray crystal structures. In the structures reported for both free Hsp90 protein and Hsp90/p50Cdc37 complex, the lid segment residues were close to residues #26 to #33, similar to Hsp90/celastrol complex. In the structure of Hsp90/p23 complex, Hsp90 was in a different conformation in which the lid segment was completely displaced and was close to residues #36 to #50. Moreover, the aforementioned celastrol-binding pocket of Hsp90 is filled by residues #376 to #385 on the Hsp90 C-terminal in Hsp90/p23 complex. The conformation of Hsp90 in the Hsp90/ p23 complex is clearly not suitable for binding with celastrol. Hence, celastrol is not expected to disrupt the Hsp90/p23 complex.

2.4.3 Celastrol has no effect on ATP binding to Hsp90

The molecular docking results showed that celastrol disrupted Hsp90 and p50Cdc37 interaction without blocking the nucleotide binding pocket of Hsp90. To further confirm this finding, we employed the ATP-Sepharose pull-down assay using purified human Hsp90β protein. As shown in Figure 2.2A, ATP-Sepharose beads

successfully pulled down Hsp90 in the solution. GA has been reported to block the ATP binding pocket of Hsp90. We also found that 1 μM of GA was able to block more than 90% of ATP binding to Hsp90β. In contrast, celastrol (0.1 to 100 μM) did not have an effect on ATP binding. This result provides further evidence that celastrol functioned differently from classic Hsp90 inhibitors (GA).

2.4.4 Celastrol disrupts Hsp90/p50Cdc37 complex in pancreatic cancer cells

Hsp90 has interaction with various cochaperones at different stages of the catalytic cycle. Current studies have suggested that Hsp90, p50Cdc37, and Hop co-exist with Hsp90 in the intermediate complex [13, 30]. To confirm the molecular modeling results that celastrol disrupts Hsp90/p50Cdc37 complex, we did immunoblotting of p50Cdc37 and Hop after immunoprecipitation of Hsp90. As shown in Figure 2.2B, immunoprecipitation of Hsp90 did pull down p50Cdc37 and Hop as detected by Western blotting, suggesting that Hsp90/p50Cdc37 and Hsp90/Hop may exist in a complex. Celastrol (10 μM) decreased the amount of p50Cdc37 dramatically in the immunoprecipitated Hsp90 complex as early as 1 h after treatment, however, celastrol did not affect Hsp90 and Hop interaction which was indicated by the unchanged amount of Hop. In contrast, GA (10 μM) did not change the level of either Hop or p50Cdc37 in immunoprecipitated Hsp90 complex. These results indicate that celastrol acts differently from GA by inhibiting Hsp90 via disruption of the Hsp90/p50Cdc37complex. The unchanged levels of Hop and p50Cdc37 in the immunoprecipitated complex after GA treatment further confirmed that p50Cdc37 and Hop coexist in the intermediate Hsp90 superchaperone complex.

Unlike p50Cdc37, p23 is believed to be a member of the mature multichaperone complex after ATP binding [28, 31, 32]. To confirm our molecular docking results that the Hsp90/p23 complex could not accommodate celastrol binding, we performed Western blotting analysis of p23 after Hsp90 immunoprecipitation. Anti-Hsp90 antibody was able to pull down p23, indicating their interaction (Figure 2.3A). Interestingly, after 24 h of celastrol treatment, p23 was still present in the immunoprecipitated Hsp90 complex (Figure 2.3A). The presence of Hsp90/p23 complex after celastrol treatment was further confirmed after immunoprecipitation of p23 (Figure 2.3B), suggesting that celastrol does not disrupt Hsp90/p23 complex in pancreatic cancer cells. Since GA locks Hsp90 in the intermediate complex with Hop and p50Cdc37, as a comparison, Hsp90 is unlikely to bind p23 after GA treatment. Indeed, GA excluded p23 in the immunoprecipitated Hsp90 complex (Figure 2.3A), and excluded Hsp90 after immunoprecipitation of p23 (Figure 2.3B). These data suggest that celastrol shows a different mechanism of Hsp90 inhibition compared to GA.

2.4.5 p23 does not co-exist with p50Cdc37 or Hop in one complex

Our data showed that celastrol and GA treatment led to distinct results, in which celastrol disrupted the Hsp90/p50Cdc37 complex. Since GA has been reported to lock Hsp90 in the intermediate complex without Hsp90 and p23 interaction, we intend to further elucidate the sequence of protein-protein interaction for Hsp90/p50Cdc37 and Hsp90/p23. We used antibodies against p50Cdc37, Hop, and Hsp90 to detect protein levels after p23 immunoprecipitation. The results showed that Hsp90 was detected in the immunoprecipitated p23 complex, while neither Hop nor p50Cdc37 was detected (Figure 2.3C). These results suggest that p50Cdc37 and Hop do not co-exist with p23 in the

Hsp90 superchaperone complex. This further confirms that p50Cdc37 and Hop are in the intermediate complex of Hsp90 while p23 is in the mature complex. Our data is in agreement with the recent crystal structure of Hsp90/p50Cdc37 and Hsp90/p23. The structural analysis has revealed that p50Cdc37 binds to the N-terminal nucleotide-binding domain of Hsp90 and arrests the chaperoning cycle in the conformation that could inhibit the binding of p23 to Hsp90 [17]. Subsequently, *in vitro* difference circular dichroism suggests that binding of p23 and p50Cdc37 to Hsp90 is mutually exclusive [33].

2.4.6 Celastrol decreases Hsp90 client protein levels

Since celastrol resulted in the dissociation of p50Cdc37 from Hsp90, we next tested whether the compound could inhibit Hsp90 function and induce the degradation of its client proteins in pancreatic cells (Panc-1). Panc-1 cells were treated with various concentrations of celastrol or GA. The protein levels of Akt and Cdk4, two well-known Hsp90 clients [34, 35], were measured. Celastrol decreased the protein levels of Akt and Cdk4 in a time- and concentration-dependent manner. A 24-h treatment of Panc-1 cells with 1 μM celastrol slightly decreased Akt and Cdk4, but 5 μM celastrol was able to decrease Akt and Cdk4 by 80% and 70%, respectively (Figure 2.4A and B). Similarly, GA induced similar levels of Akt and Cdk4 degradation (Figure 2.4A). These data suggest that celastrol can induce Hsp90 client protein degradation, albeit via a different mechanism.

In addition, GA generally has no effect on the levels of Hsp90, but induces Hsp70 protein expression. Western blotting analysis confirmed that neither celastrol nor GA had any effect on Hsp90 protein levels. On the contrary, both celastrol (5 μM) and GA (5 and

10 μM) were able to increase Hsp70 protein expression by more than 12-fold after 24 h (Figure 2.4C).

2.4.7 Celastrol inhibits Panc-1 cell growth and induces apoptosis

Pancreatic cancer cells are usually resistant to various chemotherapeutic compounds. We selected the pancreatic cancer cell line (Panc-1) to test the anticancer effect of celastrol. MTS assay showed that celastrol exhibited stronger anticancer activity (IC_{50} = 3 μM) than GA (IC_{50} = 8 μM) (Figure 2.5A). Annexin-V staining indicated that celastrol (5 μM) induced apoptosis in approximately 15% to 40% of pancreatic cancer cells after one to five hours incubation (Figure 2.5B). Pancreatic cancer cells became rounded and congregated after incubation with celastrol as early as 1 hour after drug treatment.

2.4.8 Celastrol shows strong anticancer activity *in vivo*

Since celastrol showed anticancer activity against pancreatic cancer cells *in vitro*, we then tested its activity *in vivo* with two animal models.

In Panc-1 cell xenograft mice, celastrol inhibited 80% of tumor growth ($p<0.001$) after the last injection (Figure 2.5C). The anticancer effect of celastrol was slightly better than that of GA. Three weeks after the last injection, the average tumor size of the control group reached over 500 mm^3, while the tumor size in celastrol treatment group was four- to five-fold smaller than the control group. It is worth noting that celastrol treatment caused 5% of weight loss in mice (data not shown).

We next used the RIP1-Tag2 transgenic mouse model of pancreatic islet carcinogenesis. Although pancreatic islet cell carcinoma are rare tumors with approximately 1 in 100 000 population, representing only 1-2% of all pancreatic

neoplasms, they are quite resistant to standard therapy [36]. The RIP1-Tag2 transgenic mice expressing multistage islet and metastatic tumors have served as a good animal model for studying pancreatic endocrine tumors. In the positive mice, hyperplastic islets begin to appear by 3-4 weeks of age, and solid tumors emerge in the pancreas at about 8-9 weeks. The tumors usually metastasize to other sites such as mesenterium in the peritoneal cavity at 10-12 week. We found that celastrol treatment decreased metastatic tumors in the mesenterium by 80% ($P < 0.05$) compared to the control group after four-week treatment (Figure 2.5D&E). In comparison, GA inhibited metastatic tumors in the mesenterium by 50% ($P < 0.05$) (Figure 2.5D&E).

The RIP1-Tag2 transgenic mice generally have a life span of 11-13 weeks due to pancreatic tumor burden and related symptoms. Surprisingly, the inhibitory effect of celastrol on tumor growth led to a significant life prolongation. As shown in Figure 2.5F, the median survival time for control and celastrol treatment group was 84 and 96 days, representing an average increase of 12 days ($P < 0.001$). The GA treatment group only increased survival by 6 days ($P < 0.001$). These data indicate that celastrol can inhibit the proliferation and metastasis of pancreatic islet carcinomas. Again it is worth noting that celastrol resulted in a 10% weight loss for the mice (data not shown).

2.4.9 Celastrol is different from other proteasome inhibitors

To test whether celastrol also inhibited the proteasome, we measured two well-known client proteins (p27 and IκB-α) of proteasome in pancreatic cancer cells [37, 38]. The results showed that celastrol rendered the accumulation of cyclin-dependent kinase inhibitor p27 and IκB-α (Figure 2.6A). Interestingly, GA also showed a similar effect as celastrol for the protein levels of p27 and IκB-α (Figure 2.6A). To distinguish celastrol

from other proteasomal inhibitors, we next compared celastrol with two well-known proteasome inhibitor MG132 and lactacystin [39, 40] for their effect on Hsp90 client proteins (Akt and Cdk4). Different from celastrol, MG132 or lactacystin (10 μM) did not change the levels of the Cdk4 and Akt proteins (Figure 2.6B). MTS assay was used to show the anti-proliferation effect (Figure 2.6B). These results suggest that celastrol, which inhibits Hsp90-Cdc37 interaction, is distinct from other proteasome inhibitors.

2.5 Discussion

Targeted therapy appears to be an attractive approach for cancer therapy since it specifically targets malfunctioning proteins and signaling pathways [41]. However, how to inhibit multiple molecules and pathways remains a major challenge since cancer is usually present with multiple mutations. The Hsp90 protein has emerged as a promising target due to the regulation of many oncogenic proteins [9]. In human pancreatic cancer, Hsp90 is expressed 6- to 7-fold higher than normal tissues [42]. Recent data have revealed that Hsp90 inhibitor (GA) has exhibited anti-tumor effect in nude mice implanted with human pancreatic cancer cells in combination with the glycolysis inhibitor [43].

Hsp90 protein is a weak ATPase and its function depends on the ability to bind and hydrolyze ATP [44]. The early Hsp90 inhibitors represented by GA, herbinmycin A and radicicol, target at the N-terminal nucleotide binding domain [45, 46]. Many studies have focused on this mechanism and these naturally occurring compounds, producing GA derivatives (such as 17-AAG) [47], or synthesizing new compounds with similar binding capacity, e.g., CCT018159 [48]. Considering the side effects like hepatotoxicity and

induction of heat shock response, it is premature to conclude that targeting the ATP binding sites is a viable strategy for Hsp90 inhibition.

In the current study, we provided evidence of a novel Hsp90 inhibitor which disrupts protein-protein interaction in the Hsp90 superchaperone complex without blocking ATP binding. Celastrol disrupts the Hsp90/p50Cdc37 complex and leads to the degradation of Hsp90 client proteins. Celastrol exhibits anti-pancreatic tumor activity both *in vitro* and *in vivo*. This class of compounds may offer a new strategy to develop Hsp90 inhibitors for treatment of pancreatic cancers.

The Hsp90 multichaperone complex cycle has been studied extensively [10, 49]. A client protein first binds to the Hsp70/Hsp40 complex, followed by Hop recruits the "open" state Hsp90 to the Hsp70/Hsp40/client complex. The binding of ATP alters Hsp90 conformation and results in the "closed" state. Hsp70, Hsp40 and Hop are subsequently released and replaced by another set of cochaperones including p23 and immunophilins. With regard to the cochaperone p50Cdc37, the Hsp70/Hsp40 complex prepares the kinase for interacting with p50Cdc37, and then p50Cdc37 recruits Hsp90 to the complex [13, 30, 50]. However, upon ATP binding, it remains unclear whether p50Cdc37 dissociates before p23 binding. Our immunoprecipitation data suggest that p23 does not coexist with either p50Cdc37 or Hop (Fig. 3C). The recent structural study of Hsp90/p50Cdc37 has demonstrated that p50Cdc37 binds to the N-terminal domain of Hsp90 by inserting its C-terminal side chain into the nucleotide binding pocket, holding Hsp90 in an "open" conformation [17]. Therefore, progression from this stage to complete the ATPase cycle may require the ejection of p50Cdc37 side chain from the binding pocket [17]. *In vitro* protein binding analysis also suggests that binding of

p50Cdc37 and p23 to Hsp90 is mutually exclusive and the p23/Hsp90/p50Cdc37 complex could not exist [33]. All these data imply that p50Cdc37 dissociates from the Hsp90 multichaperone complex after ATP binding. Moreover, p50Cdc37 and p23 bind at different stages in the chaperoning cycle.

It has been proved that GA locks Hsp90 at the client protein loading phase [9]. Therefore, GA effectively halts the chaperoning cycle and leads to proteasomal degradation of client protein [9, 10]. Consistent with these findings, our data showed that GA inhibited the binding of ATP to Hsp90 (Figure 2.2A). Incubating pancreatic cancer cells with GA led to degradation of Hsp90 client proteins (Akt and Cdk4) (Figure 2.4A). Since GA locks Hsp90 in the intermediate complex, Hsp90 is unlikely to proceed to the subsequent stage to bind p23 [28, 31, 32]. Consistently, the Hsp90/p23 complex was not detected in Panc-1 cells after GA treatment (Figure 2.3A&B), which is also supported by previous studies showing that p23 only binds to ATP-bound form of Hsp90. However, the Hsp90/p50Cdc37 or Hsp90/Hop complex showed no change before and after GA treatment (Figure 2.2B), indicating that both p50Cdc37 and Hop may bind with Hsp90 in the intermediate complex.

Different from GA, celastrol has provided a distinct mechanism of Hsp90 inhibition. Our computational modeling and co-immunoprecipitation data confirmed that celastrol interfered with the Hsp90/p50Cdc37 interaction (Figure 2.1G & 2.2B). As a consequence, Hsp90 clients were not stabilized and thus degraded in a time- and dose-dependent manner (Figure 2.4A&B). However, celastrol did not interrupt the Hsp90/p23 complex in pancreatic cancer cells (Figure 2.3A&B), although different results were reported in SKBR-3 cells [16]. The computer modeling also showed p23 blocked

celastrol's access to its binding site in Hsp90 (Figure 2.1H). Our data and previous studies may explain the sequence cochaperone or nucleotide binding in chaperoning cycle. Previous results have shown that p50Cdc37 C-terminus inserts into the ATP binding pocket of Hsp90 (Open state), and later ATP binding to Hsp90 ejects p50Cdc37 from Hsp90 [17], preparing Hsp90 for p23 binding. Therefore, p50Cdc37 and p23 bind to Hsp90 at different stages of the chaperoning cycle. They are not likely to co-exist in one complex. Disruption of the Hsp90/p50Cdc37 complex by celastrol may not affect the Hsp90/p23 complex.

Recent studies have not only investigated the direct effect of Hsp90 inhibition on on cancer cell survival but also focused on the cellular mechanisms related to tumor invasion and metastasis. Some Hsp90 client proteins can promote cancer invasion and metastasis [51]. It has also been shown that Hsp90 inhibitor GA suppresses extrinsic stimuli-induced signaling pathways contributing to tumor invasion and angiogenesis in T24 bladder carcinoma model [52]. Consistent with those findings, administration of celastrol or GA to RIP1-Tag2 transgenic mice has dramatically reduced the metastatic tumor sizes by 80% and 30%, which are much larger than the reduction in primary pancreatic islet carcinomas (30% and 13%, respectively) (Figure 2.5D&E). The higher dependence on Hsp90 in metastasis may account for the better effect compared with shrinkage of primary tumors. However, further studies are warranted to reveal the underlying mechanism.

It has been reported that celastrol is a proteasome inhibitor [29]. Consistent with that, we also confirmed that celastrol induced the accumulation of proteasomal target proteins p27 and IκB-α in Panc-1 cells (Figure 2.6A). Interestingly, the classical Hsp90

inhibitor GA also showed similar effect (Figure 2.6A). Furthermore, celastrol is different from other proteasome inhibitors (MG132 and lactacystin) by inducing Hsp90 client proteins degradation (Figure 2.6B).

Celastrol has exhibited potent anticancer activity against pancreatic cancer cells (Panc-1) *in vitro* and *in vivo* in xenografts. Celastrol inhibited the tumor metastasis in the RIP-tag2 transgenic mice model with pancreatic islet carcinomas. Computer modeling and immunoprecipitation confirmed that celastrol disrupted the protein-protein interaction of Hsp90 and p50Cdc37, resulting in Hsp90 client protein degradation. In contrast to the classical Hsp90 inhibitor GA, celastrol did not interfere with ATP binding to Hsp90. In conclusion, these data suggest that celastrol disrupts Hsp90/p50Cdc37 complex and provides a novel mechanism of Hsp90 inhibition.

2.6 Acknowledgments

We thank Dr. David Toft for the generous gifts of the purified Hsp90β protein and H9010 antibody to Hsp90. We also thank the Center for Computational Sciences (CCS) at University of Kentucky for support in supercomputing time.

2.7 References

1. Jemal, A., et al., *Cancer statistics, 2007.* CA Cancer J Clin, 2007. **57**(1): p. 43-66.
2. EVANS, D.B., J.L. ABBRUZZESE, and T.R. RICH, *Cancer of the pancreas. In: De Vita VT , Hellman S , Rosenberg SA , editors.* Cancer Principles and Practice of Oncology, 1997: p. 1054-1087.
3. Sawyers, C., *Targeted cancer therapy.* Nature, 2004. **432**(7015): p. 294-7.
4. Iwata, H., *Perspective of trastuzumab treatment.* Breast Cancer, 2007. **14**(2): p. 150-5.
5. Kindler, H.L., et al., *Phase II trial of bevacizumab plus gemcitabine in patients with advanced pancreatic cancer.* J Clin Oncol, 2005. **23**(31): p. 8033-40.

6. Xiong, H.Q., et al., *Cetuximab, a monoclonal antibody targeting the epidermal growth factor receptor, in combination with gemcitabine for advanced pancreatic cancer: a multicenter phase II Trial.* J Clin Oncol, 2004. **22**(13): p. 2610-6.
7. Safran, H., et al., *Herceptin and gemcitabine for metastatic pancreatic cancers that overexpress HER-2/neu.* Cancer Invest, 2004. **22**(5): p. 706-12.
8. Neckers, L., *Hsp90 inhibitors as novel cancer chemotherapeutic agents.* Trends Mol. Med, 2002. **8**: p. 55-61.
9. Kamal, A., M.F. Boehm, and F.J. Burrows, *Therapeutic and diagnostic implications of Hsp90 activation.* Trends Mol Med, 2004. **10**(6): p. 283-290.
10. Neckers, L., *Development of small molecule Hsp90 Inhibitors: utilizing both forward and reverse chemical genomics for drug identification.* Current Medicinal Chemistry, 2003. **10**(9): p. 733-739.
11. Ramanathan, R.K., et al., *Phase I Pharmacokinetic-Pharmacodynamic Study of 17-(Allylamino)-17-Demethoxygeldanamycin (17AAG, NSC 330507), a Novel Inhibitor of Heat Shock Protein 90, in Patients with Refractory Advanced Cancers.* Clin. Cancer Res., 2005. **11**(9): p. 3385-3391.
12. Brandt, G.E. and B.S. Blagg, *Alternate strategies of Hsp90 modulation for the treatment of cancer and other diseases.* Curr Top Med Chem, 2009. **9**(15): p. 1447-61.
13. Pearl, L.H., *Hsp90 and Cdc37 -- a chaperone cancer conspiracy.* Curr Opin Genet Dev, 2005. **15**(1): p. 55-61.
14. Smith, J.R. and P. Workman, *Targeting CDC37: an alternative, kinase-directed strategy for disruption of oncogenic chaperoning.* Cell Cycle, 2009. **8**(3): p. 362-72.
15. Westerheide, S.D., et al., *Celastrols as inducers of the heat shock response and cytoprotection.* J Biol Chem, 2004. **279**(53): p. 56053-60.
16. Hieronymus, H., et al., *Gene expression signature-based chemical genomic prediction identifies a novel class of HSP90 pathway modulators.* Cancer Cell 2006. **10**(4): p. 321-30.
17. Roe, S.M., Ali, M.M.U., Meyer, P., Vaughan, C.K., Panaretou, B., Piper, P.W., Prodromou, C. and Pearl, L.H., *The mechanism of Hsp90 regulation by the protein kinase-specific cochaperone p50(cdc37).* Cell, 2004. **116**: p. 87-98.
18. Bernstein, F.C., et al., *The Protein Data Bank: a computer-based archival file for macromolecular structures.* J Mol Biol, 1977. **112**(3): p. 535-42.
19. Ali, M.M., et al., *Crystal structure of an Hsp90-nucleotide-p23/Sba1 closed chaperone complex.* Nature, 2006. **440**(7087): p. 1013-7.
20. Hamza, A. and C.G. Zhan, *How can (-)-epigallocatechin gallate from green tea prevent HIV-1 infection? Mechanistic insights from computational modeling and the implication for rational design of anti-HIV-1 entry inhibitors.* J Phys Chem B Condens Matter Mater Surf Interfaces Biophys, 2006. **110**(6): p. 2910-7.
21. Kuntz, I.D., E.C. Meng, and B.K. Shoichet, *Receptor-Based Molecular Design.* Acc. Chem. Res., 1994. **27**: p. 117-123.
22. Jorgensen, W.L., et al., *Comparison of simple potential functions for simulating liquid water.* J. Chem. Phys., 1983. **79**: p. 926-935.

23. Bayly, C.I., et al., *A WELL-BEHAVED ELECTROSTATIC POTENTIAL BASED METHOD USING CHARGE RESTRAINTS FOR DERIVING ATOMIC CHARGES - THE RESP MODEL* J. Phys. Chem., 1993. **97**: p. 10269-10280.
24. Cornell, W.D., et al., *Application of RESP charges to calculate conformational energies, hydrogen bond energies and free energies of solvation.* J. Am. Chem. Soc., 1993. **115**: p. 9620-9631.
25. Ryckaert, J.P., G. Ciccotti, and H.J.C. Berendsen, *Numerical Integration of the Cartesian Equations of Motion of a System with Constraints: Molecular Dynamics of n Alkanes.* J. Comput. Phys. , 1977. **23**(327-341).
26. Essmann, U., et al., *A smooth particle mesh Ewald method.* J. Chem. Phys., 1995. **103**: p. 8577-8593.
27. Kollman, P.A., et al., *Calculating structures and free energies of complex molecules: combining molecular mechanics and continuum models.* Acc Chem Res, 2000. **33**(12): p. 889-97.
28. Grenert, J.P., et al., *The amino-terminal domain of heat shock protein 90 (hsp90) that binds geldanamycin is an ATP/ADP switch domain that regulates hsp90 conformation* J. Biol. Chem, 1997. **272**: p. 23843-23850.
29. Yang, H., et al., *Celastrol, a triterpene extracted from the Chinese "Thunder of God Vine," is a potent proteasome inhibitor and suppresses human prostate cancer growth in nude mice.* Cancer Res, 2006. **66**(9): p. 4758-65.
30. Lee, P., et al., *Sti1 and Cdc37 Can Stabilize Hsp90 in Chaperone Complexes with a Protein Kinase.* Mol. Biol. Cell 2004. **15**: p. 1785-1792.
31. Johnson, J.L. and D.O. Toft, *Binding of p23 and hsp90 during the assembly with the. progesterone receptor.* Mol Endocrinol 1995. **9**: p. 670-678.
32. Sullivan, W., et al., *Nucleotides and two functional states of hsp90.* J Biol Chem, 1997. **272**(12): p. 8007-12.
33. Siligardi, G., et al., *Co-chaperone regulation of conformational switching in the Hsp90 ATPase cycle.* J Biol Chem 2004. **279**(50): p. 51989-51998.
34. Sato, S., N. Fujita, and T. Tsuruo, *Modulation of Akt kinase activity by binding to Hsp90.* Proc Natl Acad Sci U S A, 2000. **97**(20): p. 10832-7.
35. Stepanova, L., et al., *Mammalian p50(Cdc37) is a protein kinase-targeting subunit of Hsp90 that binds and stabilizes Cdk4.* Genes Dev., 1996. **10**: p. 1491-1502.
36. Oberg, K. and B. Eriksson, *Endocrine tumours of the pancreas.* Best Pract Res Clin Gastroenterol, 2005. **19**(5): p. 753-81.
37. Schulte, T.W., W.G. An, and L.M. Neckers, *Geldanamycin-induced destabilization of Raf-1 involves the proteasome.* Biochem Biophys Res Commun, 1997. **239**: p. 655-659.
38. Verma, I.M., et al., *Rel/NF-kappa B/I kappa B family: intimate tales of association and dissociation.* Genes Dev., 1995. **9**(22): p. 2723-2735.
39. Kisselev, A.F. and A.L. Goldberg, *Proteasome inhibitors: from research tools to drug candidates.* Chem Biol, 2001. **8**(8): p. 739-58.
40. Fenteany, G., et al., *Inhibition of proteasome activities and subunit-specific amino-terminal threonine modification by lactacystin.* Science, 1995. **268**(5211): p. 726-31.

41. Xiong, H.Q., *Molecular targeting therapy for pancreatic cancer.* Cancer Chemother Pharmacol, 2004. **54 Suppl 1**: p. S69-77.
42. Ogata, M., et al., *Overexpression and localization of heat shock proteins mRNA in pancreatic carcinoma.* Journal of Nippon Medical School, 2000. **67**: p. 177-185.
43. Cao, X., et al., *Synergistic antipancreatic tumor effect by simultaneously targeting hypoxic cancer cells with HSP90 inhibitor and glycolysis inhibitor.* Clin Cancer Res, 2008. **14**(6): p. 1831-9.
44. Prodromou, C., et al., *Identification and structural characterization of the ATP/ADP-binding site in the Hsp90 molecular chaperone.* Cell, 1997. **90**(1): p. 65-75.
45. Whitesell, L., et al., *Inhibition of heat shock protein HSP90-pp60v-src heteroprotein complex formation by benzoquinone ansamycins: essential role for stress proteins in oncogenic transformation.* Proc Natl Acad Sci U S A, 1994. **91**(18): p. 8324-8.
46. Schulte, T.W., et al., *Antibiotic radicicol binds to the N-terminal domain of Hsp90 and shares important biologic activities with geldanamycin.* Cell Stress Chaperones, 1998. **3**(2): p. 100-108
47. Schulte, T.W., Neckers, L.M., *The benzoquinone ansamycin 17-allylamino-17-demethoxygeldanamycin binds to HSP90 and shares important biologic activities with geldanamycin. .* Cancer Chemother. Pharmacol., 1998. **42**: p. 273-279.
48. Dymock, B.W., et al., *Novel, potent small-molecule inhibitors of the molecular chaperone Hsp90 discovered through structure-based design. .* J. Med. Chem., 2005. **48**: p. 4212-4215.
49. Richter, K. and J. Buchner, *Hsp90: chaperoning signal transduction.* J Cell Physiol 2001. **188**: p. 281-290.
50. Arlander, S.J., et al., *Chaperoning checkpoint kinase 1 (Chk1), an Hsp90 client, with purified chaperones.* J Biol Chem, 2006. **281**(5): p. 2989-98.
51. Xu, W. and L. Neckers, *Targeting the molecular chaperone heat shock protein 90 provides a multifaceted effect on diverse cell signaling pathways of cancer cells.* Clin Cancer Res, 2007. **13**(6): p. 1625-9.
52. Koga, F., S. Tsutsumi, and L.M. Neckers, *Low dose geldanamycin inhibits hepatocyte growth factor and hypoxia-stimulated invasion of cancer cells.* Cell Cycle, 2007. **6**(11): p. 1393-402.

Figure 2.1 Molecular docking of celastrol with Hsp90 and Hsp90/p50Cdc37 complex

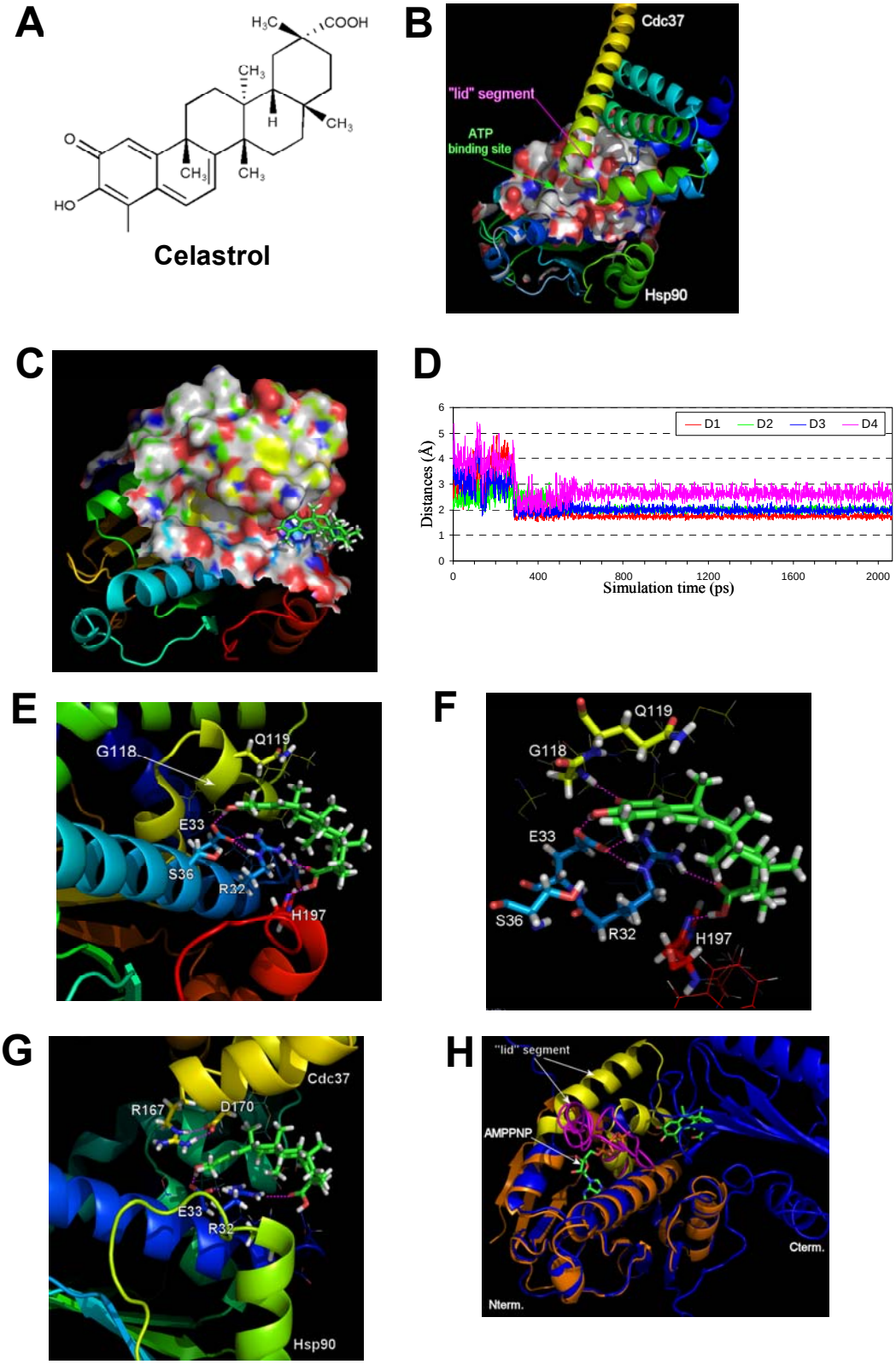

Figure 2.2 Celastrol disrupts the Hsp90/p50Cdc37 interaction in pancreatic cancer cells

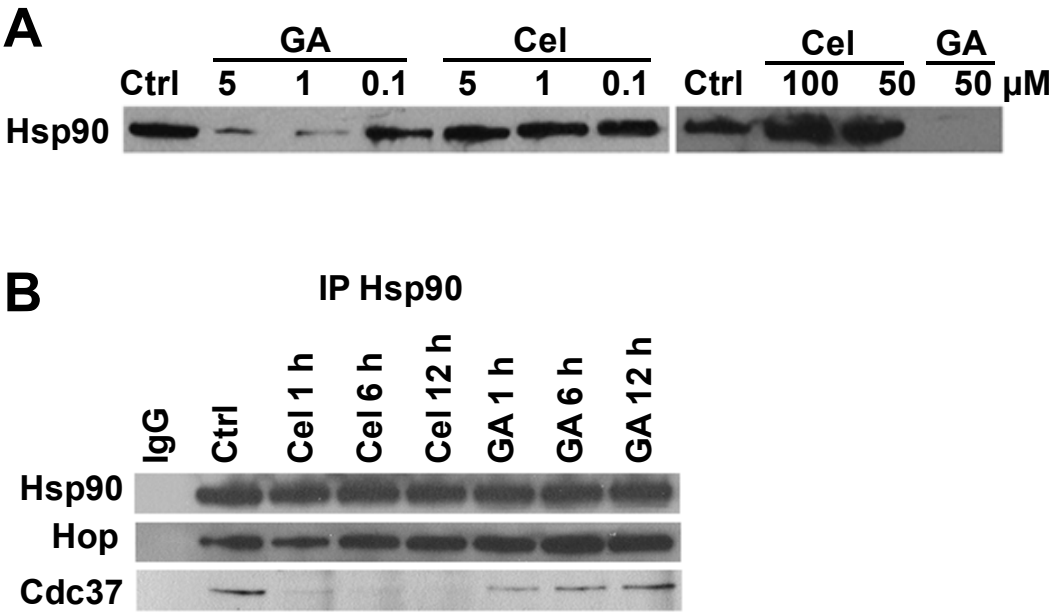

Figure 2.3 Celastrol does not disrupt Hsp90/p23 complex as GA

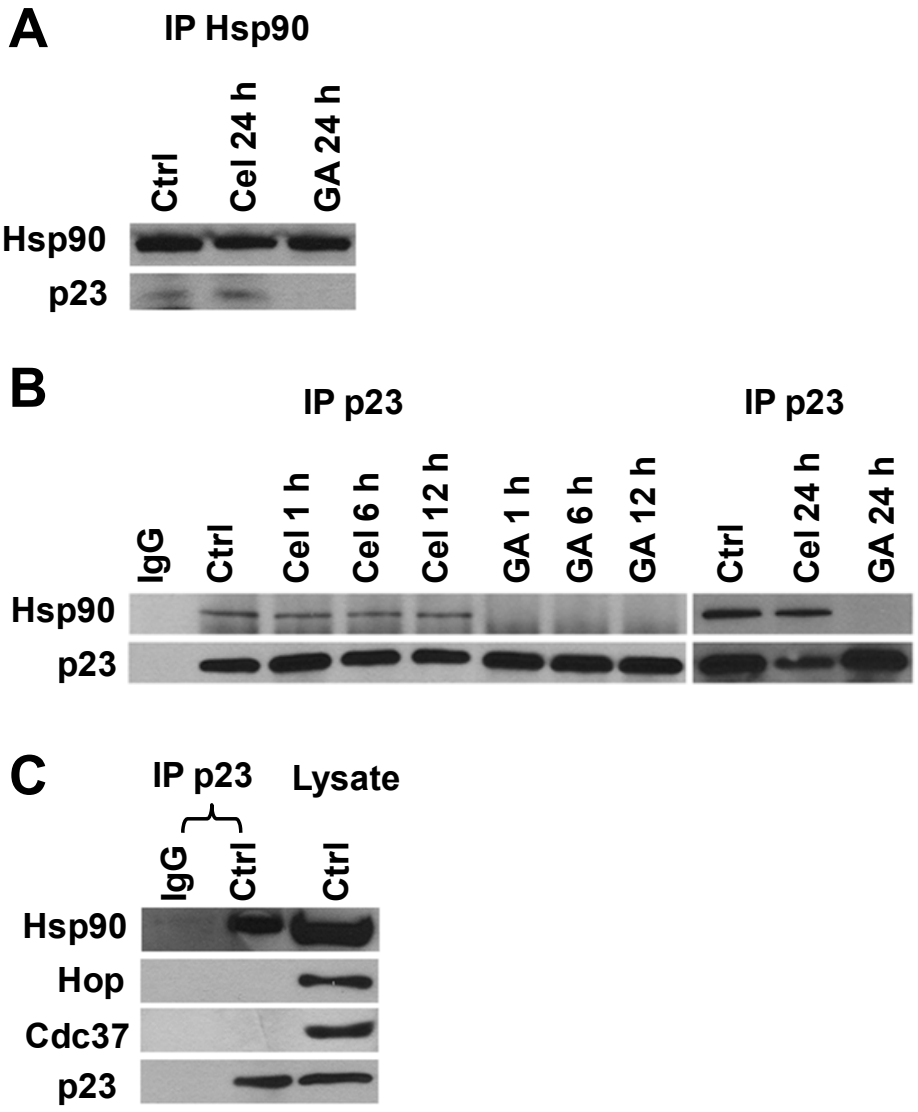

Figure 2.4 Effects of celastrol on client protein degradation and Hsp70 induction

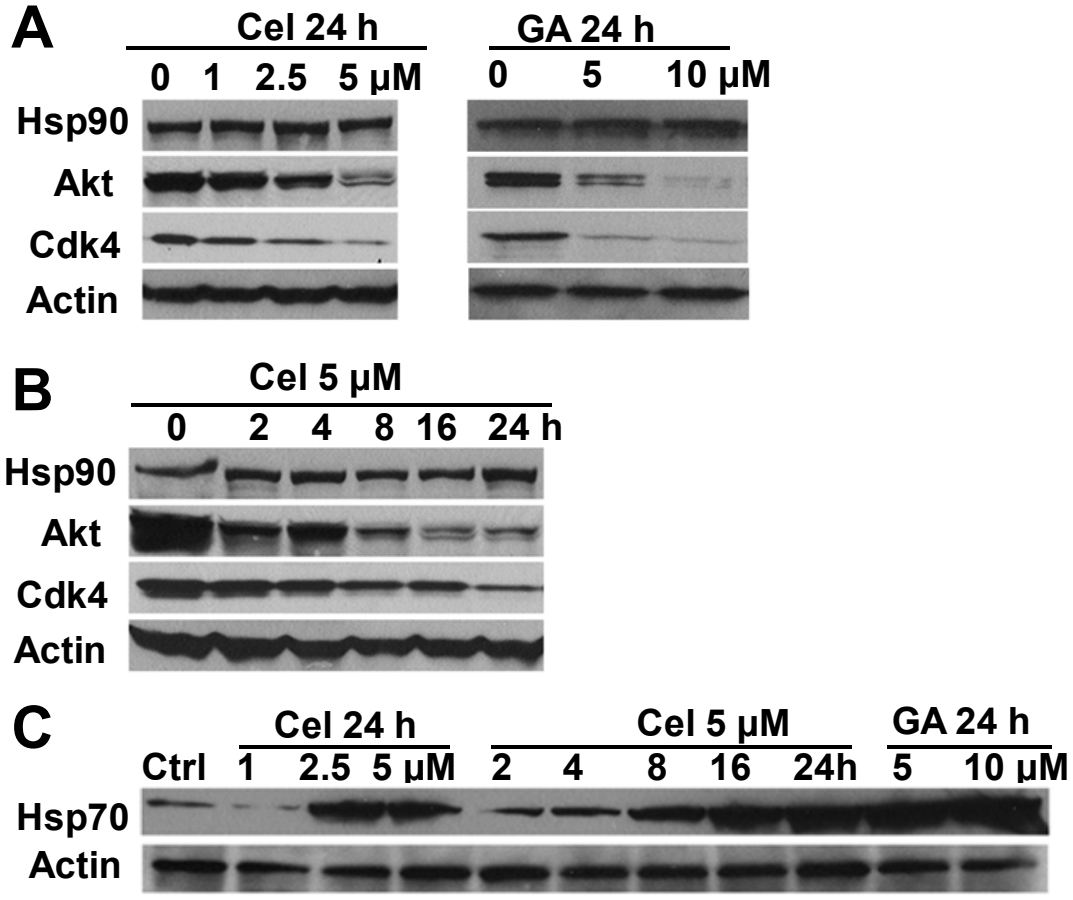

Figure 2.5 Antitumor effects of celastrol in vitro and in vivo

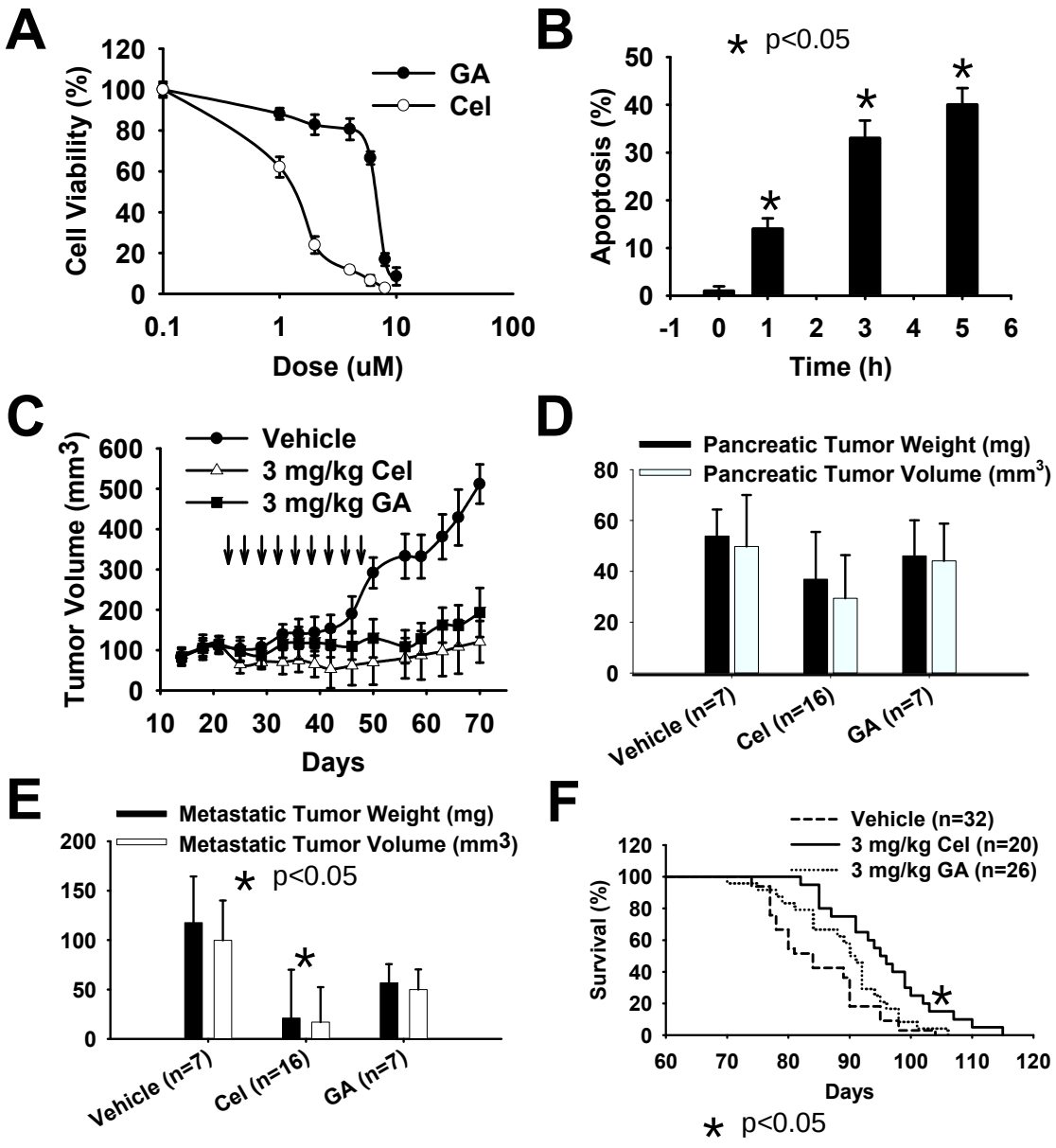

Figure 2.6 Celastrol is different from other proteasome inhibitors

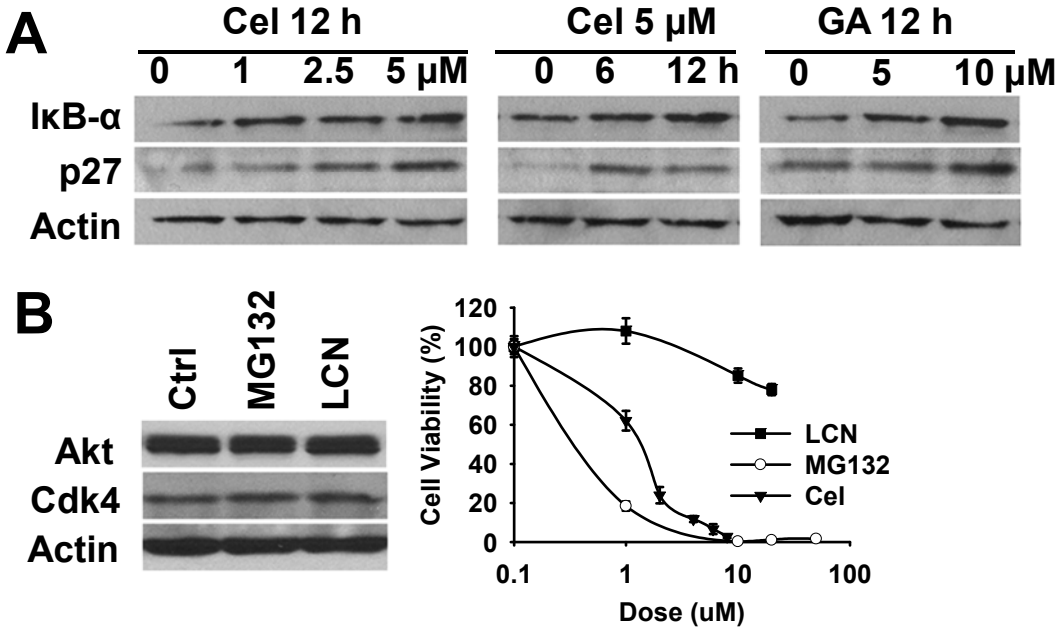

CHAPTER 3

Characterization of Celastrol to Inhibit Hsp90 and p50Cdc37 Interaction

3.1 Abstract

The molecular chaperone heat shock protein 90 (Hsp90) is required for the stabilization and conformational maturation of various oncogenic proteins in cancer. The loading of protein kinases to Hsp90 is actively mediated by the cochaperone p50Cdc37. The crucial role of the Hsp90/p50Cdc37 complex has made it an exciting target for cancer treatment. In this study, we characterize the Hsp90 and p50Cdc37 interaction and drug disruption using a reconstituted protein system. GST pull-down and ELISA assays show that p50Cdc37 binds to ADP-bound/nucleotide-free Hsp90 but not ATP-bound Hsp90. Celastrol disrupts the Hsp90/p50Cdc37 complex formation whereas the classical Hsp90 inhibitors (eg, geldanamycin) have no effect. Celastrol inhibits Hsp90 ATPase activity without blocking ATP binding. Proteolytic fingerprinting indicates that celastrol binds to the Hsp90 C-terminal domain to protect it from trypsin digestion. These data suggest that celastrol may represent a new class of Hsp90 inhibitors by modifying the Hsp90 C-terminus to allosterically regulate its chaperone activity and thereby disrupt the Hsp90/p50Cdc37 complex.

3.2 Introduction

Heat shock protein 90 (Hsp90) is a highly abundant and essential molecular chaperone in eukaryotic cells, accounting for as much as 1-2% of the cytosolic protein

even under nonstressed conditions [1]. Hsp90 protects cells not only through correcting the misfolded proteins under stress conditions, but also plays a key role under normal conditions in regulating the stability, maturation and activation of a wide range of client substrates, including kinases, hormone receptors, and transcription factors [2]. There are strong evidences that Hsp90 plays an important role in disease states, particularly in cancer. Hsp90 is expressed 2- to 10-fold higher in cancer cells compared to their normal counterparts, implying its crucial role in tumor cell growth or survival [3]. The largest subset of Hsp90 clients is the protein kinase, many of which are mutated and/or overexpressed signaling proteins in cancers [4-6]. Furthermore, cancer cells are significantly more sensitive to Hsp90 inhibition than non-transformed cells [7]. Therefore, Hsp90 has emerged as a promising target for cancer treatment.

The crystal structure reveals that Hsp90 consists of three highly conserved domains: an N-terminal ATP-binding domain (25 kDa), a middle domain (35 kDa) and a C-terminal dimerization domain (12 kDa) [8-10]. Hsp90 exists as a homodimer [11]. The N-terminal domain contains a specific ATP binding pocket, which has been well characterized [9, 12]. The middle domain is highly charged and its major role is to distinguish various types of client proteins and adjust the molecular chaperone for proper substrate activation [13]. The C-terminal domain strengthens the weak association between the two N-terminal domains of the Hsp90 dimer [10]. A second ATP-binding site is located in the C-terminus, which does not exhibit ATPase activity [14].

Hsp90 chaperone function depends on the conformational changes driven by its ATPase activity [15]. Numerous Hsp90 inhibitors, ranging from the original natural products and their derivatives to fully synthetic small molecules, have been discovered or

developed to inhibit its chaperone function by binding to the ATP/ADP pocket[16]. The antibiotic benzoquinone ansamycins, represented by geldanamycin (GA), are the first identified Hsp90 inhibitors [17]. Binding of GA in the N-terminal ATP pocket restrains Hsp90 in its ADP-bound conformation and prevents the subsequent "clamping" of Hsp90 around a client protein, resulting in ubiquitination and proteasomal degradation of the client proteins [18-20]. GA has exhibited potent anticancer effect, but the strong hepatotoxicity prevented its clinical development [21]. As a result, many GA derivatives have been generated to decrease toxicity but maintain anti-cancer activities [22-26], among which 17-AAG (17-allylamino-17-demethoxygeldanamycin), 17-DMAG (17-(dimethylaminoethylamino)-17-demethoxygeldanamycin), and IPI-504 (17-allylamino-17-demethoxy-geldanamycin hydroquinone hydrochloride) are currently in clinical trials for various solid tumors and leukemia [27-30]. Inhibitors binding to the newly discovered Hsp90 C-terminal ATP binding site have also been identified, such as novobiocin, cisplatin, epilgallocatechin-3-gallate (EGCG) and taxol [31]. Inhibition of Hsp90 by novobiocin induces similar cellular responses as N-terminal inhibitors and destabilizes a range of Hsp90 client proteins via the ubiquitin-proteasome pathway [32, 33]. Although the biochemical and molecular modeling techniques have made considerable advancements in understanding the Hsp90 C-terminus, much still remains speculative or controversial due to the lack of co-crystal structures. Currently, most of the Hsp90 inhibitors are targeting the ATP binding site in the N-terminal region [34].

The wide-ranging functions of Hsp90 result from its ability to chaperone many client proteins through an ordered formation of multichaperone complexes with cochaperones [2, 34]. Accompanying with the increasing understanding of Hsp90

function cycle and the promising results of ATP binding blockers of Hsp90, interest in Hsp90 inhibition expands from the central component Hsp90 to various modulators in the chaperone machinery. Inhibition of cochaperones (Aha1, p50Cdc37, CHIP, Hop, Hsp70, and PP5) has exhibited therapeutic anticancer potentials as well [34]. Silencing of Aha1, the only known Hsp90 ATPase activator, decreases client protein activation and increases cellular sensitivity to the Hsp90 inhibitor 17-AAG [35]. Simultaneous knockdown both Hsc70 and Hsp72 induces proteasome-dependent degradation of Hsp90 client proteins, G1 cell-cycle arrest, and extensive tumor-specific apoptosis [36]. p50Cdc37 silencing promotes the proteasome-mediated degradation of kinase clients via a degradation pathway independent of Hsp90 binding, and enhances apoptosis in combination with 17-AAG [37]. Not only targeting cochaperones has exhibited pharmacological benefits, the interference of Hsp90/cochaperone complex has shown therapeutic potential as well. The compounds disrupting Hsp90 and Hop interaction have been identified and shown activity in human breast cancer cells [38, 39]. More recently, we have demonstrated that celastrol, a natural triterpene compound isolated from the plant family *Celastraceae* [40], can disrupt Hsp90 and p50Cdc37 interaction in pancreatic cancer cells, resulting in Hsp90 client protein degradation and cell apoptosis [41]. These findings have highlighted the pharmacological potential of the cochaperone p50Cdc37.

p50Cdc37, also known as p50, was originally discovered in yeast as an essential cell cycle protein [42]. Later studies proved it to be an Hsp90 cochaperone, acting as an adaptor to load protein kinase to Hsp90 complex [34, 43]. Most of the Hsp90 clients p50Cdc37 associated with are crucial elements implicated in signal transduction, cell proliferation and survival [34]. In addition, p50Cdc37 overexpression is found in cancer

cells and tissues, and its induction can promote tumorigenesis [44, 45]. p50Cdc37 can be dissected into three domains [34, 46]. The N-terminal domain is the kinase binding domain containing a conserved phosphorylated residue (Ser-13) [47-49]. The middle region of p50Cdc37 is the most stable domain [50], which binds the N-terminus of Hsp90 [4]. The C-terminal domain is also involved in Hsp90 binding and probably required for the dimer formation [4, 51].

In previous studies we have shown that celastrol disrupts Hsp90 and p50Cdc37 interaction in pancreatic cancer cells and exhibited anticancer effect [41]. Here, using a purified protein system, we present that p50Cdc37 binds to ADP-bound/nucleotide-free Hsp90, which can be directly inhibited by celastrol. Through the comparison of celastrol with nucleotides and other Hsp90 inhibitors, we prove that celastrol functions via a distinct mechanism. It interacts with Hsp90 C-terminal domain and inhibits its ATPase activity without blocking ATP binding pocket.

3.3 Experimental Procedures

3.3.1 Chemicals

Celastrol was purchased from Sigma-Aldrich. Dihydrocelastrol diacetate (DDCel) was from Gaia Chemical Corporation. Geldanamycin (GA) was kindly provided by Dr. George Wang (Department of Chemistry, The Ohio State University). The mixture of celastrol and DTT was analyzed using proton nuclear magnetic resonance spectra (1H NMR) on a 300 MHz Bruker DPX-300 NMR spectrometer. The nucleotides ATP, ADP, AMP-PNP were from Sigma-Aldrich.

3.3.2 Protein purification

The expression plasmids pET15b-hHsp90β, pET28a(+)-hHsp90β (530-724), pGEX4T.1-p50Cdc37 for expression of human full length His-Hsp90β, C-Hsp90β and GST-p50Cdc37 protein were kindly provided by Dr. Thomas Ratajczak (University of Western Australia, Australia); plasmid pET15b-hHsp90α for expression of human His-Hsp90α was provided by Dr. Wei Li (University of Southern California Keck School of Medicine, USA). The plasmids were transformed into *E.coli* strain Rosetta 2(DE3) (EMD Biosciences Inc., San Diego, CA) according to the protocol provided by manufacturer. Primary cultures of transformed cells were grown overnight, pelleted by centrifugation, resuspended in new culture medium and grown for 1-2 h at 37°C till OD600= 0.6. Then protein expression was induced by 0.2 mM IPTG (isopropyl-beta-D-thiogalactopyranoside) (GE Healthcare, Piscataway, NJ) for 2 h. Cells were collected by centrifugation and washed once by cold PBS. His-tagged proteins were purified by affinity chromatography through mixing with HisPurTM Cobalt Resin (Pierce, Rockford, IL), and GST-tagged proteins with Glutathione 4B Sepharose (GE Healthcare, Piscataway, NJ). The GST tag of p50Cdc37 was removed by thrombin cleavage. Purified proteins were dialyzed against PBS, the purity was assessed by SDS-PAGE, and concentrations were determined by BCA assay (Pierce, Rockford, IL). Proteins were stored at -70°C after adding glycerol to 10%. The purified yeast Hsp82 protein was kindly provided by Dr. Dan Bolon (University of Massachusetts Medical School, USA).

3.3.3 GST pull-down assay

Purified Hsp90 protein (~5 μg) was pre-incubated with different compounds or control (DMSO) at 30°C for 30 min in 200 μl incubation buffer (10 mM Tris-HCl, 50

mM KCl, 5 mM $MgCl_2$, 0.01% Nonidet P-40, pH 7.5). Following incubation, GST-p50Cdc37 protein (~10 μg) was added and further incubated at 4°C for 1 h. After that, Glutathione Sepharose 4B (20 μl) pre-equilibrated with incubation buffer was added and incubated at 4°C for 2 h. The incubation was performed with gentle shaking. Sepharose was then pelleted by centrifugation, washed five times with 1 ml incubation buffer, analyzed by SDS-PAGE and Western blotting.

3.3.4 ELISA microtiter plate assay

The ELISA assay was modified from the previous reported method [52]. Purified hHsp90α/β protein (80 nM) or control (bovine serum albumin) in ELISA Coating buffer (Biolegend, San Diego, CA) was applied to Immulon 4HBX 96-well Microtiter plates with 50 μl/well (triplicate per sample) and incubated at 4 °C overnight. Wells were washed three times with TBST (*50 mM Tris*-HCl pH 7.6, 150 *mM* NaCl, 0.075% Tween 20) and blocked with 100 μl of 1% BSA in PBS overnight at 4°C. Afterwards wells were washed three times again with TBST. Compound in 100 μl TBST was added at indicated concentrations and incubated at 30°C for 30 min. Depending on different experimental design, the compounds were either removed by washing five times, or this step was excluded, before adding 0.25 μM of GST-p50Cdc37 protein in TBST. The mixture was incubated at 4°C for 1 h. Unbound proteins were removed by washing with TBST for five times. Rabbit anti-p50Cdc37 antibody (H271, Santa Cruz Biotechnology, Santa Cruz, CA) was added at 1:2000 dilutions in 100 μl TBST containing 1% BSA and incubated at room temperature for 1 h. After washing five times, goat anti-rabbit IgG antibody conjugated with horseradish peroxidase *(*HRP) at 1:150,000 dilution in TBST containing 1% BSA was added in 100 μl aliquot to each well and incubated at room temperature for

1 h. After washing, each well was added with 100 µl of the substrate 3,3',5,5'-tetramethylbenzidine (Sigma Chemical Company, St. Louis, MO) and incubated at 30°C for 5-15 min with gentle shaking., The reactions were stopped with 100 µl of 0.5 M sulfuric acid, producing a yellow end product which was quantified at 450 nm.
For a complementary assay, purified Cdc37 protein (untagged, 80 nM) was coated to the plate while His-tagged hHsp90α/β (250 nM) was added later. All the assay steps were the same except that mouse anti-His antibody (GE Healthcare, Piscataway, NJ) and anti-mouse secondary antibody were employed.

3.3.5 ATPase activity assay

The ATPase activity assay is based on the conversion of phosphoenolpyruvate (PEP) to pyruvate by pyruvate kinase (PK) coupled to the conversion of pyruvate to lactate by lactate dehydrogenase (LDH) at the expense of NADH [53]. The oxidation of NADH to NAD^+ produces a decrease of absorbance at 340 nm. The reaction buffer contained 100 mM Tris-HCl (pH 7.4), 20 mM KCl, 6 mM $MgCl_2$, 0.8 mM ATP, 0.1 mM NADH, 2 mM PEP, 10 µl of Pyruvate Kinase/Lactic Dehydrogenase enzymes (Sigma Chemical Company, St. Louis, MO). The reaction was started by addition of 2.5 µM yeast Hsp82 protein at 37°C. The ATPase activity was determined by tracking the decrease in the absorbance at 340 nm. The compounds (GA or celastrol) was dissolved in DMSO and added to the reaction mixture to test the inhibition of Hsp90 ATPase activity.

3.3.6 Biotinylated GA binding assay

Purified human Hsp90β protein (5 µg) in 200 µl incubation buffer (10 mM Tris-HCl, 50 mM KCl, 5 mM $MgCl_2$, 0.01% Nonidet P-40, pH 7.5) was incubated with increasing concentrations of 17-AAG or celastrol for 30 min at 30°C, and then incubated

with biotin-GA (Invivogen, San Diego, CA) for 1 h at 4 °C. The biotinylated GA-bound hsp90 was immunoprecipitated with Streptavidin-agarose beads and Hsp90 was detected by Western blotting.

3.3.7 Proteolytic fingerprinting

The experiment was performed following previously described procedure [54]. Purified recombinant protein (0.1-0.5 µg) was incubated with DMSO or celastrol in 20 µl assay buffer (10 mM Tris-HCl, 50 mM KCl, 5 mM $MgCl_2$, 0.1 mM EDTA, pH 7.4) at room temperature for half an hour. The samples were digested on ice with different concentrations of trypsin for 6 min. The reactions were terminated by adding SDS sample buffer followed by boiling for 3-5 min. The digested products were analyzed by Western blotting with Hsp90 (H-114) antibody (Santa Cruz Biotechnology, Santa Cruz, CA) and Hsp90 (AC88) antibody (Assay Designs, Inc., Ann Arbor, MI).

3.4 RESULTS

3.4.1 p50Cdc37 binding to Hsp90.

Previous studies about Hsp90 and cochaperones interaction have shown that the ingredients and various conditions of the incubation buffer can dramatically affect the protein interactions [55-57]. To test these conditions, we performed GST pull-down assay by mixing Hsp90 and p50Cdc37 in different buffers (Figure 3.1A). We started with pure water, in which no obvious interaction between Hsp90 and p50Cdc37 was noticed (Figure 3.1A, lane 1). A weak interaction was detected using the basic incubation buffer previously reported for characterizing Hsp90 and p23 interaction (Figure 3.1A, lane 2), which is surprising because Hsp90 and p23 can not bind to each other under the same

condition [55]. The maximal interaction was noticed when Nonidet P-40 was added (Figure 3.1A, lane 3). In fact, the Hsp90/p50Cdc37 complex was present upon simply mixing them in a PBS buffer, although the interaction is slightly weaker (Figure 3.1A, lane 4). These results demonstrate that Hsp90 and p50Cdc37 can form complex in the absence of other proteins.

Hsp90 exists at two different functional states, the ADP-bound and ATP-bound forms [55]. The nucleotides have proved to be effective to switch the conformation of Hsp90 [55]. We tested these effectors in the Hsp90/p50Cdc37 complex formation by GST pull-down assay. The addition of ADP has no influence on Hsp90 and p50Cdc37 interaction (Figure 3.1B), indicating Hsp90 is in its ADP-bound state in the complex. It has been shown that molybdate maintains Hsp90 in a pseudo-ATP-bound state, which is completely dependent on the presence of ATP [55]. Indeed, the addition of molybdate alone has no effect on Hsp90 and p50Cdc37 interaction (Figure 3.1B). The addition of both molybdate and ATP completely disrupted Hsp90/P50Cdc37 complex (Figure 3.1B), suggesting that the ATP-bound state of Hsp90 is not capable of binding p50Cdc37. This was further confirmed when AMP-PNP, the nonhydrolysable analog of ATP, was added (Figure 3.1B). Because molybdate is only effective with a readily metabolized nucleotide [55], we added AMP-PNP without molybdate. Similar to ATP, AMP-PNP inhibited Hsp90/p50Cdc37 complex formation (Figure 3.1B).

3.4.2 Celastrol inhibits Hsp90/p50P50Cdc37 complex formation

We first examined the effect of Hsp90 inhibitors on Hsp90/p50Cdc37 interaction using GST pull-down assay. As one of the most well-known Hsp90 inhibitors, geldanamycin (GA) blocks Hsp90 function by binding to the N-terminal ATP binding

pocket [2]. Our previous results have shown that GA has no effect on Hsp90 and p50Cdc37 interaction in pancreatic cancer cells [41]. Consistent with the *in vivo* studies, as high as 500 μM of GA was not able to change Hsp90 and p50Cdc37 binding in the purified protein system, as shown in Figure 3.1C. No disruption was noticed with its derivatives 17-AAG and 17-DMAG either (Figure 3.1C).

In contrast, celastrol can disrupt Hsp90/p50Cdc37 complex in the same GST pull-down assay. A progressive decline in the complex formation was observed with increasing concentrations of celastrol (Figure 3.1D). As low as 1 μM of celastrol has exhibited moderate effect, 10 μM inhibited more than 70% of complex formation, and up to 100 μM completely abrogated Hsp90 and p50Cdc37 interaction (Figure 3.1D). These results are consistent with what we observed in pancreatic cancer cells upon celastrol treatment [41]. Moreover, the inhibitory effect was not restricted to human Hsp90β protein, but applicable to human Hsp90α and yeast Hsp82 proteins as well (Figure 3.1D). To confirm these results, we performed ELISA microtiter plate assay using both Hsp90α and Hsp90β proteins. Purified Hsp90α/β was coated on the Immulon 4HBX 96-well Microtiter plate and incubated with celastrol before p50Cdc37 was added. Bound p50Cdc37 was detected by antibody specific to p50Cdc37. The results showed that celastrol (1-200 μM) was able to disrupt Hsp90 and p50Cdc37 interaction in a concentration-dependent manner (Figure 3.1E), while GA did not interfere with Hsp90/p50Cdc37 complex.

3.4.3 Inhibitory activity resides within the A/B rings of celastrol

It has been predicted there are two electrophilic centers residing within the A and B rings of celastrol [58-60]. They are active structures responsible for the biological

activity of celastrol [58-60]. To test the importance of these moieties in compromising Hsp90/p50Cdc37 complex formation, we used the derivative of celastrol, dihydrocelastrol diacetate (DDCel). Compared with celastrol, DDCel has an altered double bond arrangement within A/B ring, and two acetoxyl groups attached to the A ring carbonyl and hydroxyl groups of celastrol (Figure 3.2A). DDCel showed a significantly weaker effect in disrupting Hsp90/p50Cdc37 complex. A minor disruption of the complex was observed only in response to as high as 100-200 μM concentrations (Figure 3.2B), which indicates the importance of the unique quinone methide structure of celastrol.

Previous studies have shown that the activation of the heat shock response by celastrol can be inactivated by mixing with excess thiols [61], therefore we tested whether thiols can affect the effect of celastrol on Hsp90/p50Cdc37 complex. Celastrol was premixed with dithiothreitol (DTT) before incubation with Hsp90. It seems that these two chemicals react with each other as the red color of celastrol faded away right after DTT was added. The results showed that the mixture was incapable of affecting Hsp90/p50Cdc37 complex formation (Figure 3.2C). The NMR analysis of the mixture indicated altered bond arrangement in the A and B rings of celastrol (data not shown). Therefore, the reactive activity of the A/B rings may contribute to the inhibitory effect of celastrol on Hsp90/p50Cdc37 complex formation.

3.4.4 Inhibitory effect of celastrol on Hsp90/p50Cdc37 complex formation is via Hsp90

The ELISA microtiter plate assay can be applied either by coating Hsp90 on the well and detecting bound p50Cdc37, or by coating p50Cdc37 on the well and detecting

bound Hsp90. The data above (Figure 3.1E) have shown that when Hsp90 was immobilized on the plate, p50Cdc37 binds immobilized Hsp90. Similarly, when p50Cdc37 was immobilized onto the plate, purified Hsp90 also binds to immobilized p50Cdc37 (Figure 3.3A). The addition of celastrol to the mixture disrupts Hsp90/p50Cdc37 interaction, whereas GA did not, regardless which protein was immobilized onto the plate (Figure 3.1E & 3.3A).

To investigate which protein in the Hsp90/p50Cdc37 complex is the main target of celastrol, we modified the ELISA microtiter plate assay by adding one washing step to remove the free drug after incubating celastrol with the coated protein on the wells. First, Hsp90 was coated on the wells and incubated with celastrol followed by washing. Under such condition, as shown in Figure 3.3B, p50Cdc37 was incapable of binding immobilized Hsp90, which indicates celastrol has rendered Hsp90 unable to bind p50Cdc37. On the contrary, when the immobilized p50Cdc37 was incubated with celastrol, Hsp90 was still able to form Hsp90/p50Cdc37 complex after drug removal (Figure 3.3C). This suggests that either celastrol does not affect p50Cdc37, or the effect is weaker or transient which can be abrogated by washing. However, the effect of celastrol on Hsp90 was persistent, implying that celastrol may mainly target Hsp90 to impair Hsp90/p50Cdc37 complex formation.

3.4.5 Celastrol inhibits ATPase activity of Hsp90

As a molecular chaperone, the intrinsic ATPase activity of Hsp90 is critical for its function in the folding and maturation of client proteins [15]. Since Hsp90 is likely to be the target of celastrol, we next examined whether celastrol could interfere with the essential ATPase activity of Hsp90. As shown in Figure 3.4A, 10 μM of celastrol

exhibited marked inhibitory effect on ATPase activity of Hsp90, while 100 μM of celastrol completely abolished the activity, comparable to that of GA.

Given that celastrol inhibits ATPase activity, it is reasonable to suspect that celastrol binds to the ATP site because the Hsp90 inhibitors (eg, GA) occupy the ATP binding pocket of Hsp90 to inhibit its ATPase activity. However, our previous results have shown that celastrol did not inhibit ATP binding to Hsp90 with the ATP sepharose binding assay [50]. We further confirmed the phenomenon with the biotinylated GA binding assay. Purified Hsp90 protein was first incubated with DMSO, 17-AAG or celastrol before biotin-GA was added. If the compound binds to the ATP-binding pocket of Hsp90, it will affect biotin-GA binding to Hsp90, thus less Hsp90 will be precipitated. The results confirmed that celastrol can not inhibit GA-biotin binding to Hsp90 while 17-AAG can (Figure 3.4B). These results verified that celastrol did not bind to the ATP pocket of Hsp90 to inhibit its ATPase activity.

3.4.6 Celastrol binds to C-terminus of Hsp90

The ATP pocket binding may not be the only way to modulate the ATPase activity of Hsp90, the inhibition can be achieved by alteration or interaction with other domains of the molecule far from the ATP-binding pocket [62]. Recent studies have provoked the importance of the Hsp90 C-terminus in the regulation of its function [63, 64]. Therefore, we tested whether celastrol can interact with C-terminal domain of Hsp90 by performing proteolytic fingerprinting assay with purified full-length and C-terminal (residues 530-724) Hsp90 proteins. The proteins were incubated with DMSO or celastrol and the fingerprint was obtained by treatment with increasing concentrations of trypsin. The fragments of the C-terminal domain were detected by antibodies specifically

recognizing epitopes within this region. As shown in Figure 3.4C, in the absence of celastrol, the full-length Hsp90 protein is highly sensitive to trypsin digestion. After the protein was pre-incubated with celastrol, the stabilization of a ~50 kDa fragment was observed, which was detected by the antibody specific to the C-terminus. This indicates that celastrol induces the conformational changes of full-length Hsp90, resulting in the altered susceptibility to trypsin mediated degradation. To further investigate the location of interaction, we examined the effect of celastrol on the proteolysis of the purified Hsp90 C-terminus protein containing residues 530-724. As expected, the recombinant protein was sensitive to trypsin digestion (Figure 3.4D). Celastrol protected the entire C-terminal region from trypsin cleavage (Figure 3.4D). Therefore, we interpret that celastrol binds directly to a site on the C-terminal region of Hsp90.

3.5 Dicussion

The molecular chaperone Hsp90 has become an exciting target for cancer therapeutics. A number of Hsp90 inhibitors have exhibited anticancer activity in xenograft models and several of them are in clinical trials [65]. Although Hsp90 remains to be the main target, there is increasing interest in the functionally related cochaperones involved in the multichaperone complex, such as Hop, p50Cdc37, p23, and Aha1 [34]. Our previous studies have shown that celastrol disrupts Hsp90 and p50Cdc37 interaction in pancreatic cancer cells, and it showed potent anticancer activity in pancreatic cell lines and animal models. The present study establishes a reconstituted protein system to characterize the effect of celastrol on Hsp90/p50Cdc37 complex. Using purified proteins, we find that p50Cdc37 binds to Hsp90 in the ADP-bound/nucleotide-free state but not in ATP-bound state. Celastrol directly disrupts their interaction in the purified protein

system in a dose-dependent manner, excluding the possibility that in pancreatic cancer cells the disruption of Hsp90/p50Cdc37 complex upon celastrol treatment was merely indirect consequence of other factors. Moreover, celastrol completely abrogates the ATPase activity of Hsp90 but does not inhibit GA binding to Hsp90. The functional group of celastrol may reside in the A/B rings and its inhibitory effect may result from its interaction with Hsp90 C-terminal domain.

The chaperoning cycle of Hsp90, which depends on an ordered assembly and disassembly of various cochaperones driven by the ATPase activity, has been studied extensively [2]. However, because it is a dynamic process with many cochaperones (eg, Hsp70, Hsp40, Hop, Hip, p50Cdc37, p23, IP, and Aha1) involved and new members being identified [66], much detailed information remains inconclusive and controversial. Our results show that the Hsp90/p50Cdc37 complex forms by simply mixing Hsp90 and P50Cdc37 in the incubation buffer (Figure 3.1A). When the agents (molybdate, ATP, and AMP-PNP) that promote the conversion of Hsp90 into the ATP-bound state were included, p50Cdc37 can no longer associate with Hsp90 (Figure 3.1B). These results reveal that p50Cdc37 prefers to bind the nucleotide-free or ADP-bound Hsp90. The same conclusion has been drawn on the cochaperone Hop as well [56]. In addition, it has been proposed that p50Cdc37 acts as an adaptor or scaffold that loads client/Hsp70/Hsp40 to Hsp90 with the help of Hop in the early complex during the chaperoning cycle [4, 67]. Therefore, p50Cdc37 and Hop are likely to bind Hsp90 at the same stage. This is consistent with the recent data that p50Cd37 co-associate with Hop in the early complex [43, 68, 69]. Another similarity of p50Cdc37 and Hop is that neither of them can associate with the ATP-bound Hsp90 in the mature complex (Figure 3.1B) [56]. The

crystal structure has shown that p50Cdc37 binds to Hsp90 by inserting its C-terminal side chain into the nucleotide binding pocket of Hsp90, suggesting the binding of ATP would have to eject this side chain out of ATP binding pocket [2]. Therefore, it is possible that p50Cdc37 and Hop are removed from the Hsp90 early complex simultaneously due to the binding of ATP to Hsp90. However, more direct evidence is required to confirm these hypotheses.

The disruption of Hsp90/p50Cdc37 complex by celastrol could be through Hsp90, p50Cdc37, or both. Our results confirmed that Hsp90 definitely contributes to the disruption (Figure 3.3B), and thus we consider celastrol as an Hsp90 inhibitor. There are two well-known classes of Hsp90 inhibitors. The first identified are ATP pocket inhibitors at the N-terminal region, represented by GA and its derivatives [15]. GA blocks ATP binding to Hsp90 and locks the chaperone cycle in the early complex containing Hsp70, Hop, and p50Cdc37 [15] [41]. Therefore, it should not disrupt Hsp90 and P50Cdc37 interaction, which is clearly supported by our results (Figsure 3.1C & E). A second nucleotide-binding domain has been reported to exist in the carboxyl terminus of Hsp90, and specific inhibitors to this domain are represented by novobiocin and the related coumarin antibiotics [32]. Similar with novobiocin, celastrol interacts with a domain in the C-terminal portion of Hsp90 (Figure 3.4C & D). They both interfere with the chaperone function of Hsp90 and deplete a series of Hsp90-dependent signaling proteins in tumor cells [32, 41]. However, novobiocin and celastrol showed major differences in their effects on the interaction of cochaperones with Hsp90. Novobiocin (4 mM) significantly reduced the interaction of Hsc70 and p23 with Hsp90 in reticulocyte lysate [54]. The same result was reported by Marcu and co-workers with a lower

concentration (1 mM) of novobiocin [70]. Novobiocin (10 mM) moderately decreased the interaction of Hop with Hsp90 [54]. However, novobiocin (5 mM) has little effects on the interaction of p50Cdc37 with Hsp90, while higher concentration (10 mM) of novobicin even caused a slight increase in Hsp90/p50Cdc37 complex formation [54]. In contrast, the effect of celastrol is quite different from that of novobiocin. In a reconstituted protein system, 0.001-0.01 mM celastrol induced a dramatic reduction of p50Cdc37 binding to Hsp90, while 0.1 mM celastrol blocked their interaction completely (Figure 3.1D). Celastrol (0.01 mM) also disrupted Hsp90 and P50Cdc37 interaction in cancer cells while no inhibition of Hsp90/Hsc70/Hop and Hsp90/p23 complexes was noticed under the same condition [41]. Therefore, the mechanism by which celastrol inhibits Hsp90 function appears to be distinct from that of Hsp90 C-terminal inhibitors.

Hsp90 function depends on its ability to bind and hydrolyze ATP, and its ATPase activity can be regulated not only by small molecules, but also other modulators such as cochaperones or post-translational modifications [62]. Cochaperones preferentially bind to a specific conformation of Hsp90 to modulate its ATPase activity, either by inhibition (such as p23, p50Cdc37) or activation (such as Aha1) [62]. Although the ATP binding and hydrolysis occur at the N-terminal domain, its ATPase activity can be modulated through interaction beyond this site. Sti1, the yeast homolog of Hop, binds to the C-terminus of Hsp90 and completely inhibits the ATPase activity of Hsp90 without affecting ATP binding [63, 71]. The reason for Sti1 to function like this is because it binds a specific conformation of Hsp90 to prevent the dimerization of N-terminus and association of the N- and M- domains [63] [62]. Similarly, celastrol interacts with the C-terminus of Hsp90 protecting it from cleavage by trypsin digestion (Figure 3.4C & D),

and inhibits Hsp90 ATPase activity (Figure 3.4A) without inhibiting ATP binding (Figure 3.4B). In addition, other modifications of Hsp90 in the C-terminus have also shown altered ATPase activity [64]. For instance, S-nitrosylation in the Hsp90 C-terminal domain inhibits its ATPase activity [64], although whether it affects ATP binding to Hsp90 was not reported. All these findings reveal the importance of the C-terminus in the regulation of Hsp90 ATPase activity. Therefore, we speculate that the inhibition of the ATPase activity by celastrol maybe relates to its interaction with Hsp90 C-terminus. Thus, celastrol may represent another class of Hsp90 inhibitor that "allosterically" modulates Hsp90 chaperone activity and superchaperone complex. While this manuscript was under review, Sridhar and colleagues showed that celastrol does not bind to Hsp90 N-terminus but modifies the cysteine residues in p50Cdc37[72]. Interestingly, the susceptible target of S-nitrosylation is also a cysteine residue in the Hsp90 C-terminal domain [64]. Moreover, our recent data proved that withaferin A, which has been reported to react with protein thiol-nucleophiles, is able to affect Hsp90 and p50Cdc37 interaction in cells as well [73-75]. Therefore, we would not be surprised if celastrol modifies Hsp90 C-terminus cysteine residues to inhibit ATPase activity and disrupt Hsp90/p50Cdc37 complex. However, more work is warranted to map the exact site in Hsp90 where celastrol interacts with.

Our study reveals that p50Cdc37 can only bind ADP-bound or nucleotide-free Hsp90 but not ATP-bound Hsp90, which indicates that p50Cdc37 can only associate with the early but not the mature complex of Hsp90. The data demonstrates that celastrol directly disrupts Hsp90 and p50Cdc37 interaction in a reconstituted protein system, which confirmed the previously reported *in vivo* data [41]. Celastrol interacts with Hsp90

C-terminus, inhibiting its ATPase activity without blocking ATP-binding site, which is distinct from the current Hsp90 inhibitors. Additional work is required to locate the exact residues that celastrol interacts with.

3.6 Acknowledgments

This study is partially supported by NIH funding RO1 CA 120023, UM cancer center research grant (Munn), UM cancer center core grant to DS. We thank Dr. Thomas Ratajczak (University of Western Australia, Australia) and Dr. Wei Li (University of Southern California Keck School of Medicine, USA) for the generous gifts of expression plasmids, pET15b-hHsp90β, pET28a(+)-hHsp90β (530-724) and pET15b-hHsp90α. We also acknowledge Dr. Dan Bolon (University of Massachusetts Medical School) for the generous gift of purified yeast Hsp82 protein.

3.7 References

1. Lai, B.T., et al., *Quantitation and intracellular localization of the 85K heat shock protein by using monoclonal and polyclonal antibodies.* Mol Cell Biol, 1984. **4**(12): p. 2802-10.
2. Kamal, A., M.F. Boehm, and F.J. Burrows, *Therapeutic and diagnostic implications of Hsp90 activation.* Trends Mol Med, 2004. **10**(6): p. 283-90.
3. Ferrarini, M., et al., *Unusual expression and localization of heat-shock proteins in human tumor cells.* Int J Cancer, 1992. **51**(4): p. 613-9.
4. Roe, S.M., et al., *The Mechanism of Hsp90 regulation by the protein kinase-specific cochaperone p50(cdc37).* Cell, 2004. **116**(1): p. 87-98.
5. Whitesell, L. and S.L. Lindquist, *HSP90 and the chaperoning of cancer.* Nat Rev Cancer, 2005. **5**(10): p. 761-72.
6. Chiosis, G. and L. Neckers, *Tumor selectivity of Hsp90 inhibitors: the explanation remains elusive.* ACS Chem Biol, 2006. **1**(5): p. 279-84.
7. Solit, D.B. and G. Chiosis, *Development and application of Hsp90 inhibitors.* Drug Discov Today, 2008. **13**(1-2): p. 38-43.
8. Stebbins, C.E., et al., *Crystal structure of an Hsp90-geldanamycin complex: targeting of a protein chaperone by an antitumor agent.* Cell, 1997. **89**(2): p. 239-50.
9. Prodromou, C., et al., *Identification and structural characterization of the ATP/ADP-binding site in the Hsp90 molecular chaperone.* Cell, 1997. **90**(1): p. 65-75.

10. Terasawa, K., M. Minami, and Y. Minami, *Constantly updated knowledge of Hsp90.* J Biochem, 2005. **137**(4): p. 443-7.
11. Minami, Y., et al., *Analysis of native forms and isoform compositions of the mouse 90-kDa heat shock protein, HSP90.* J Biol Chem, 1991. **266**(16): p. 10099-103.
12. Dutta, R. and M. Inouye, *GHKL, an emergent ATPase/kinase superfamily.* Trends Biochem Sci, 2000. **25**(1): p. 24-8.
13. Hawle, P., et al., *The middle domain of Hsp90 acts as a discriminator between different types of client proteins.* Mol Cell Biol, 2006. **26**(22): p. 8385-95.
14. Soti, C., et al., *Comparative analysis of the ATP-binding sites of Hsp90 by nucleotide affinity cleavage: a distinct nucleotide specificity of the C-terminal ATP-binding site.* Eur J Biochem, 2003. **270**(11): p. 2421-8.
15. Neckers, L., *Development of small molecule Hsp90 inhibitors: utilizing both forward and reverse chemical genomics for drug identification.* Curr Med Chem, 2003. **10**(9): p. 733-9.
16. Workman, P., et al., *Drugging the cancer chaperone HSP90: combinatorial therapeutic exploitation of oncogene addiction and tumor stress.* Ann N Y Acad Sci, 2007. **1113**: p. 202-16.
17. Whitesell, L., et al., *Inhibition of heat shock protein HSP90-pp60v-src heteroprotein complex formation by benzoquinone ansamycins: essential role for stress proteins in oncogenic transformation.* Proc Natl Acad Sci U S A, 1994. **91**(18): p. 8324-8.
18. Mimnaugh, E.G., C. Chavany, and L. Neckers, *Polyubiquitination and proteasomal degradation of the p185c-erbB-2 receptor protein-tyrosine kinase induced by geldanamycin.* J Biol Chem, 1996. **271**(37): p. 22796-801.
19. Blagg, B.S. and T.D. Kerr, *Hsp90 inhibitors: small molecules that transform the Hsp90 protein folding machinery into a catalyst for protein degradation.* Med Res Rev, 2006. **26**(3): p. 310-38.
20. Neckers, L., *Chaperoning oncogenes: Hsp90 as a target of geldanamycin.* Handb Exp Pharmacol, 2006(172): p. 259-77.
21. Supko, J.G., et al., *Preclinical pharmacologic evaluation of geldanamycin as an antitumor agent.* Cancer Chemother. Pharmacol., 1995. **36**: p. 305-315.
22. Schnur, R.C., et al., *erbB-2 oncogene inhibition by geldanamycin derivatives: synthesis, mechanism of action, and structure-activity relationships.* J Med Chem, 1995. **38**(19): p. 3813-20.
23. Schnur, R.C., et al., *Inhibition of the oncogene product p185erbB-2 in vitro and in vivo by geldanamycin and dihydrogeldanamycin derivatives.* J Med Chem, 1995. **38**(19): p. 3806-12.
24. Mandler, R., et al., *Modifications in Synthesis Strategy Improve the Yield and Efficacy of Geldanamycin-Herceptin Immunoconjugates.* Bioconjugate Chemistry, 2002. **13**(4): p. 786-791.
25. Kuduk, S.D., et al., *Synthesis and evaluation of geldanamycin-testosterone hybrids.* Bioorganic & Medicinal Chemistry Letters, 2000. **10**(11): p. 1303-1306.
26. Kuduk, S.D., et al., *Synthesis and evaluation of geldanamycin-estradiol hybrids.* Bioorganic & Medicinal Chemistry Letters, 1999. **9**(9): p. 1233-1238.

27. Heath, E.I., et al., *A phase II trial of 17-allylamino-17- demethoxygeldanamycin in patients with hormone-refractory metastatic prostate cancer.* Clin Prostate Cancer, 2005. **4**(2): p. 138-41.
28. Ronnen, E.A., et al., *A phase II trial of 17-(Allylamino)-17-demethoxygeldanamycin in patients with papillary and clear cell renal cell carcinoma.* Invest New Drugs, 2006. **24**(6): p. 543-6.
29. Pacey, S., et al., *Hsp90 inhibitors in the clinic.* Handb Exp Pharmacol, 2006(172): p. 331-58.
30. Peng, C., et al., *Inhibition of heat shock protein 90 prolongs survival of mice with BCR-ABL-T315I-induced leukemia and suppresses leukemic stem cells.* Blood, 2007. **110**(2): p. 678-85.
31. Donnelly, A. and B.S. Blagg, *Novobiocin and additional inhibitors of the Hsp90 C-terminal nucleotide-binding pocket.* Curr Med Chem, 2008. **15**(26): p. 2702-17.
32. Marcu, M.G., T.W. Schulte, and L. Neckers, *Novobiocin and related coumarins and depletion of heat shock protein 90-dependent signaling proteins.* J Natl Cancer Inst, 2000. **92**(3): p. 242-8.
33. Allan, R.K., et al., *Modulation of chaperone function and cochaperone interaction by novobiocin in the C-terminal domain of Hsp90: evidence that coumarin antibiotics disrupt Hsp90 dimerization.* J Biol Chem, 2006. **281**(11): p. 7161-71.
34. Smith, J.R. and P. Workman, *Targeting CDC37: an alternative, kinase-directed strategy for disruption of oncogenic chaperoning.* Cell Cycle, 2009. **8**(3): p. 362-72.
35. Holmes, J.L., et al., *Silencing of HSP90 cochaperone AHA1 expression decreases client protein activation and increases cellular sensitivity to the HSP90 inhibitor 17-allylamino-17-demethoxygeldanamycin.* Cancer Res, 2008. **68**(4): p. 1188-97.
36. Powers, M.V., P.A. Clarke, and P. Workman, *Dual targeting of HSC70 and HSP72 inhibits HSP90 function and induces tumor-specific apoptosis.* Cancer Cell, 2008. **14**(3): p. 250-62.
37. Smith, J.R., et al., *Silencing the cochaperone CDC37 destabilizes kinase clients and sensitizes cancer cells to HSP90 inhibitors.* Oncogene, 2008.
38. Cortajarena, A.L., F. Yi, and L. Regan, *Designed TPR modules as novel anticancer agents.* ACS Chem Biol, 2008. **3**(3): p. 161-6.
39. Yi, F. and L. Regan, *A novel class of small molecule inhibitors of Hsp90.* ACS Chem Biol, 2008. **3**(10): p. 645-54.
40. Ngassapa, O., et al., *Quinone-methide triterpenes and salaspermic acid from Kokoona ochracea.* J Nat Prod, 1994. **57**(1): p. 1-8.
41. Zhang, T., et al., *A novel Hsp90 inhibitor to disrupt Hsp90/Cdc37 complex against pancreatic cancer cells.* Mol Cancer Ther, 2008. **7**(1): p. 162-70.
42. Reed, S.I., *The selection of S. cerevisiae mutants defective in the start event of cell division.* Genetics, 1980. **95**(3): p. 561-77.
43. Pearl, L.H., *Hsp90 and Cdc37 -- a chaperone cancer conspiracy.* Curr Opin Genet Dev, 2005. **15**(1): p. 55-61.
44. Schwarze, S.R., V.X. Fu, and D.F. Jarrard, *Cdc37 enhances proliferation and is necessary for normal human prostate epithelial cell survival.* Cancer Res, 2003. **63**(15): p. 4614-9.

45. Stepanova, L., et al., *Induction of human Cdc37 in prostate cancer correlates with the ability of targeted Cdc37 expression to promote prostatic hyperplasia.* Oncogene, 2000. **19**(18): p. 2186-93.
46. MacLean, M. and D. Picard, *Cdc37 goes beyond Hsp90 and kinases.* Cell Stress Chaperones, 2003. **8**(2): p. 114-119.
47. Grammatikakis, N., et al., *p50cdc37 acting in concert with Hsp90 is required for Raf-1 function.* Mol. Cell Biol., 1999. **19**: p. 1661-1672.
48. Shao, J., et al., *Hsp90 Regulates p50cdc37 Function during the Biogenesis of the Active Conformation of the Heme-regulated eIF2alpha Kinase.* J. Biol. Chem., 2001. **276**: p. 206-214.
49. Shao, J., et al., *Phosphorylation of serine 13 is required for the proper function of the Hsp90 co-chaperone, Cdc37.* J Biol Chem, 2003. **278**(40): p. 38117-20.
50. Zhang, W., et al., *Biochemical and structural studies of the interaction of Cdc37 with Hsp90.* J Mol Biol, 2004. **340**(4): p. 891-907.
51. Siligardi, G., et al., *Regulation of Hsp90 ATPase activity by the co-chaperone Cdc37p/p50cdc37.* J Biol Chem, 2002. **277**(23): p. 20151-9.
52. Ward, B.K., et al., *A structure-based mutational analysis of cyclophilin 40 identifies key residues in the core tetratricopeptide repeat domain that mediate binding to Hsp90.* J Biol Chem, 2002. **277**(43): p. 40799-809.
53. Ali, J.A., et al., *The 43-kilodalton N-terminal fragment of the DNA gyrase B protein hydrolyzes ATP and binds coumarin drugs.* Biochemistry, 1993. **32**(10): p. 2717-24.
54. Yun, B.G., et al., *Novobiocin induces a distinct conformation of Hsp90 and alters Hsp90-cochaperone-client interactions.* Biochemistry, 2004. **43**(25): p. 8217-29.
55. Sullivan, W., et al., *Nucleotides and two functional states of hsp90.* J Biol Chem, 1997. **272**(12): p. 8007-12.
56. Johnson, B.D., et al., *Hop modulates Hsp70/Hsp90 interactions in protein folding.* J Biol Chem, 1998. **273**(6): p. 3679-86.
57. Sullivan, W.P., B.A. Owen, and D.O. Toft, *The influence of ATP and p23 on the conformation of hsp90.* J Biol Chem, 2002. **277**(48): p. 45942-8.
58. Huang, F.C., et al., *Novel cytokine release inhibitors. Part I: Triterpenes.* Bioorg Med Chem Lett, 1998. **8**(14): p. 1883-6.
59. Yang, H., et al., *Celastrol, a triterpene extracted from the Chinese "Thunder of God Vine," is a potent proteasome inhibitor and suppresses human prostate cancer growth in nude mice.* Cancer Res, 2006. **66**(9): p. 4758-65.
60. Trott, A., et al., *Activation of heat shock and antioxidant responses by the natural product celastrol: transcriptional signatures of a thiol-targeted molecule.* Mol Biol Cell, 2008. **19**(3): p. 1104-12.
61. Lee, J.H., et al., *Inhibition of NF-kappa B activation through targeting I kappa B kinase by celastrol, a quinone methide triterpenoid.* Biochem Pharmacol, 2006. **72**(10): p. 1311-21.
62. Wandinger, S.K., K. Richter, and J. Buchner, *The Hsp90 chaperone machinery.* J Biol Chem, 2008. **283**(27): p. 18473-7.
63. Richter, K., et al., *Sti1 is a non-competitive inhibitor of the Hsp90 ATPase. Binding prevents the N-terminal dimerization reaction during the atpase cycle.* J Biol Chem, 2003. **278**(12): p. 10328-33.

64. Martinez-Ruiz, A., et al., *S-nitrosylation of Hsp90 promotes the inhibition of its ATPase and endothelial nitric oxide synthase regulatory activities.* Proc Natl Acad Sci U S A, 2005. **102**(24): p. 8525-30.
65. Onuoha, S.C., et al., *Structural studies on the co-chaperone Hop and its complexes with Hsp90.* J Mol Biol, 2008. **379**(4): p. 732-44.
66. Zhao, R. and W.A. Houry, *Hsp90: a chaperone for protein folding and gene regulation* Biochem Cell Biol, 2005. **83**: p. 703-710.
67. Caplan, A.J., A.K. Mandal, and M.A. Theodoraki, *Molecular chaperones and protein kinase quality control.* Trends Cell Biol, 2007. **17**(2): p. 87-92.
68. Hartson, S.D., et al., *p50cdc37 is a nonexclusive Hsp90 cohort which participates intimately in Hsp90-mediated folding of immature kinase molecules.* Biochemistry, 2000. **39**: p. 7631-7644.
69. Lee, P., et al., *Sti1 and Cdc37 Can Stabilize Hsp90 in Chaperone Complexes with a Protein Kinase.* Mol. Biol. Cell 2004. **15**: p. 1785-1792.
70. Marcu, M.G., et al., *The heat shock protein 90 antagonist novobiocin interacts with a previously unrecognized ATP-binding domain in the carboxyl terminus of the chaperone.* J Biol Chem, 2000. **275**(47): p. 37181-6.
71. Prodromou, C., et al., *Regulation of Hsp90 ATPase activity by tetratricopeptide repeat (TPR)-domain co-chaperones.* EMBO J, 1999. **18**(3): p. 754-62.
72. Sreeramulu, S., et al., *Molecular mechanism of inhibition of the human protein complex Hsp90-Cdc37, a kinome chaperone-cochaperone, by triterpene celastrol.* Angew Chem Int Ed Engl, 2009. **48**(32): p. 5853-5.
73. Fuska, J., et al., *Novel cytotoxic and antitumor agents. IV. Withaferin A: relation of its structure to the in vitro cytotoxic effects on P388 cells.* Neoplasma, 1984. **31**(1): p. 31-6.
74. Kaileh, M., et al., *Withaferin a strongly elicits IkappaB kinase beta hyperphosphorylation concomitant with potent inhibition of its kinase activity.* J Biol Chem, 2007. **282**(7): p. 4253-64.
75. Yu, Y., et al., *Withaferin A targets heat shock protein 90 in pancreatic cancer cells.* Biochem Pharmacol, 2009, in Press.

Figure 3.1 Disruption of Hsp90/p50Cdc37 complex by celastrol but not GA and its derivatives

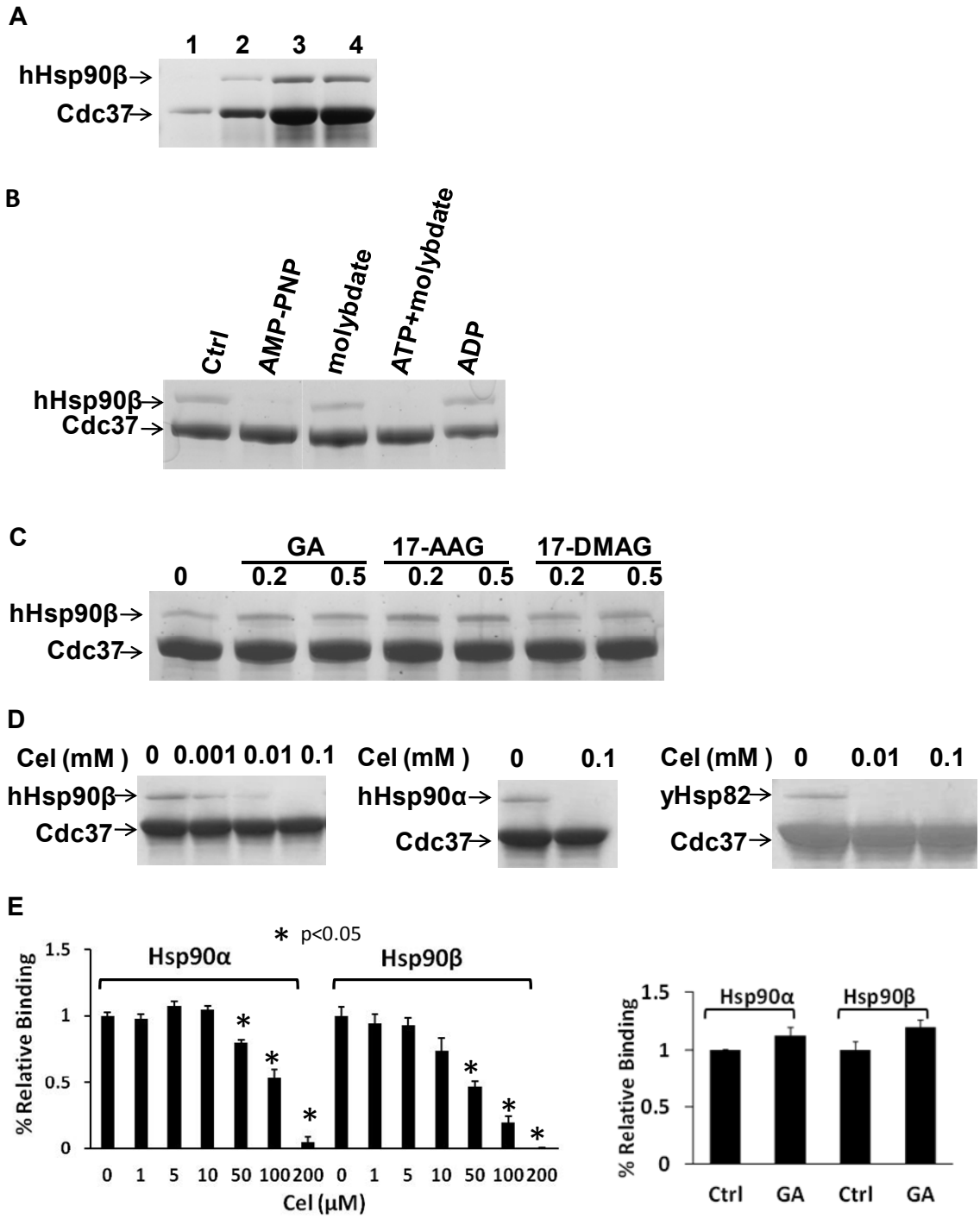

Figure 3.2 Chemical specificity of celastrol on Hsp90/p50Cdc37 complex disruption

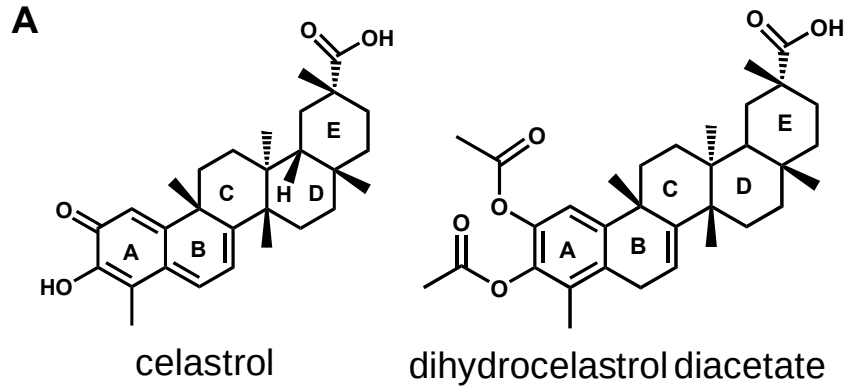

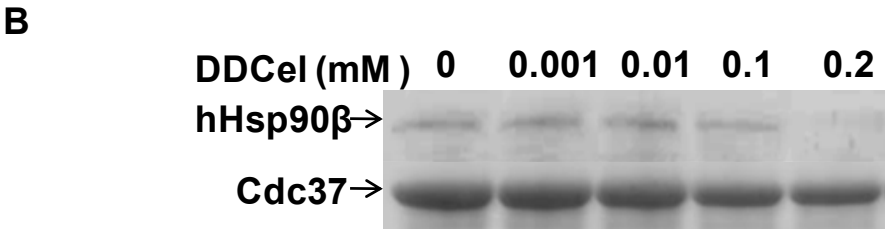

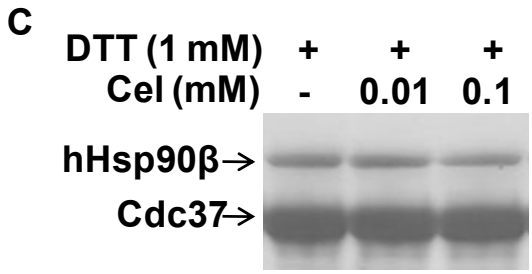

Figure 3.3 Celastrol targets on Hsp90

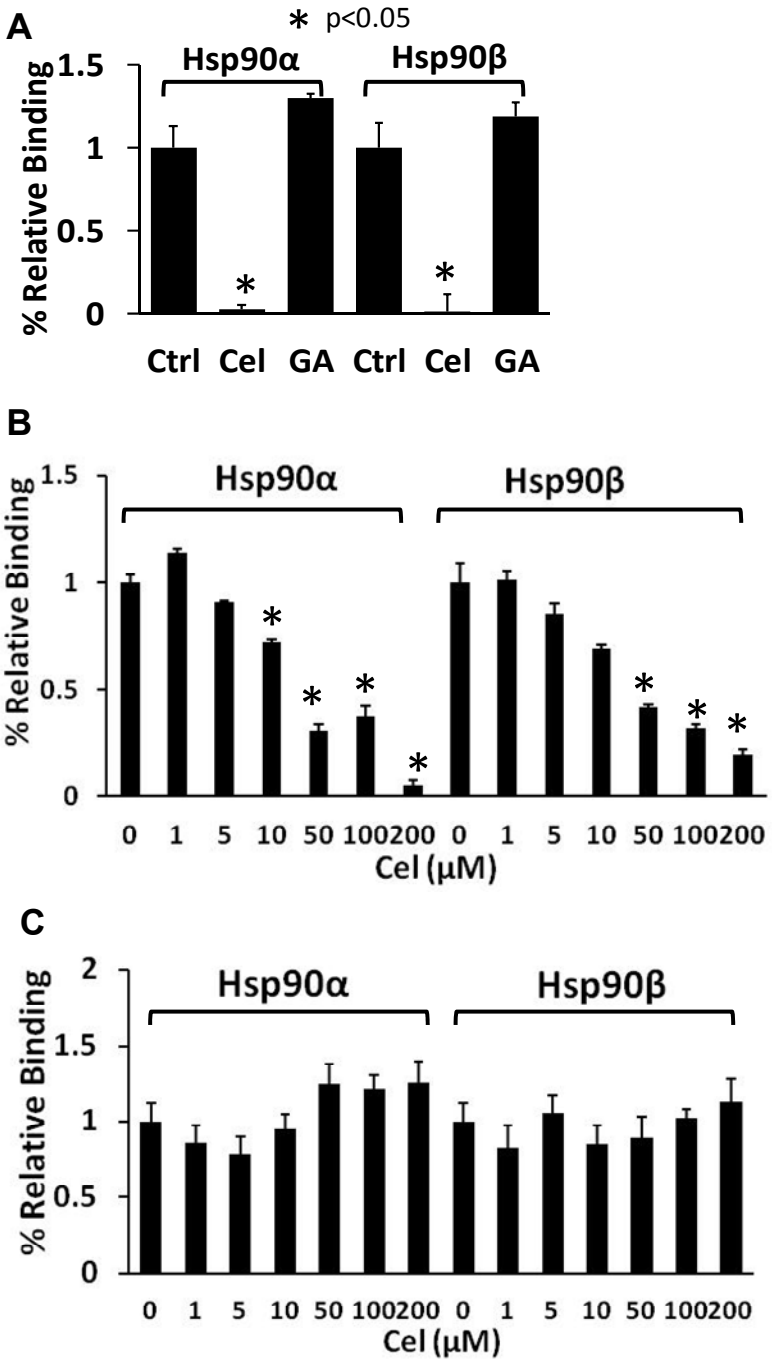

Figure 3.4 Celastrol inhibits Hsp90 ATPase activity and binds to its C-terminal domain

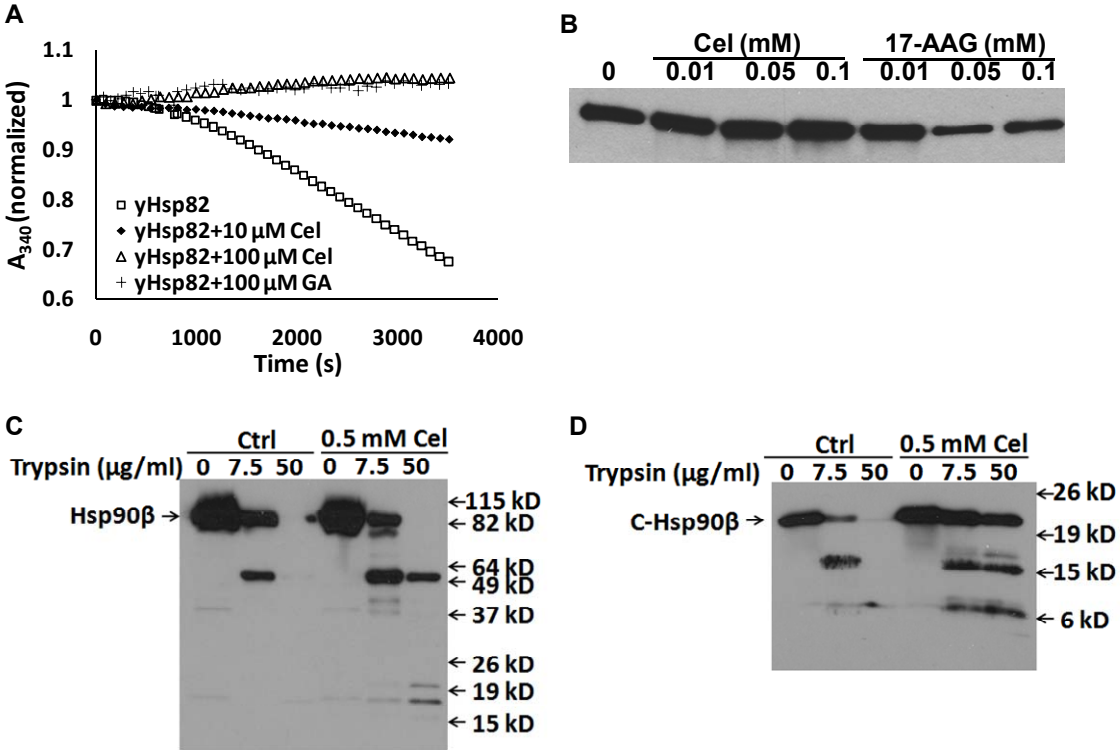

CHAPTER 4

MEK Inhibition Potentiates the Activity of Hsp90 Inhibitor 17-AAG against Pancreatic Cancer Cells

4.1 Abstract

The Ras/Raf/MEK/ERK signaling cascade has been implicated in uncontrolled cell proliferation and tumor progression in pancreatic cancer. The purpose of this study is to evaluate the antitumor activity of the MEK inhibitor U0126 in combination with the Hsp90 inhibitor 17-allylamino-17-demethoxygeldanamycin (17-AAG) in pancreatic cancer cells. Western blotting showed that 17-AAG caused a 2- to 3-fold transient activation of MEK/ERK signaling in pancreatic cancer cells. The activation was sustained for 6 h before phospho-ERK (p-ERK) destabilization. The selective MEK inhibitor U0126 completely abolished the 17-AAG induced ERK1/2 activation and resulted in more than 80% of phosphor-ERK degradation after only a 15 min treatment. Moreover, U0126 had a complementary effect on 17-AAG regulated oncogenic and cell cycle related proteins. Although 17-AAG downregulated cyclin D1, cyclin E, CDK4 and CDK6, it led to cyclin A and CDK2 accumulation, which was reversed by the addition of U0126. Anti-proliferation assay showed that the combination of U0126 and 17-AAG resulted in a synergistic cytotoxic effect. More importantly, 17-AAG alone only exhibited moderate inhibition of cell migration *in vitro*, while addition of U0126 dramatically enhanced the inhibitory effect by 2- to 5-fold. Taken together, these data demonstrate that the MEK inhibitor U0126 potentiates the activity of the Hsp90 inhibitor 17-AAG against

pancreatic cancer cells. The combination of Hsp90 and MEK inhibition could provide a promising avenue for the treatment of pancreatic cancer.

4.2 Introduction

Pancreatic cancer is the fourth leading cause of cancer death in the United States [1]. It is an aggressive and devastating disease, and most patients diagnosed with pancreatic cancer die of their disease within months [2]. Despite efforts in the past several decades, conventional treatments such as surgery, radiation, chemotherapy, or the combination of these have had little impact on the progression of this disease [3]. The average one-year and five-year survival of pancreatic cancer patients is merely 24% and 5%, respectively [4]. The low survival rate of pancreatic cancer patients is attributable to the fact that less than 20% of patients have confined tumors in pancreas at the time of diagnosis; a majority of patients (>80%) are present with advanced or distant metastases which cannot be treated with surgical removal [2]. Even within the 15-20% of patients who are able to undergo potentially curative resection, the 5-year survival is only 20% [5].

The advances in molecular biology have dramatically improved our knowledge of pancreatic cancer pathogenesis and provided the foundation for targeted therapy. Some of the important genetic and epigenetic changes have been targeted for therapy of various solid tumors, such as cetuximab against EGFR, Herceptin against HER2/Neu and tyrosine kinase inhibitors [6]. However, the clinical results for those single targeted agents have not shown impressive efficacy for pancreatic cancer therapy [6]. Considering that pancreatic cancer has multiple biochemical and genetic abnormalities, targeting a single pathway is unlikely to be effective. Thus, discovery of molecular targets that

modulate multiple signaling pathways, such as molecular chaperone Hsp90, has emerged as a promising strategy.

Hsp90 is a highly abundant molecular chaperone in eukaryotic cells [7]. It simultaneously regulates the conformation, activation, maturation, and stability of a wide range of client proteins, many of which are mutated and/or overexpressed signaling proteins in cancers [8-10]. Hsp90 inhibition results in ubiquitination and proteasomal degradation of client proteins, thus rendering potent anticancer activity [11]. Currently, several Hsp90 inhibitors, such as 17-allylamino-17-demethoxygeldanamycin (17-AAG) and 17-allylamino-17-demethoxy-geldanamycin hydroquinone hydrochloride (IPI-504), are in clinical trials to treat various types of cancer [12, 13]. However, the detailed kinetics of Hsp90 client protein activation and degradation and their impact on cancer development have not yet been fully understood. It is generally accepted that Hsp90 inhibition shows anticancer activity via degradation of various oncogenic proteins. However, Price et al have reported that 17-AAG and other Hsp90 inhibitors can enhance osteoclast formation and may potentiate bone metastasis of a human breast cancer cell line MDA-Mb-231SA [14]. Hsp90 inhibition also promotes growth of prostate carcinoma cells (PC-3M) in bone in the xenograft model, which may be due to transient activation of ERK, Akt and Src kinase [15].

Therefore, preventing the short-lived kinase activation induced by Hsp90 inhibition may further enhance the therapeutic efficacy of 17-AAG. In the present study, we found that 17-AAG induced the transient activation of ERK and Src kinase in pancreatic cancer cells. U0126, a potent and selective MEK inhibitor [16], abolished the transient ERK activation induced by 17-AAG and potentiated the growth inhibitory effect

of 17-AAG against pancreatic cancer cells. Combination of U0126 with 17-AAG also suppressed pancreatic cancer cell migration. These data support the combinational use of Hsp90 inhibitors with specific Raf/MEK/ERK signaling inhibitors in pancreatic cancer treatment.

4.3 Materials and Methods

4.3.1 Cell culture and reagents

Human pancreatic cancer cell lines PANC-1, MIA PaCa-2, BxPC-3 and AsPC-1 were obtained from the American Type Culture Collection (Rockville, MD, USA). PANC-1, BxPC-3 and AsPC-1 were maintained in RPMI-1640, and MIA PaCa-2 in Dulbecco's Modified Eagle's Medium (DMEM) (Gibco, Grand Island, NY). All growth media contain 10% Fetal Bovine Serum, 100 units/ml penicillin, and 100 μg/ml streptomycin. Hsp90 inhibitors 17-AAG and radicicol were purchased from LC Labs (Woburn, MA). MEK1/2 inhibitor U0126 was obtained from Cell Signaling Technologies Inc. (Beverly, MA). The compounds were dissolved in dimethyl sulfoxide (DMSO)/ethanol and 20 mM stock aliquots were stored at -20 °C.

4.3.2 Western blotting

Cells were seeded in 100-mm tissue culture dishes and grown to 80% confluence in medium supplemented with 10% FBS. Drug treated or control cells were washed twice in cold phosphate-buffered saline (PBS), scraped off the plate, and lysed in RIPA lysis buffer containing 25 mM Tris-HCl pH 7.6, 150 mM NaCl, 1% NP-40, 1% sodium deoxycholate, 0.1% SDS, and protease inhibitors. After incubation on ice for 20 min, cell extracts were clarified by centrifugation at 14 000 g for 10 min at 4 °C, and protein

concentrations were determined by BCA method (Pierce, Rockford, IL). Equal amount of protein was separated by SDS-PAGE and transferred onto PVDF membrane (Biorad, Hercules, CA). To detect pERK and pSrc, cells were starved in serum-free medium for 20 h before drug treatment. Antibodies to Akt, phospho-Src (Tyr-416), Src, phospho-ERK1/2, ERK1/2 were purchased from Cell Signaling Technology (Beverly, MA); antibodies to Hsp90, Hsp70, Raf-1, cyclin A, cyclin D1, cyclin E, CDK2, CDK4, CDK6, p27 were from Santa Cruz Biotechnology (Santa Cruz, CA). Immunodetection was performed with corresponding horseradish peroxide-conjugated secondary antibodies and detected by enhanced chemiluminescence assay (ECl, Amersham, Piscataway, NJ). Quantification of Western blotting bands was performed by densitomery analysis with Image J software (NIH, Bethesda, MD).

4.3.3 Cell proliferation assay

Cells were seeded in 96-well plates at a density of 3000-5000 cells per well. After an overnight attachment period, cells were exposed to various concentrations of 17-AAG and U0126, alone or in combination for 48 h. Control cells received DMSO only. The percentage of viable cells was assessed with a colorimetric MTS (3,4-(5-dimethylthiazol-2-yl)-5-(3-carboxymethoxyphenyl)-2-(4-sulfophenyl)-2H-tetrazolium salt) cell proliferation assay (Promega, Madison, WI). The IC_{50} values for cytotoxicity were calculated with WinNonlin software (Pharsight, Mountain View, CA). All experiments were carried out in hexaplicate and repeated at least twice independently.

4.3.4 Cell migration assay

Cell migration assays were performed using 24-well Costar Transwell chambers with 8.0 μm pore polycarbonate membranes (Corning Inc., Corning, NY). The bottom

chambers were filled with 600 µl of cell culture medium supplemented with 10% FBS. Pancreatic cancer cells (Mia PaCa-2, AsPC-1) were detached with 0.05% trypsin/EDTA, and resuspended at 1×10^6 cells/ml in serum-free medium. An 100 µl aliquot of cell suspension was added to the upper chamber. After 2 h incubation to allow cell attachment, inhibitors or DMSO was added to the upper chambers and cells were allowed to migrate for 24 h at 37 °C. Cells on the upper side of the membrane were gently removed with cotton swabs, while those that have penetrated to the bottom side of the membrane were fixed with ice-cold methanol for 10 min and stained with 0.5% crystal violet solution. After rinsing with water, the dye was extracted by the addition of 10% acetic acid. The absorbance at 570 nm, which is corresponding to the number of live adherent cells, was measured with a microplate reader.

4.3.5 Wound healing assay

Cells were seeded into 6-well plates to obtain 80%-90% confluence. After serum starvation, wounds were made by dragging a sterile pipette tip through the monolayer. Cells were washed to remove debris and 17-AAG and/or U0126 was added with 25 ng/ml mitomycin C, which was used to inhibit proliferation. Images were taken under an inverted microscope and migration index was calculated as follows: migration index= [(width of wound at time 0 h - width of wound at time t h)/ width of wound at time 0 h] × 100%.

4.3.6 Statistics

All values are expressed as means ±SD. When appropriate, statistical significance (defined as $p < 0.05$) was determined by Student *t* test.

4.4 Results

4.4.1 Src and ERK activation after 17-AAG treatment

We investigated the ability of 17-AAG to activate ERK by Western blotting (Figure 4.1). Mia PaCa-2 cells were exposed to 17-AAG for 24 h. We observed a slight increase of p-ERK1/2 level upon 0.03 μM (~IC50, shown later in Figure 4.3) 17-AAG treatment, which peaked at 3 h with a 2-fold increase (Figure 4.1A). Thereafter, it progressively declined to basal level. At 24 h, there was no discernible difference in p-ERK level compared with non-treatment control at 0 h. The transient increase of p-ERK was dose-dependent, which reached maximum level upon 0.5-1 μM 17-AAG treatment (Figure 4.1B). After treatment with 1 μM 17-AAG, p-ERK protein level increased about 3-fold at 1 h followed by gradual degradation (Figure 4.1C). At 24h, the p-ERK protein level reduced to approximately 60% of control. There was no obvious change in total ERK protein. Similar ERK activation was also observed in another Hsp90 inhibitor radicicol (Figure 4.1D).

It has been reported that in T24 cell, a cell line derived from transitional cancers of human bladder, Src activation accounts for the transient increase of p-ERK caused by GA treatment [17]. To examine the possible involvement of Src in 17-AAG induced ERK activation in pancreatic cancer cells, we tested Src phosphorylation on Tyr-418, which indicates Src activation. We noticed a similar trend of p-Src increase, with slightly stronger magnitude and longer duration compared with p-ERK transient increase (Figure 4.1E). The accumulation of p-Src started after 15 min treatment and reached peak at 1 h with a 4-fold increase. The protein level of total Src had no change. These data suggest

that the activation of Src and ERK may correlate with each other in pancreatic cancer cells after 17-AAG treatment.

4.4.2 MEK inhibitor abolished 17-AAG induced Src and ERK activation

The activation of MEK/ERK signal transduction cascade has been implicated in human pancreatic cancer [18]. We used selective MEK inhibitor U0126 to test whether it inhibits 17-AAG stimulated MEK/ERK activation. MTS assay has shown that 10-20 μM of U0126 had very little anti-proliferative effect, therefore, we treated Mia PaCa-2 cells with 10 μM of U0126 and collected cells at various time points to monitor the protein levels of p-ERK and p-Src. Surprisingly, U0126 (10 μM) exhibited dramatic inhibition on p-ERK (Figure 4.2A). P-ERK decreased to under detection level after only 15 min treatment, and the inhibition sustained for at least 24 h. Although p-Src degradation did not occur immediately upon U0126 treatment, p-Src did decrease progressively and we never noticed any increase as that after 17-AAG treatment (Figure 4.2B). Next, we treated cells with the combination of 17-AAG and U0126 (Figure 4.2C&D). The data showed that U0126 completely abrogated 17-AAG induced p-ERK activation, and the effect is comparable with that treated with U0126 alone (Figure 4.2C). Similarly, 17-AAG stimulated Src activation was also blocked by U0126 (Figure 4.2D). Thus, MEK inhibitors efficiently suppresses the transient MEK/ERK activation caused by 17-AAG.

4.4.3 Combination effect of Hsp90 and MEK inhibition on the signaling proteins

Because the impact of transient Src and ERK activation has not been fully studied, we next evaluated the changes of various signaling proteins in pancreatic cancer cells when treated with 17-AAG and U0126, alone or in combination (Figure 4.2E). 17-AAG exerted broad effects on various oncogenic proteins. For instance, 0.5 μM 17-AAG

resulted in 50% decrease of Raf-1 and over 70% reduction of Akt. As a molecular signature of Hsp90 inhibition, 17-AAG induced the expression of Hsp70. In contrast, U0126 treatment had no effect on Hsp70, little impact on Raf which is upstream of MEK, and minor influence on Akt which has cross-talk with MEK/ERK pathway.

In addition, different response patterns were observed on the expression of cell cycle regulatory proteins after 17-AAG or U0126 treatment (Figure 4.2E). 17-AAG (0.5 μM) treatment decreased cyclin D1 by 70%, cyclin E by 40%, CDK4 by 62% and CDK6 by 53%. Meanwhile, 17-AAG caused marked induction of cyclin A by 3-fold and CDK2 by 1.4-fold. In comparison, U0126 (20 μM) either did not change or only caused a little decrease in the levels of cyclin D1, cyclin E, CDK4, and CDK6, but it downregulated cyclin A by 40% and CDK2 by 80%.

Furthermore, the expression of p27, a critical cell cycle regulator, increased 2- to 3-fold upon U0126 treatment (Figure 4.2E). In contrast, 17-AAG (0.5 μM) exhibited little effect on the expression of p27.

Combination of the two inhibitors exhibited complementary inhibitory effect on various proteins (Figure 4.2E). Using both 17-AAG and U0126 decreased cyclin E levels by more than 67%. In addition, U0126 also reversed the induction of cyclin A and CDK2 caused by 17-AAG.

4.4.4 U0126 potentiated 17-AAG induced cytotoxicity

17-AAG has shown anti-proliferation effect in many cancers including pancreatic carcinoma. Since U0126 blocked 17-AAG induced transient activation and accumulation of signaling proteins, we examined whether this inhibition can sensitize pancreatic cancer cells to 17-AAG. Four pancreatic cancer cell lines (Mia PaCa-2, AsPC-1, BxPC-3,

PANC-1) were treated with 17-AAG or U0126 alone. 17-AAG exhibited potent anti-proliferation effect with IC50 less than 0.05 μM in AsPC-1, BxPC-3 and Mia PaCa-2 (Figure 4.3). In contrast, the efficacy of U0126 was much weaker. Up to 40 μM of U0126 was not able to inhibit 50% of cell growth. This is consistent with the previous studies that U0126 does not possess strong anti-proliferative activity [19]. Next, we examined the combination effect of 17-AAG and U0126 (Figure 4.3). Cells were treated with various concentrations of 17-AAG and 5 μM of U0126. At this concentration, U0126 had produced little anti-proliferative effect. However, this low concentration of U0126 potentiated dose-dependent inhibitory effect of 17-AAG as shown in Figure 4.3. The IC50 of 17-AAG decreased by 50-80% when combined with 17-AAG.

4.4.5 MEK inhibition prevented pancreatic cancer cell migration

It is unknown whether the transient activation of MEK/ERK and Src caused by Hsp90 inhibition undermines the anticancer effect of Hsp90 inhibitors because Hsp90 inhibition will eventually result in the degradation of those kinases and lead to cell death. A few studies suggest that transient activation of AKT and Src in MDA-Mb-231SA breast cancer cells and PC-3M prostate cancer cells may involve in cell migration and metastasis [14, 15] . Since we also observed that 17-AAG induced Src and ERK activation in pancreatic cancer cells, we tested the effect of 17-AAG on pancreatic cell motility by two assays. In wound healing assay, an injury line was marked with a pipette tip and cells were incubated with 17-AAG, U0126 or the combination. In this assay, the concentrations used for 17-AAG and U0126 were 0.02 and 10 μM, because these concentrations exhibited little/minor effect on cell survival determined by MTS assay (Figure 4.3A). The data showed that cell migration index from wound edge to empty

surface in control Mia PaCa-2 and AsPC-1 cells were 76% and 64%, respectively (Figure 4.4A&B). Incubation with 0.02 μM 17-AAG did not show much inhibitory effect on cell migration, with migration index of 67% and 57% in these two pancreatic cancer cell lines. In contrast, 10 μM of U0126 significantly decreased cell migration index, which were 43% and 20% in Mia PaCa-2 and AsPc-1, respectively. The combination of the two inhibitors resulted in maximum inhibitory effect with migration index of 27% and 13% in Mia PaCa-2 and AsPC-1, respectively.

Next, we tested cell migration with Transwell chambers. Pancreatic cancer cells were plated on Transwell membranes in the presence of drug and experiments were conducted as described in materials and methods. As shown in Figure 4.4C&D, 0.02 μM 17-AAG decreased the number of cells penetrating through the membrane to lower surface by 18% and 11% in Mia PaCa-2 and AsPC-1, respectively. Higher concentration of 17-AAG (0.05 μM) inhibited cell penetration by 30% and 17% in these two cell lines. Combination of 0.02 μM 17-AAG and 5 μM U0126 inhibited cell penetration by 47% and 55% in Mia PaCa-2 and AsPC-1, while 0.05 μM 17-AAG and 10 μM U0126 inhibited by 66% and 80% in Mia PaCa-2 and AsPC-1, respectively.

4.5 Discussion

Pancreatic cancer is one of the most lethal human cancers, which causes over 30,000 deaths per year in the United States [20]. Most patients diagnosed with pancreatic cancer are present with locally advanced or metastatic disease, and their average survival duration is within 4-10 months due to the aggressive nature of pancreatic carcinoma [21]. There is no effective treatment for this disease. The study on pathogenesis of pancreatic cancer has revealed that pancreatic carcinogenesis is driven by multiple genetic and

epigenetic changes [6]. Thus, targeting a single molecule that exerts control over multiple oncogenes involved in tumor development and progression may offer advantages to treat this disease. Hsp90 has emerged as a new therapeutic target to simultaneously regulate numerous oncogenic client proteins, which are pathological hallmarks of malignancy [22].

The antibiotic benzoquinone ansamycins, represented by geldanamycin (GA), are the first identified Hsp90 inhibitors [23]. GA has exhibited potent anticancer effect, but the strong hepatotoxicity prevented its clinical development [24]. 17-AAG is a geldanamycin derivative that has less side effect than its parent compound [13]. As the first-in-class Hsp90 inhibitor, 17-AAG has been studied in a number of phase I trials for both solid tumors including prostate, breast, pancreatic cancer and hematological malignancies [13]. At the given doses, 17-AAG resulted in good pharmacokinetic exposures and showed molecular signatures of Hsp90 inhibition such as degradation of CDK4 and induction of Hsp70 [25, 26]. Although cancer patients with prolonged stable disease were observed in several phase I trials using 17-AAG, results from three phase II trials were less impressive, which was likely due to the limited potency and high toxicity of 17-AAG [13]. This suggests that combination of differently targeted therapeutic agents may be required to achieve desired antitumor activity. In this context, several studies have shown a synergistic or additive cytotoxicity via combinational treatment with 17-AAG and other targeted agents against a variety of cancer cells [27-32]. In the current study, we also observed the selective MEK inhibitor U0126 can potentiate the efficacy of 17-AAG in pancreatic cancer cells (Figure 4. 3). A low concentration of U0126 (5 μM), which showed no inhibitory effect alone, substantially enhanced the anti-proliferation effect of 17-AAG.

The potentiation of 17-AAG activity by U0126 may result from the complete inhibition of the MEK/ERK signaling because U0126 is a MEK-specific inhibitor [16]. The Ras/Raf/MEK/ERK cascade, which has been studied intensively, is the first signal transduction cascade delineated from the cell membrane to the nucleus [33]. It is a key intracellular signaling pathway regulating diverse cellular functions including cell proliferation, survival, and migration [34]. The cascade is generally described as a linear signaling pathway initiated by Ras activation, followed by Raf, MEK and ERK activation [34]. The only known targets of MEK1/2 is ERK protein, which in principle are capable of mediating all the diverse functions attributed to this pathway [33, 34]. Active ERK can phosphorylate over 100 possible substrates with diverse functions, either in the nucleus or cytoplasm [35, 36]. Hsp90 inhibitors and specific MEK inhibitors interfered with MEK/ERK signaling in distinct ways. Hsp90 inhibition by 17-AAG initially caused a transient activation of ERK, which could last several hours and then led to the destabilization of activated ERK in pancreatic cancer cells (Figure 4.1A&C). On the contrary, specific MEK inhibitor U0126 resulted in a rapid and complete blockade of the MEK/ERK signaling (Figure 4.2A). This difference could exert diverse influence on related signaling proteins.

The downstream of MEK/ERK pathway include many cell cycle protein kinases, cyclins and mitotic inhibitors [37-39].The cyclin/cyclin-dependent kinase (CDK) complexes, together with the flow of information from outside the cell, play a crucial role in regulating cell cycle progression [40]. Various combinations of the complexes include cyclin D1/CDK4, cylin D1/CDK6, cylcin E/CDK2, cyclin A/CDK1, cyclin A/CDK2, and cyclin B/CDK1 [40, 41]. Several molecules that inhibit cell cycle kinases have been

developed as potential anticancer agents [40]. However, none of these have been approved as an effective strategy to control malignant cell proliferation [40]. A major obstacle is that much remains to be determined on the complicated functions of cyclin/CDK complexes. In our study, we found that 17-AAG caused the degradation of cyclin D1, cyclin E, CDK4 and CDK6, while induced the expression of cyclin A and CDK2 (Fig. 2E). Studies have shown that sensitivity to CDK inhibition depends on tumor type, and CDKs may have compensatory roles in cell cycle control [40]. Therefore, the accumulation of some cyclins and CDKs after 17-AAG treatment might in a sense favor tumor progression, correlating with the activation of ERK. The addition of U0126 could reverse 17-AAG induced accumulation of cyclin A and CDK2 (Figure 4.2E). The activities of cyclin/CDK complexes are regulated by p27, which suppresses cell cycle by binding to and inhibiting cyclin E/CDK2 [42]. 17-AAG did not significantly induce p27 expression, while U0126 dramatically increased p27 expression (Figure 4.2E). Taken together, the combination of MEK and Hsp90 inhibitor exerts more intensive inhibition on proteins downstream of MEK/ERK.

Although there is no direct evidence that transient activation of MEK/ERK attenuates the anti-proliferative effect of Hsp90 inhibitors, there is evidence that it can affect cancer cell motility and promote tumor metastasis under certain circumstances in some breast cancer and prostate cancer cell lines [14, 15, 17]. In evaluation of pancreatic cancer cell motility, we found that 17-AAG showed a relatively weak inhibitory effect on pancreatic cancer cell migration (Figure 4.4). It is worth noting that at the same concentrations (0.02 and 0.05 μM) 17-AAG exhibited potent cytotoxity (Figure 4.3), and thus the inhibition on migration may be over-estimated due to the contribution of cell

death. On the contrary, U0126, at non-growth-inhibitory concentrations, displayed dramatic inhibition of cell migration (Figure 4.4). This is consistent with the studies that MEK inhibitor can effectively inhibit cancer cell motility and metastasis [43-45].

In summary, we have shown that Hsp90 inhibition transiently activates MEK/ERK signaling in pancreatic cancer cells. MEK/ERK inhibition completely suppressed 17-AAG-induced transient ERK activation. Combinational use of Hsp90 and MEK/ERK inhibitors in pancreatic cancer cells may achieve higher efficacy in preventing tumor progression and metastasis.

4.6 Acknowledgments

This work was partially supported by the National Institutes of Health (RO1 CA120023, R21CA143474); University of Michigan Cancer Center Research Grant (Munn); and University of Michigan Cancer Center Core Grant to DS.

4.7 References

1. Jemal, A., et al., *Cancer statistics, 2007.* CA Cancer J Clin, 2007. **57**(1): p. 43-66.
2. Gronborg, M., et al., *Biomarker discovery from pancreatic cancer secretome using a differential proteomic approach.* Mol Cell Proteomics, 2006. **5**(1): p. 157-71.
3. Li, D., et al., *Pancreatic cancer.* Lancet, 2004. **363**(9414): p. 1049-57.
4. *Cancer Facts & Figures 2009.* America Cancer Society
5. Ahrendt, S.A. and H.A. Pitt, *Surgical management of pancreatic cancer.* Oncology (Williston Park), 2002. **16**(6): p. 725-34; discussion 734, 736-8, 740, 743.
6. Xiong, H.Q., *Molecular targeting therapy for pancreatic cancer.* Cancer Chemother Pharmacol, 2004. **54 Suppl 1**: p. S69-77.
7. Lai, B.T., et al., *Quantitation and intracellular localization of the 85K heat shock protein by using monoclonal and polyclonal antibodies.* Mol Cell Biol, 1984. **4**(12): p. 2802-10.
8. Roe, S.M., et al., *The Mechanism of Hsp90 regulation by the protein kinase-specific cochaperone p50(cdc37).* Cell, 2004. **116**(1): p. 87-98.
9. Whitesell, L. and S.L. Lindquist, *HSP90 and the chaperoning of cancer.* Nat Rev Cancer, 2005. **5**(10): p. 761-72.

10. Chiosis, G. and L. Neckers, *Tumor selectivity of Hsp90 inhibitors: the explanation remains elusive.* ACS Chem Biol, 2006. **1**(5): p. 279-84.
11. Kamal, A., M.F. Boehm, and F.J. Burrows, *Therapeutic and diagnostic implications of Hsp90 activation.* Trends Mol Med, 2004. **10**(6): p. 283-90.
12. Messaoudi, S., et al., *Recent advances in Hsp90 inhibitors as antitumor agents.* Anticancer Agents Med Chem, 2008. **8**(7): p. 761-82.
13. Usmani, S.Z., R. Bona, and Z. Li, *17 AAG for HSP90 inhibition in cancer--from bench to bedside.* Curr Mol Med, 2009. **9**(5): p. 654-64.
14. Price, J.T., et al., *The heat shock protein 90 inhibitor, 17-allylamino-17-demethoxygeldanamycin, enhances osteoclast formation and potentiates bone metastasis of a human breast cancer cell line.* Cancer Res, 2005. **65**(11): p. 4929-38.
15. Yano, A., et al., *Inhibition of Hsp90 activates osteoclast c-Src signaling and promotes growth of prostate carcinoma cells in bone.* Proc Natl Acad Sci U S A, 2008. **105**(40): p. 15541-6.
16. Favata, M.F., et al., *Identification of a novel inhibitor of mitogen-activated protein kinase kinase.* J Biol Chem, 1998. **273**(29): p. 18623-32.
17. Koga, F., et al., *Hsp90 inhibition transiently activates Src kinase and promotes Src-dependent Akt and Erk activation.* Proc Natl Acad Sci U S A, 2006. **103**(30): p. 11318-22.
18. Wallace, E.M., et al., *Progress towards therapeutic small molecule MEK inhibitors for use in cancer therapy.* Curr Top Med Chem, 2005. **5**(2): p. 215-29.
19. Hoadley, K.A., et al., *EGFR associated expression profiles vary with breast tumor subtype.* BMC Genomics, 2007. **8**: p. 258.
20. Jemal, A., et al., *Cancer statistics, 2009.* CA Cancer J Clin, 2009. **59**(4): p. 225-49.
21. EVANS, D.B., J.L. ABBRUZZESE, and T.R. RICH, *Cancer of the pancreas. In: De Vita VT , Hellman S , Rosenberg SA , editors.* Cancer Principles and Practice of Oncology, 1997: p. 1054-1087.
22. Workman, P., et al., *Drugging the cancer chaperone HSP90: combinatorial therapeutic exploitation of oncogene addiction and tumor stress.* Ann N Y Acad Sci, 2007. **1113**: p. 202-16.
23. Whitesell, L., et al., *Inhibition of heat shock protein HSP90-pp60v-src heteroprotein complex formation by benzoquinone ansamycins: essential role for stress proteins in oncogenic transformation.* Proc Natl Acad Sci U S A, 1994. **91**(18): p. 8324-8.
24. Supko, J.G., et al., *Preclinical pharmacologic evaluation of geldanamycin as an antitumor agent.* Cancer Chemother. Pharmacol., 1995. **36**: p. 305-315.
25. Banerji, U., et al., *Phase I pharmacokinetic and pharmacodynamic study of 17-allylamino, 17-demethoxygeldanamycin in patients with advanced malignancies.* J Clin Oncol, 2005. **23**(18): p. 4152-61.
26. Goetz, M.P., et al., *Phase I trial of 17-allylamino-17-demethoxygeldanamycin in patients with advanced cancer.* J Clin Oncol, 2005. **23**(6): p. 1078-87.
27. Premkumar, D.R., et al., *Synergistic interaction between 17-AAG and phosphatidylinositol 3-kinase inhibition in human malignant glioma cells.* Mol Carcinog, 2006. **45**(1): p. 47-59.

28. Premkumar, D.R., B. Arnold, and I.F. Pollack, *Cooperative inhibitory effect of ZD1839 (Iressa) in combination with 17-AAG on glioma cell growth.* Mol Carcinog, 2006. **45**(5): p. 288-301.
29. Sain, N., et al., *Potentiation of paclitaxel activity by the HSP90 inhibitor 17-allylamino-17-demethoxygeldanamycin in human ovarian carcinoma cell lines with high levels of activated AKT.* Mol Cancer Ther, 2006. **5**(5): p. 1197-208.
30. Cao, X., et al., *Synergistic antipancreatic tumor effect by simultaneously targeting hypoxic cancer cells with HSP90 inhibitor and glycolysis inhibitor.* Clin Cancer Res, 2008. **14**(6): p. 1831-9.
31. Jane, E.P. and I.F. Pollack, *The heat shock protein antagonist 17-AAG potentiates the activity of enzastaurin against malignant human glioma cells.* Cancer Lett, 2008. **268**(1): p. 46-55.
32. Roforth, M.M. and C. Tan, *Combination of rapamycin and 17-allylamino-17-demethoxygeldanamycin abrogates Akt activation and potentiates mTOR blockade in breast cancer cells.* Anticancer Drugs, 2008. **19**(7): p. 681-8.
33. Galabova-Kovacs, G., et al., *ERK and beyond: insights from B-Raf and Raf-1 conditional knockouts.* Cell Cycle, 2006. **5**(14): p. 1514-8.
34. Friday, B.B. and A.A. Adjei, *Advances in targeting the Ras/Raf/MEK/Erk mitogen-activated protein kinase cascade with MEK inhibitors for cancer therapy.* Clin Cancer Res, 2008. **14**(2): p. 342-6.
35. Dhillon, A.S., et al., *MAP kinase signalling pathways in cancer.* Oncogene, 2007. **26**(22): p. 3279-90.
36. Ramos, J.W., *The regulation of extracellular signal-regulated kinase (ERK) in mammalian cells.* Int J Biochem Cell Biol, 2008. **40**(12): p. 2707-19.
37. Greulich, H. and R.L. Erikson, *An analysis of Mek1 signaling in cell proliferation and transformation.* J Biol Chem, 1998. **273**(21): p. 13280-8.
38. Cheng, M., et al., *Assembly of cyclin D-dependent kinase and titration of p27Kip1 regulated by mitogen-activated protein kinase kinase (MEK1).* Proc Natl Acad Sci U S A, 1998. **95**(3): p. 1091-6.
39. Tachibana, K., et al., *MAP kinase links the fertilization signal transduction pathway to the G1/S-phase transition in starfish eggs.* Embo J, 1997. **16**(14): p. 4333-9.
40. Lapenna, S. and A. Giordano, *Cell cycle kinases as therapeutic targets for cancer.* Nat Rev Drug Discov, 2009. **8**(7): p. 547-66.
41. Masaki, T., et al., *Cyclins and cyclin-dependent kinases: comparative study of hepatocellular carcinoma versus cirrhosis.* Hepatology, 2003. **37**(3): p. 534-43.
42. Larrea, M.D., S.A. Wander, and J.M. Slingerland, *p27 as Jekyll and Hyde: regulation of cell cycle and cell motility.* Cell Cycle, 2009. **8**(21): p. 3455-61.
43. Klemke, R.L., et al., *Regulation of cell motility by mitogen-activated protein kinase.* J Cell Biol, 1997. **137**(2): p. 481-92.
44. Honma, N., et al., *MEK/ERK signaling is a critical mediator for integrin-induced cell scattering in highly metastatic hepatocellular carcinoma cells.* Lab Invest, 2006. **86**(7): p. 687-96.
45. Takino, T., et al., *Membrane type 1 matrix metalloproteinase regulates collagen-dependent mitogen-activated protein/extracellular signal-related kinase activation and cell migration.* Cancer Res, 2004. **64**(3): p. 1044-9.

Figure 4.1 Transient activation of ERK and Src by Hsp90 inhibition

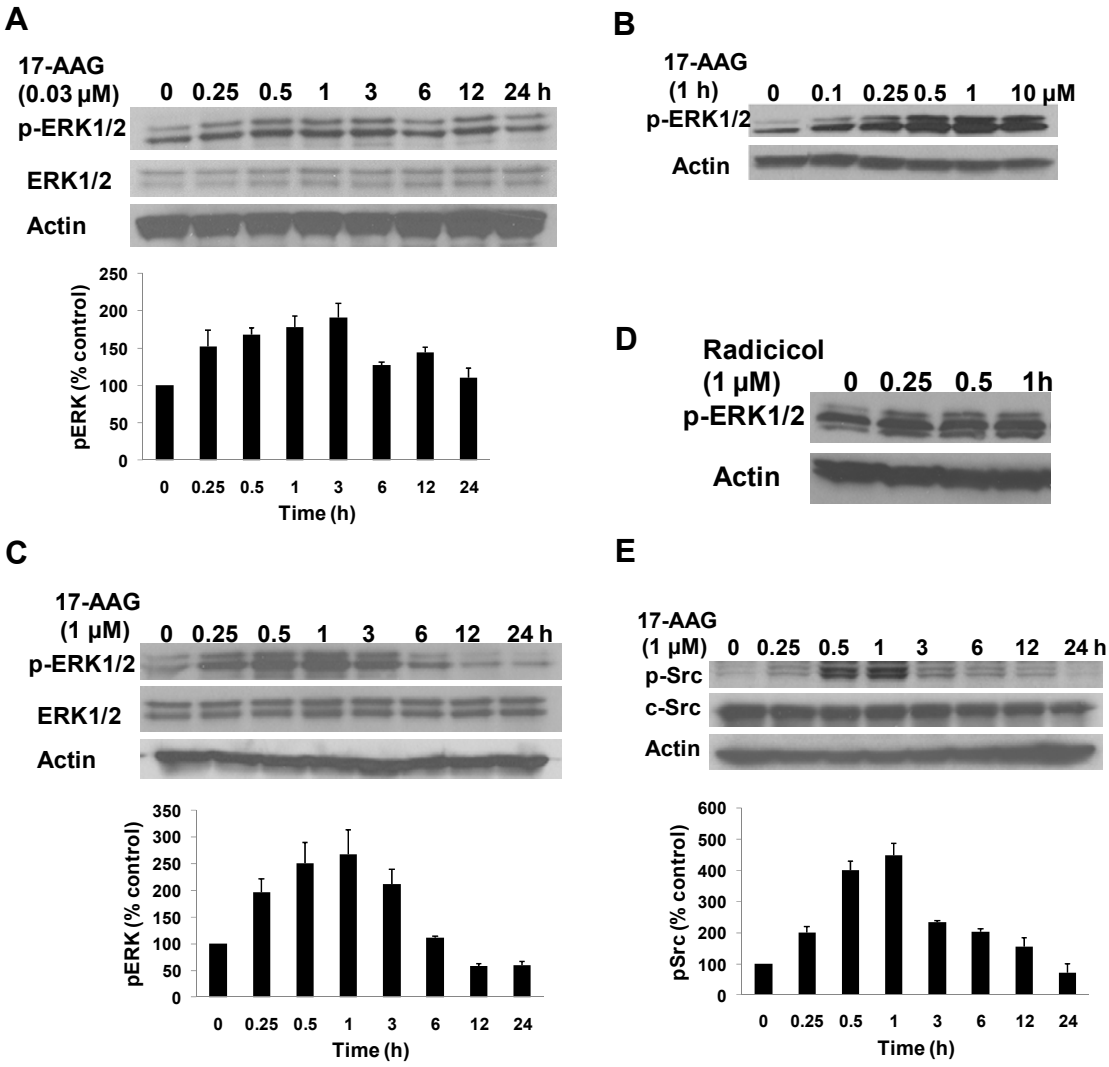

Figure 4.2 MEK inhibitor U0126 blocked 17-AAG induced ERK activation

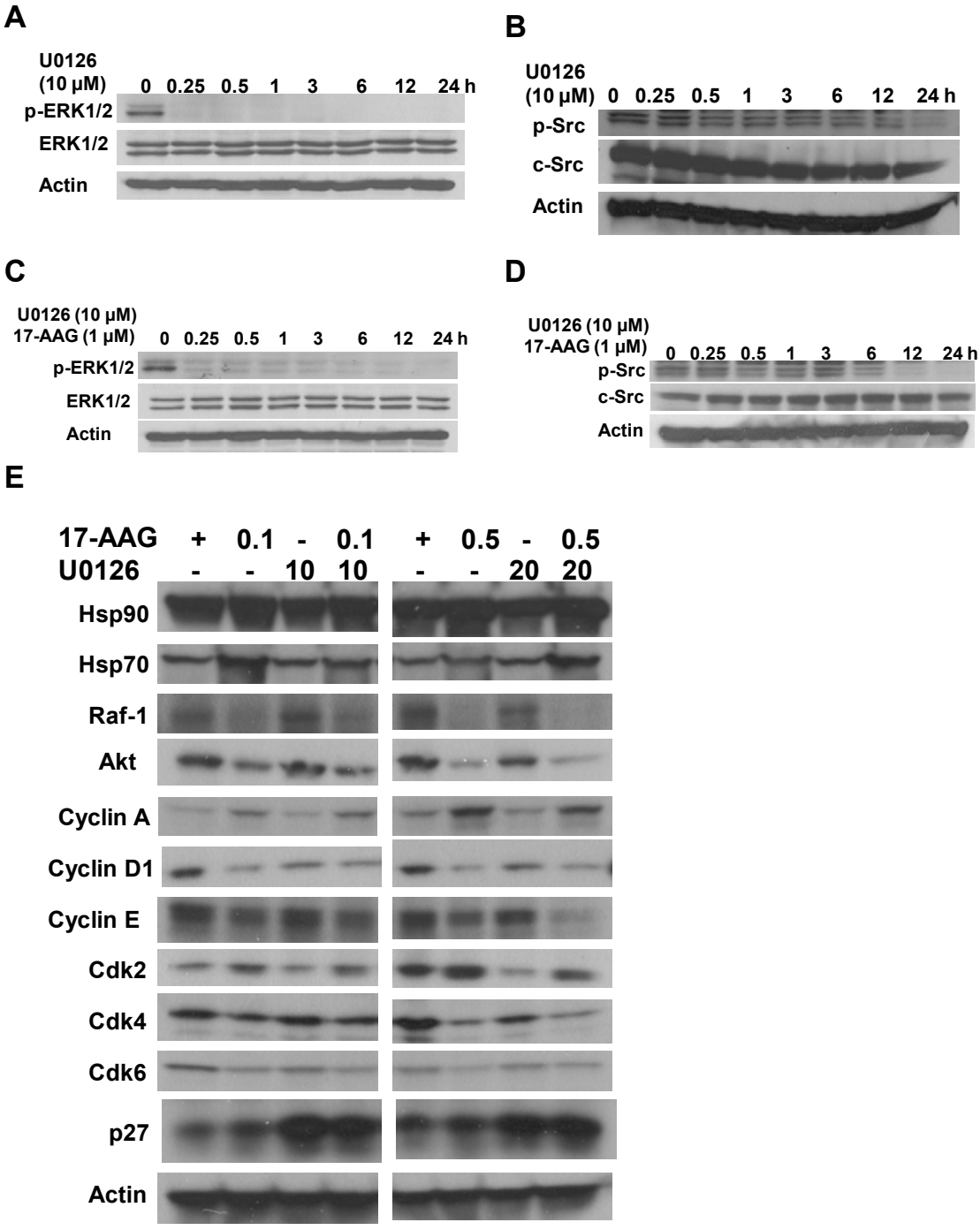

Figure 4.3 MEK inhibitor U0126 enhanced the anti-proliferation activity of 17-AAG

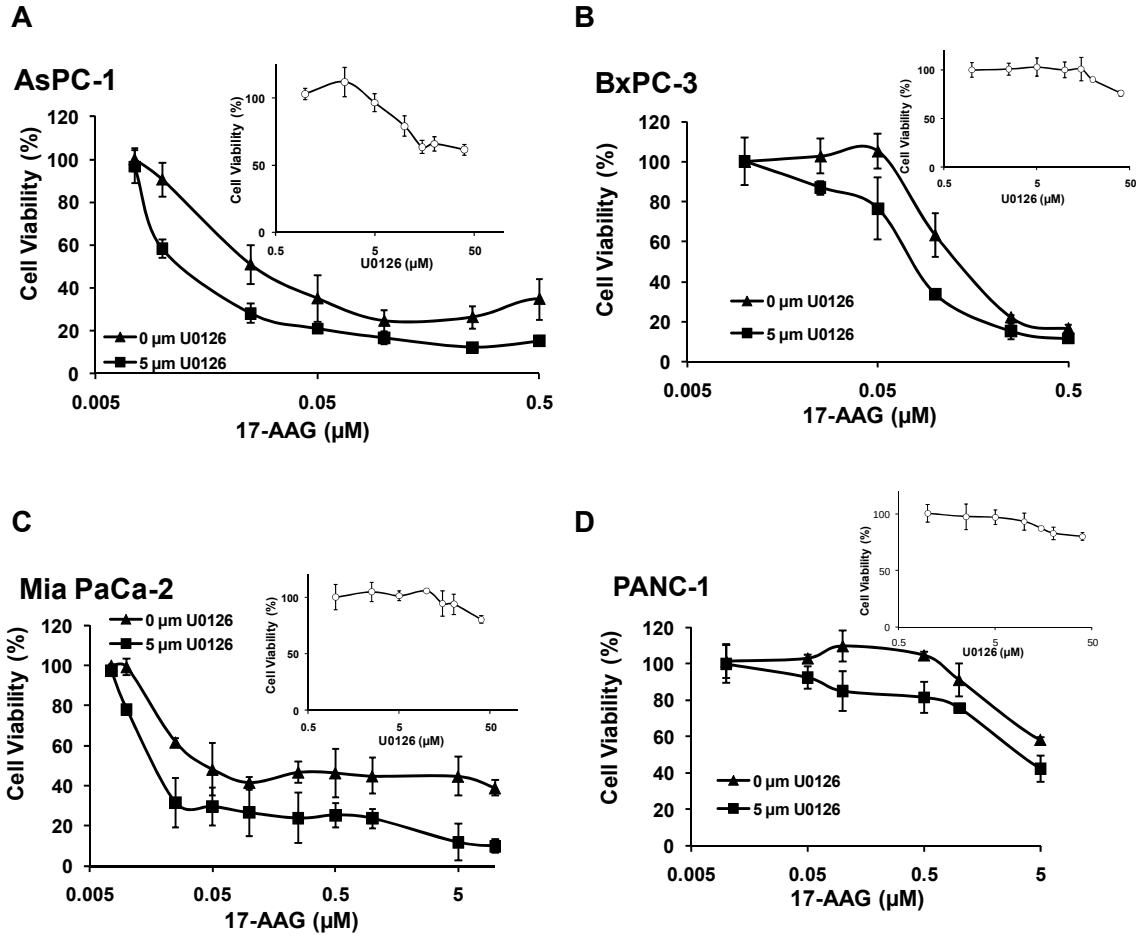

Figure 4.4 Effects of 17-AAG and U0126 alone or in combination on cell motility and migration

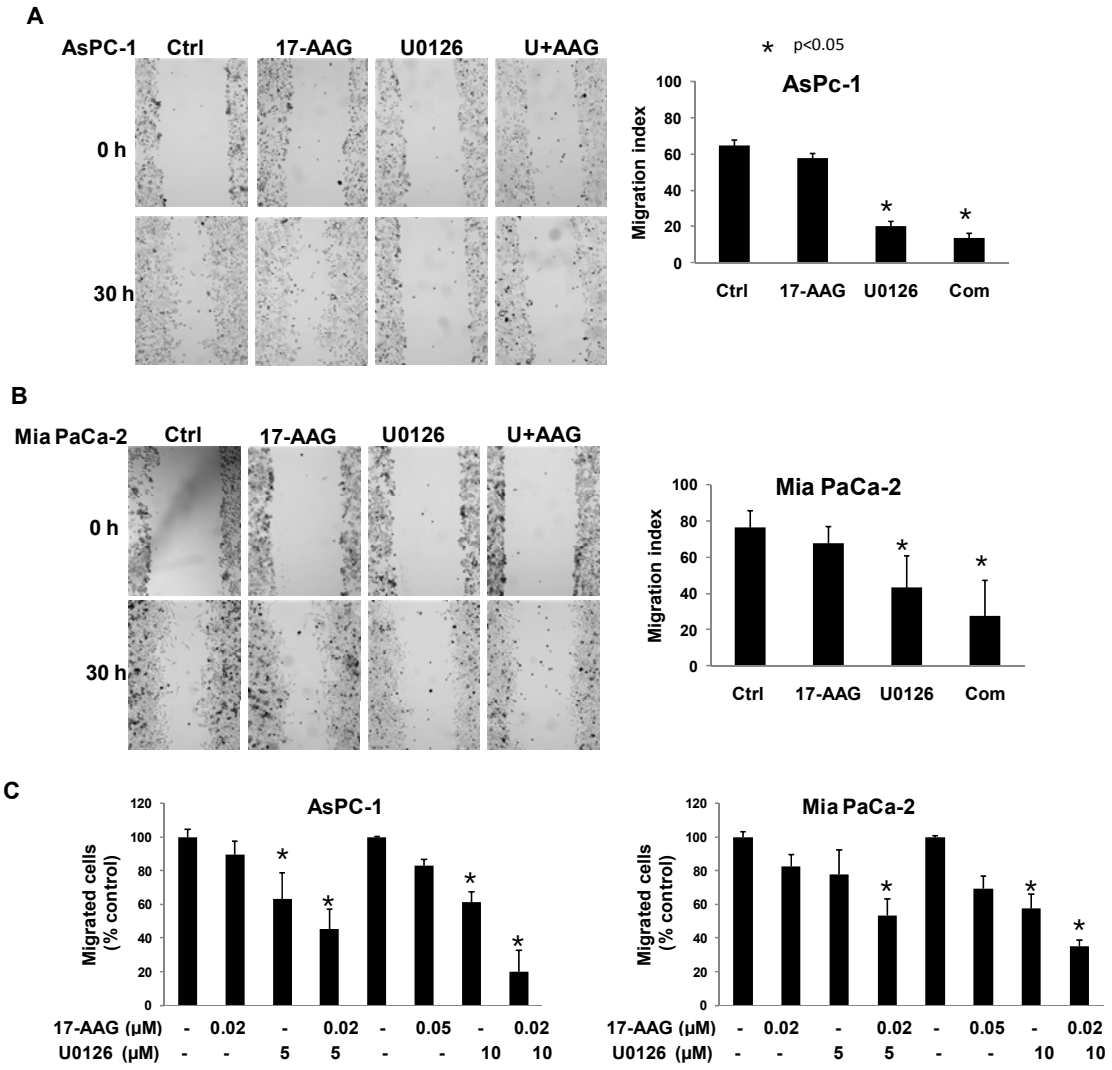

CHAPTER 5
SUMMARY

This primary goal of this study is to identify novel Hsp90 inhibitors which can disrupt the Hsp90/p50Cdc37 interaction for pancreatic cancer therapy.

Traditional Hsp90 inhibitors in clinical trials employ the mechanism of blocking nucleotide binding to the N-terminal ATP-binding site of Hsp90 [1]. Although they have shown efficacy, therapeutic limitations were noticed as well. Here, we reported that celastrol, a quinone methide triterpene purified from tripterygium wilfordii Hook F., provided an alternative strategy of Hsp90 inhibition via disrupting the Hsp90/p50Cdc37 complex. The evidence supporting a focus on this compound is that celastrol has been demonstrated as an inducer of heat shock response for many years [2], and a chemical genomic screen showed that celastrol can interfere with the Hsp90 pathway [3].

We started to investigate the relation between celastrol and Hsp90 in pancreatic cancer cells. Celastrol treatment can induce Hsp90 client protein degradation and result in Hsp70 overexpression, which are the molecular signatures of Hsp90 inhibition. However, further studies using immunoprecipitation found that celastrol did not affect the interaction between Hsp90 and the cochaperone p23, which is distinct from other Hsp90 inhibitors. The ATP-Sepharose assay also proved that celastrol did not interfere with ATP binding to Hsp90, which further suggested the distinction of celastrol on Hsp90 pathway. To investigate the underlying mechanism of celastrol on Hsp90, we employed various in silico and in vitro assays. Molecular docking and molecular dynamic

simulations showed that celastrol blocked the critical interaction between the Glu33 of Hsp90 and the Arg167 of p50Cdc37. Co-immunoprecipitation showed that celastrol disrupted the Hsp90 and p50Cdc37 interaction in the pancreatic cancer cell line Panc-1. GST pull-down and ELISA assays show that p50Cdc37 binds to ADP-bound/nucleotide-free Hsp90 but not ATP-bound Hsp90. Celastrol inhibits Hsp90 ATPase activity without blocking ATP binding. Proteolytic fingerprinting indicates that celastrol binds to the Hsp90 C-terminal domain to protect it from trypsin digestion. However, except computational modeling, we have not had other evidence that celastrol binds to Hsp90 N-terminus.

The anticancer effect of celastrol was tested in pancreatic cancer models in vitro and in vivo. Celastrol inhibited pancreatic cancer cell proliferation with an IC_{50} of 3 μM. Celastrol induced apoptosis in approximately 15% to 40% of pancreatic cancer cells after one to five hours of incubation. In Panc-1 cell xenograft mice, celastrol inhibited 80% of tumor growth ($p<0.001$) after i.p. administration of 3 mg/kg of celastrol for two weeks. Three weeks after the last injection, the average tumor size of the control group reached over 500 mm^3, while tumor size in the celastrol treatment group was four- to five-fold smaller than the control group. Celastrol treatment caused a 5% weight loss in mice. We next used the RIP1-Tag2 transgenic mouse model of pancreatic islet carcinogenesis. We found that celastrol treatment decreased metastatic tumors in the mesenterium by 80% ($P < 0.05$) compared to the control group after a four-week treatment. Celastrol treatment also led to a significant prolongation of life in RIP1-Tag2 mice. The median survival time for the control and celastrol treatment groups was 84 and 96 days, respectively, representing an average increase of 12 days ($P < 0.001$).

Although celastrol disrupted Hsp90/p50Cdc37 complex and showed anti-pancreatic cancer activity in vitro and in vivo in preclinical setting, our study did not provide direct evidence that the anticancer activity of celastrol was absolutely due to the disruption of the Hsp90/p50Cdc37 complex. Further studies using synthesized specific Hsp90/p50Cdc37 inhibitors can address this question.

Another disadvantage of traditional Hsp90 inhibitors is that they may promote metastasis, especially in the bone [4, 5]. The promotion of bone metastasis has been related to the transient activation of Erk, Akt and Src kinase [5]. In pancreatic cancer cells, we noticed a similar transient activation after 17-AAG treatment. Western blotting showed that 17-AAG caused a 2- to 3-fold transient activation of MEK/ERK signaling in pancreatic cancer cells. The activation was sustained for 6 h before phospho-ERK (p-ERK) destabilization. We demonstrated that the selective MEK inhibitor U0126 completely abolished 17-AAG induced ERK1/2 activation and resulted in > 80% of phosphor-ERK degradation after only a 15 min treatment. Moreover, U0126 had complementary effect on 17-AAG regulated oncogenic and cell cycle related proteins. Although 17-AAG downregulated cyclin D1, cyclin E, CDK4 and CDK6, it led to cyclin A and CDK2 accumulation, which was reversed by the addition of U0126. Anti-proliferation assay showed that the combination of U0126 and 17-AAG resulted in a synergistic cytotoxic effect. More importantly, 17-AAG alone only exhibited moderate inhibition of cell migration *in vitro*, while addition of U0126 dramatically enhanced the inhibitory effect by 2- to 5-fold. Taken together, these data demonstrate that the MEK inhibitor U0126 potentiates the activity of the Hsp90 inhibitor 17-AAG against

pancreatic cancer cells. The combination of Hsp90 and MEK inhibition could provide a promising avenue for the treatment of pancreatic cancer.

References

1. Brandt, G.E. and B.S. Blagg, *Alternate strategies of Hsp90 modulation for the treatment of cancer and other diseases.* Curr Top Med Chem, 2009. **9**(15): p. 1447-61.
2. Westerheide, S.D., et al., *Celastrols as inducers of the heat shock response and cytoprotection.* J Biol Chem, 2004. **279**(53): p. 56053-60.
3. Hieronymus, H., et al., *Gene expression signature-based chemical genomic prediction identifies a novel class of HSP90 pathway modulators.* Cancer Cell 2006. **10**(4): p. 321-30.
4. Price, J.T., et al., *The heat shock protein 90 inhibitor, 17-allylamino-17-demethoxygeldanamycin, enhances osteoclast formation and potentiates bone metastasis of a human breast cancer cell line.* Cancer Res, 2005. **65**(11): p. 4929-38.
5. Yano, A., et al., *Inhibition of Hsp90 activates osteoclast c-Src signaling and promotes growth of prostate carcinoma cells in bone.* Proc Natl Acad Sci U S A, 2008. **105**(40): p. 15541-6.

APPENDICES

APPENDIX I

Drug Transporter and CYP P450 mRNA Expression in Human Ocular Barriers: Implications for Ocular Drug Disposition

I.1 Abstract

Studies were designed to quantitatively assess the mRNA expression of (1) 10 CYP P450 enzymes in human cornea, iris-ciliary body and retina/choroid relative to their levels in the liver, and of (2) 21 drug transporters in these tissues relative to their levels in human small intestine, liver or kidney. Potential species differences in mRNA expression of PEPT1, PEPT2 and MDR1 were also assessed in these ocular tissues from rabbit, dog, monkey, and human. CYP P450s expression was either absent or marginal in human cornea, iris-ciliary body and retina/choroid, suggesting a limited role for P450-mediated metabolism in ocular drug disposition. In contrast, among 21 key drug efflux and uptake transporters, many exhibited relative expression levels in ocular tissues comparable to those observed in small intestine, liver or kidney. This robust ocular transporter presence strongly suggests a significant role that transporters may play in ocular barrier function and ocular pharmacokinetics. The highly expressed efflux transporter MRP1 and uptake transporters PEPT2, OCT1, OCTN1 and OCTN2 may be particularly important in absorption, distribution and clearance of their drug substrates in the eye. Evidence of cross-species ocular transporter expression differences noted in these studies supports the conclusion that transporter expression variability, along with anatomic and physiological differences, should be taken into consideration to better understand animal ocular PK and

PD data and the scalability to human for ocular drugs.

I.2 Introduction

As the vital organ of vision, the eye is equipped with sophisticated anatomic structures to maintain a highly regulated and confined environment for its function. This includes various ocular barriers, i.e. cornea epithelium, blood-aqueous barrier (BAB) and blood retina barrier (BRB), that govern the entry or exit of nutrients and xenobiotics to ocular tissues in either the anterior or posterior part of the eye [1]. For topically administered drugs, the cornea forms the primary rate-limiting permeability barrier to compound absorption into the anterior chamber of the eye. Additional barriers to reaching target sites in the anterior chambers include drug elimination through aqueous humor outflow and entering the uveal blood circulation via the BAB. For pharmaceuticals delivered directly to the back of the eye, their pharmacological effect and duration are not only controlled by the formulation, physicochemical properties, or device employed, but also by their interaction with the retina, which determines drug clearance into the systemic circulation. Conversely, BAB and especially BRB also restrict the entry of drugs and metabolites from systemic circulation into the eye.

Unlike the extensive body of knowledge that exists for drug transporters and metabolizing enzymes found in major drug disposition organs, i.e. small intestine, liver and kidney, knowledge about the expression and function of these systems in ocular tissues is very limited despite the potentially important role they may play in ocular drug disposition [2, 3]. Furthermore, available expression and function data have been largely limited to lower species and cell lines. The studies described here, by utilizing real-time quantitative PCR methods, were primarily aimed at providing the first systematic

profiling of mRNA expression levels of key CYP P450s and drug transporters that may be essential constituents of ocular barriers in such ocular tissues as cornea, iris-ciliary body (for BAB) and retina/choroid (for BRB). In addition, the potential cross-species differences for PEPT1, PEPT2 and MDR1 mRNA expression in rabbit, dog, monkey and human ocular tissues were also studied. The selection of these transporters for cross-species investigation was motivated by the fact that their functional or molecular presence in the eye has been either demonstrated or suggested in the literature [4-6], and that they are well-documented drug transporters that have been cloned from all four species intended for comparison.

I.3 Materials and Methods

I.3.1 Human and animal ocular tissues

Human whole globes, enucleated within 6 hours of death from human donors (age range 60 to 93 years old) were obtained from the San Diego Eye Bank. Upon arrival, the eyes were immediately dissected and the following tissues collected: cornea, iris-ciliary body (ICB), and retina/choroid. The tissues were snap frozen in liquid nitrogen sand stored at -80º C until processing. The cornea, ICB, choroid/retina pooled from 2-3 individuals were used for this study. All tissues were from donors free of ocular disease and other systemic complications and were processed in accordance with the guidelines outlined in the Declaration of Helsinki.

Female Dutch Belted rabbits (1.5-2.0 kg) from Myrtle's Rabbitry (Thompson Station, TN), Beagle dogs (male and female, weighing between 9-13kg) from Marshall Farms (North Rose, NY), and cynomolgus monkeys from BRF (a subsidiary of Charles

River Laboratories, Wilmington, MA) were used in this study. Prior to tissue collection, all animals underwent physical and ocular examinations and passed with no abnormal findings. The animals were euthanized intravenously with an overdose of sodium pentobarbital (Buethanasia, Butler Corp., Fredericksburg, VA) and the eyes enucleated immediately. The cornea, ICB, retina /choroid were then quickly dissected from both eyes of all species. Samples were snap frozen in liquid nitrogen and stored at -80ºC until processing. The corneas, ICB, retina /choroid pooled from 2-3 animals were used for this study. All animal-related work was conducted under a Pfizer Inc. IACUC-approved protocol in compliance with Animal Welfare Act regulations and the Guide for the Care and Use of Laboratory Animals.

I.3.2 RNA extraction and cDNA synthesis

The isolation of RNA was carried out using Trizol (Invitrogen, Carlsbad, CA) and/or Qiagen RNAeasy kit (Qiagen, Valencia, CA) performed according to manufacturer's protocols. Total RNA from the cornea was extracted with Trizol after homogenization with an Ultra-Turrax T8 (IKA, Wilmington, NC). The isolated RNA was then purified via the Qiagen RNAeasy kit. Total RNA from other ocular tissues (iris-ciliary body and retina/choroid) was extracted with the Qiagen RNAeasy kit after homogenization with a FastPrep F120 instrument (Qbiogene, Irvine, CA). The isolated RNAs were treated with DNase (DNA-free kit, Ambion, Huntington, UK) to digest genomic DNA. The integrity of RNA was visually assessed by conventional agarose gel electrophoresis and the concentration was measured by a NanoDrop spectrophotometer (Thermal Fisher Scientific, Wilmington, DE). Total RNA from the small intestine, liver and kidney (5 person pool) were obtained from BioChain Institute (Hayward, CA). The

RNA from all samples was reverse-transcribed into cDNA using the High Capacity cDNA Reverse Transcription Kit (Applied Biosystems, Foster City, CA) according to manufacturer's protocol. Parallel control reactions without the addition of reverse transcriptase were performed for each sample.

I.3.3 Real-time quantitative PCR

Real-time PCR was performed in 96-well plates using the iCycler iQ system (Bio-Rad Laboratories, Hercules, CA). Primer and probes were either purchased from Applied Biosystems (Foster City, CA) , or designed based on the sequence entries in the Genbank and synthesized from Integrated DNA Technologies (Coralville, IA; see Tables I.1 and I.2). The self-designed probes were labeled with a reporter dye (FAM) on the 5' end and quencher dye (BHQ-1) on the 3' end. The sequences of the designed probes and primers are as follows:

rabbit MDR1 (sense primer:TGAACGTGAGGTATCTGCGGGAAA; probe: TGGTGAGTCAGGAACCTGTGTTGTTCGCCA; antisense primer: ATAGCGGACGTTCTCAGCGATTGT; 89 bp);

rabbit PEPT1 (sense primer: AGTGGTGAAGTGCATCTGCTTTGC; probe: AGGCACCGCAGTAAGCAGTTTCCCAAGA; antisense primer: AAGCCGCTCGTCGTATTTCTCCTT; 115 bp);

rabbit PEPT2 (sense primer: TGAAATCTGTACTCCAGGCAGCGT; probe: TGGGAACATCATCGTGCTTGTTGTGGCACA; antisense primer: AATTCAGCCCACTGTACCAGACCA; 103 bp);

rabbit GADPH (sense primer: TCATTTGAAGGGCGGAGCCAAA; probe: CCATGTTTGTGATGGGCGTGAACCACGAGA; antisense primer:

GCAGGATGCGTTGCTGACAATCTT; 127 bp);

dog GADPH (sense primer: AGTCAAGGCTGAGAACGGGAAACT; probe: TTCCAGGAGCGAGATCCCGCCAACATCAAA; antisense primer: TCCACAACATACTCAGCACCAGCA; 114 bp).

Each PCR reaction was run in a total volume of 20 μl, containing cDNA transcribed from 10 ng of total RNA, TaqMan® Universal PCR Master Mix, and TaqMan® Gene Expression Assay mixes containing specific primers and probes. The concentrations for self-designed primers and probes were 900 nM and 250 nM, respectively. The PCR was run at 50 °C for 2 min, 95 °C for 10 min, followed by 40 cycles of 95 °C for 15 s and 60 °C for 1 min. Triplicate PCR reactions were performed for each sample. The setting of the threshold and baseline was performed according to the manufacturer's instructions.

I.3.4 Relative expression analysis

Quantification of the gene expression was performed using the relative standard curve method. The standard curve was generated by the mixtures of cDNA from the tissues of interest and serially diluted by a 1: 4 ratio. A sixpoint standard curve was made for each gene. The amplification efficiencies were close to 1 for all of the genes. Four human housekeeping genes, including β-actin, glyceraldehyde-3-phosphate dehydrogenase (GADPH), 18S and peptidylpropyl isomerase A (PPIA), were evaluated as potential internal reference genes. It was decided to exclude 18S because it had a much lower Ct value and much larger variance among the tissues studies. The geometric mean of β-actin, GAPDH, and PPIA was used as the normalization factor for the relative quantification of each human gene. To study species difference with respect to the

relative expression of PEPT1, PEPT2 and MDR1 mRNA in rabbit, dog, monkey and human ocular tissues, GAPDH from each species was used as the normalization factor.

I.4 Results

I.4.1 P450s mRNA expression in human ocular tissues

CYP1A2 and 2B6 were absent in all of the ocular tissues tested. CYP 2C9, 2C19 and 3A5 were absent in both ICB and retina/choroid. CYP 3A4 is absent in retina/choroid, and CYP 2C8 was absent in ICB. In cornea and ICB, the mRNA level of each detectable CYP genes was less than 1% of that in the liver. In retina/choroid, the mRNA levels of 2D6 and 2E1 were also less than 1% of that in the liver; the mRNA expression levels of 2A6 and 2C8 were about 4% and 2% of their corresponding levels in the liver, respectively (Figure I.1).

I.4.2 ABC efflux transporter mRNA expression in human ocular tissues

The descending order of the expression levels of MDR1 in the tissue tested were as follows: small intestine > kidney > liver >ICB > retina/choroid > cornea. The expression of MRP1 was higher in ICB and retina/choroid compared to that observed in small intestine, kidney and liver with the rank order of: ICB > retina/choroid > small intestine > kidney > cornea > liver. MPR2 was highly expressed in liver, followed by moderate expression in small intestine and kidney. Its expression was low in retina/choroid and even lower in ICB and cornea. MRP3 was highly expressed in liver with the rank order of: liver > kidney ≈small intestine > retina/choroid >cornea >ICB. BCRP was highly expressed in small intestine with the rank order of: small intestine > liver > retina/choroid ≈ ICB ≈ kidney >cornea (Figure I.2).

I.4.3 Uptake transporter mRNA expression in human ocular tissues

Peptide transporters: PEPT1 was highly expressed in small intestine and liver, followed by moderate expression in kidney. PEPT1 expression was detected at low levels in ICB and cornea, but was absent in retina/choroid. HPT1 was highly expressed in small intestine, while its expression in kidney, liver and ocular tissues was very low. PEPT2 expression in both retina/choroid and ICB was comparable to the level in kidney, which was higher than the levels in liver and small intestine. PEPT2 was also expressed in the cornea at a level similar to that observed in the small intestine and liver (Figure I.3A).

Organic anion transporting peptides (SLC21): OATP1A2 was highly expressed in both kidney and liver; the other three OATPs tested were all highly expressed in liver. OATP1B1 and 1B3 expression were absent in ocular tissues tested. OATP1A2 expression in retina/choroid was roughly 5-fold lower than the level found in the kidney. OATP2B1 was expressed in all of the ocular tissue tested, with the highest level observed in ICB, which was roughly 16% of the hepatic level. Its expression levels in retina/choroid and cornea were 6% and 1% of the hepatic level, respectively (Figure I.3B).

Organic cation/anion transporters (SLC22): OCT1 was highly expressed in ocular tissues, especially in retina/choroid, where its level was higher than those expressed in small intestine, kidney and liver. OCT2 was highly expressed in the kidney. It was detected in the ICB at about 8% of the level in the kidney, but absent in the cornea and retina/choroid. OCT3 was highly expressed in the liver. Its expression levels in the retina/choroid, ICB and cornea were about 0.3%, 2% and 5% of the hepatic level, respectively (Figure I.3C).

OCTN1 was highly expressed in ocular tissues, especially in ICB, where its expression was higher than that found in the small intestine and kidney. OCTN2 was also expressed in all ocular tissues tested. Its expression level in cornea, ICB and R/C was about 6%, 52% and 59% of the level in the kidney, respectively (Figure I.3C).

Both OAT1 and OAT3 were highly expressed in the kidney, while OAT2 was highly expressed in the liver. None of the OATs tested was detected in the cornea. OAT2 was only detected in retina/choroid at a very low level of less than 0.1% of the hepatic level. OAT1 expression in the ICB was about 5% of the level in the kidney. OAT3 expression level in retina/choroid and ICB was about 2% and 14% of the level in the kidney, respectively (Figure I.3C).

Bile salts cotransporter: ASBT was highly expressed in the small intestine, followed with a moderate expression in the kidney. ASBT mRNA was absent in all ocular tissues tested (Figure I.3D).

I.4.4 Transporter mRNA expression comparison between rabbit, dog, monkey and human ocular tissues

With respect to transporter mRNA expression in non-ocular human tissues, the small intestine had the highest expression level of PEPT1 and MDR1(Figure I.3A and Figure I.2); the kidney had the highest expression level of PEPT2 (Figure I.3A). This expression pattern was consistent across species (Figure 4). To facilitate cross-species comparison, the relative level of PEPT1 or MDR1 in each ocular tissue was normalized by the level in small intestine of the corresponding species, while the relative level of PEPT2 in each ocular tissue was normalized by the kidney level of the corresponding species.

MDR1 mRNA was detected in all of the tested ocular tissues across species. In cornea, the dog seemed to have the highest level, which was 10% of the level in dog small intestine. Human and rabbit cornea appeared to have low levels of MDR1 with less than 1% of the level in the small intestine. In ICB, rabbits seemed to have the lowest level and dog the highest level. MDR1 mRNA expression in rabbit, dog, monkey and human ICB was 0.4%, 18%, 2% and 7% of the level in the small intestine, respectively. In retina/choroid, MDR1 levels in rabbit and monkey tissues were similarly low, less than 0.3% of the level in the small intestine; MDR1 levels in dog and human retina/choroid were similar and about 2% of the level in the small intestine (Figure I.4A).

PEPT1 mRNA was detected at low levels in ocular tissues tested from rabbit, dog, monkey and human. It was not detected in the dog ICB and human retina/choroid. In the cornea, human seemed to have the highest PEPT1 level, which was about 1.5% of the level in human small intestine (Figure I.4B).

PEPT2 mRNA was detected in all of the tested ocular tissues across species. In the cornea, rabbit seemed to have the lowest level, which was less than 0.5% of the level in rabbit kidney. Dog, monkey and human cornea had higher levels, ranging from 5 to 10% of the kidney level. In ICB, dog displayed the lowest level of PEPT2, which was 3.6% of the level in dog kidney. PEPT2 levels in rabbit, monkey and human ICB were higher at 32%, 92% and 64% of the level in the kidney, respectively. In the retina/choroid, the highest levels were observed in the human (37% of the level in the kidney), while rabbit, dog and monkey had lower levels, ranging from 5% to 10% of the level found in the kidney.

I.5 Discussion

Unlike the liver, small intestine and kidney, the mammalian eye is seldom considered as a major disposition organ after drug dosing. Yet, for ophthalmic drugs, it is important to understand ocular drug disposition as the drug or metabolite concentration in the ocular tissues often dictates its pharmacodynamic effect. Ocular tissues evidently display metabolizing activities toward xenobiotic and endogenous substrates [3]. It is also recognized that drug transporter activity is an essential component for ocular barrier function [2]. However, information on the expression profile of drug metabolizing enzymes and transporters in the human eye is largely absent. In the presented studies, quantitative real time PCR methods were utilized to obtain the relative expression profiles of the CYP P450 enzymes and various transporter systems in the human eye. The expression of several transporters was also compared across species. To facilitate data interpretation, each CYP P450 enzyme expression in the ocular tissues was presented as the relative level after being normalized by its level in the liver, which is the major metabolizing organ. Similarly, each transporter expression level in ocular tissues was compared and rank-ordered with its level in the liver, small intestine and kidney, all of which are organs of rich drug transporter expression. These studies compared the relative mRNA abundance of a given enzyme or transporter in different tissue types, but did not compare mRNA expression levels between different enzymes or transporters. In addition, the relative expression level of a given enzyme or transporter in human was qualitatively described as high, moderate, low, very low or absent. It should also be noted that a limitation of using mRNA level as the surrogate for gene expression is that mRNA levels are not necessarily correlated with the functional protein expression, which may be a

better indicator for the functional role of these metabolizing enzymes and transporters in ocular drug disposition. Finally, the human ocular tissues studied here are free from ocular diseases, but are from aged donors. The effect of disease status and age on the expression of metabolizing enzymes and transporters is beyond the scope of this study.

P450s mRNA expression in human ocular tissues. The mRNA expression of the 10 studied CYP P450 enzymes in the eye was much less than their levels in the liver and in some instances was absent in ocular tissues. This limited mRNA expression suggests thatP450-mediated metabolism may contribute, but perhaps not to a significant degree, to the overall metabolism capacity of the eye. This data is consistent with a very low turn-over rate when CYP P450 probe substrates were incubated in various ocular tissue homogenates (data not shown). Although not profiled in this paper, other metabolizing enzymes including estereases, peptidases and ketone reductases are known to have functional expression in various ocular tissues across species [2, 7]. When it comes to molecular design of ophthalmic drug, the focus should be on the specificity and capacity of these non-P450 enzymes. One of the examples is the prodrug approach that successfully exploits esterases in ocular drug design [8].

Drug transporter mRNA expression in human ocular tissues. This paper reports the relative expression profiles of 21 drug transporters in human cornea, iris-ciliary body, retina/choroid, liver, kidney and small intestine. This is an extensive but by no means complete list of important drug transporters. The rank order expression levels of these transporters in the liver, kidney and small intestine in this study largely conforms to previously reported data using a similar real time PCR approach [9]. This inter-lab consistency further validates using real-time PCR as a viable method to relatively

quantify mRNA expression levels in different tissue types despite the potential differences associated with this methodology, including tissue resource, mRNA extraction method, PCR conditions, selection of house-keeping genes for normalization [10], et al.

Cornea: Considering that the cornea is in direct contact with the external environment, it is not surprising for this tissue to express efflux transporter as a part of its protective mechanism. There are conflicting reports in the literature regarding ABC efflux transporter expression in human cornea. For example, one study showed there was no detectable MDR1 mRNA expression in human cornea [11], while another reported the mRNA expression of MDR1 in human cornea as well as P-gp expression by Western blot in a human corneal cell line [5]. In the current study, MDR1 mRNA expression was found to be very low, which may help explain the literature inconsistency as many variables in real time PCR protocols (including cycle number and intersubject variability of source mRNA) could lead to conflicting results, especially for genes with low copy numbers. Similar to MDR1, both MRP2 and BCRP also demonstrated very low expression levels in the human cornea relative to their levels in the liver or small intestine, while there were moderate MRP1 and low MRP3 expression levels in the human cornea. Since these major drug efflux transporters tend to have overlapping or complementary substrate specificity (Reference to FDA drug transporter link), MRP3 and especially MRP1 in human cornea may be the primary efflux transporter to offer potential barrier protection despite the low abundance of MDR1, MRP2 and BCRP in human cornea. This data suggests that designing around MRP1 efflux may be a key consideration to enhance ocular penetration if drug efflux is aconcern for corneal permeability. Besides the

presence of efflux transporters, human cornea also has low to moderate expression of PEPT1, PEPT2 and some organic cation/anion transporters (OCT1, OCT3, OCTN1 and OCTN2). Contrary to efflux mechanism, these uptake transporters offer potential absorptive transport pathways for topically-dosed drug molecules. For example, the conversion of anti-viral drugs acyclovir and ganciclovir into their L-valyl esters significantly improved their corneal permeability, presumably by targeting the dipeptide transporters expressed in the cornea [4]. The data presented here suggests, by their presence, both PEPT1 and PEPT2 may participate in this absorptive mechanism for their drug substrates after topical dosing to the cornea.

Iris-ciliary body: ICB forms the blood-aqueous barrier. Its barrier function may not be as complete as the blood-retinal barrier, since the content exchange between plasma and aqueous humor is less restricted. This study reveals that numerous efflux and uptake transporters are expressed in ICB: MRP1 and OCTN1 mRNA levels are comparable to those levels found in small intestine and kidney; PEPT2 level is comparable to that in the kidney; other transporters including OCT1, OCTN2 and OAT3 are also substantially expressed in this tissue. The presence of these efflux and uptake transporters may provide an additional active elimination pathways for drug removal from aqueous humor to systemic circulation or vice versa, which works in concert with the less restricted passive pathway and aqueous humor turnover to eliminate drugs from the anterior chamber [1]. This may explain why some large and lipophilic drugs have clearance values exceeding the rate of aqueous humor turnover [12].

Retina/Choroid: The retina is composed of neural retina and retinal pigment epithelium cells, which are adjacent to the choroid. The blood-retina barrier includes the

endothelial cells of retinal blood vessels as the inner blood-retinal barrier and the retinal pigment epithelial cells as the outer blood-retinal barriers. The blood-retinal barrier prevents plasma contents including drug molecules from entering into the retina. The retina is in direct contact with vitreous humor; thus, retinal drug concentration and elimination halflife for drug molecules administered into the vitreous humor are partially determined by retinal penetration, which can be governed by both passive and active processes. As summarized in a recent review article [2], there is rich transporter expression in the blood-retinal barrier, but most studies were conducted in preclinical species and immortalized cell lines. This study offers a more complete profiling of transporter expression in human retina with a few noteworthy findings. All of the five efflux transporters tested are expressed in human retina, especially MRP1, which has a high relative expression level. This observation is consistent with the previous study showing both mRNA and protein expression of MRP1 in both ARPE-19 and primary human retinal pigment epithelia cells [13]. PEPT1 mRNA could not be detected in human retina; however, there is moderate PEPT2 expression in this tissue, which suggests that PEPT2 may be the dominant oligopeptide transporter in human blood-retina barrier, similar to the role of PEPT2 in the blood-brain barrier [14]. OCT1 seems to have the highest relative expression level in retina compared to all other tissues tested. OCT1 expression in ocular tissue has not been reported up to now. As many drug molecules are substrates or inhibitors of human OCT1, the functional implication of a highly expressed OCT1 in human retina remains to be further defined for ophthalmic drugs. Besides OCT1, other organic anion and cation transporters are also expressed in human retina (Fig I.3C). Further investigation of drug transporter expression regarding location, orientation, and

transport capacity in both inner and outer bloodretinal barriers will be essential to understand the role of drug transporters in retinal disposition and how drug-transporter interactions may be able to influence ophthalmic drug design.

Species differences in ocular transporter expression: The ocular mRNA expression of PEPT1, PEPT2 and MDR1 was normalized across species and presented as relative to levels in the small intestine (PEPT1 and MDR1) or kidney (PEPT2). Potential species differences were observed for the mRNA expression of these three transporters in ocular tissues. The implications of these observed differences are illustrated by the results found in the cornea. In the cornea, dog MDR1 mRNA expression is about 10% of its expression in dog small intestine, and human MDR1 mRNA level is about 1% of its expression in human small intestine. These data suggest that the corneal MDR1 expression, as well as the MDR1-mediated efflux potential, may be different between dog and human. PEPT1 mRNA level in rabbit cornea is less than 0.01% of that found in rabbit small intestine, much lower than the relative level (1.3%) of PEPT1 in human cornea normalized by the level in human small intestine. Similarly, PEPT2 mRNA level in rabbit cornea is about 0.4% of its level in rabbit kidney, much lower than the relative level (5.2%) of human corneal PEPT2 normalized by human kidney PEPT2 level. These data suggest that corneal PEPT1 and PEPT2 expression, as well as the PEPT1/PEPT2-mediated absorptive uptake, may be different between rabbit and human. These potential differences remain to be further investigated by additional protein expression data and functional comparison using probe transporter substrates. This transporter expression variability in the eye, when better understood, may help us understand the potential

limitations of different animal model with respect to ocular pharmacokinetics and perhaps help refine animal PK/PD information for better human dose prediction.

In conclusion, this study represents the most comprehensive analysis of CYP P450 enzymes and drug transporters expression in human ocular tissues to date. It provides the molecular evidence for the potentially limited role of CYP P450-mediated metabolism in the eye and the potentially important role of certain drug transporters in ocular drug disposition. In addition, this report demonstrates the importance of studying the species difference of drug transporters in the eye. Future efforts will further investigate the role of drug metabolizing enzymes and transporters in ocular drug disposition, which may provide guidance on how to optimize drug disposition properties in ophthalmic drug design.

I.6 Acknowledgments

We thank Chunze Li and Deepak Davie for insightful scientific discussions, Mike Zientek for critical reading of the manuscript, and Terri Vandegiessen, Yanfang Liu, and Helen Cho for technical assistance.

I.7 References

1. Hornof, M., E. Toropainen, and A. Urtti, *Cell culture models of the ocular barriers.* Eur J Pharm Biopharm, 2005. **60**(2): p. 207-25.
2. Mannermaa, E., K.S. Vellonen, and A. Urtti, *Drug transport in corneal epithelium and blood-retina barrier: emerging role of transporters in ocular pharmacokinetics.* Adv Drug Deliv Rev, 2006. **58**(11): p. 1136-63.
3. Duvvuri, S., S. Majumdar, and A.K. Mitra, *Role of metabolism in ocular drug delivery.* Curr Drug Metab, 2004. **5**(6): p. 507-15.
4. Anand, B.S. and A.K. Mitra, *Mechanism of corneal permeation of L-valyl ester of acyclovir: targeting the oligopeptide transporter on the rabbit cornea.* Pharm Res, 2002. **19**(8): p. 1194-202.
5. Dey, S., et al., *Molecular evidence and functional expression of P-glycoprotein (MDR1) in human and rabbit cornea and corneal epithelial cell lines.* Invest Ophthalmol Vis Sci, 2003. **44**(7): p. 2909-18.

6. Ocheltree, S.M., et al., *Preliminary investigation into the expression of proton-coupled oligopeptide transporters in neural retina and retinal pigment epithelium (RPE): lack of functional activity in RPE plasma membranes.* Pharm Res, 2003. **20**(9): p. 1364-72.
7. Lee, V.H., D.S. Chien, and H. Sasaki, *Ocular ketone reductase distribution and its role in the metabolism of ocularly applied levobunolol in the pigmented rabbit.* J Pharmacol Exp Ther, 1988. **246**(3): p. 871-8.
8. Shirasaki, Y., *Molecular design for enhancement of ocular penetration.* J Pharm Sci, 2008. **97**(7): p. 2462-96.
9. Hilgendorf, C., et al., *Expression of thirty-six drug transporter genes in human intestine, liver, kidney, and organotypic cell lines.* Drug Metab Dispos, 2007. **35**(8): p. 1333-40.
10. Vandesompele, J., et al., *Accurate normalization of real-time quantitative RT-PCR data by geometric averaging of multiple internal control genes.* Genome Biol, 2002. **3**(7): p. RESEARCH0034.
11. Becker, U., et al., *Expression of ABC-transporters in human corneal tissue and the transformed cell line, HCE-T.* J Ocul Pharmacol Ther, 2007. **23**(2): p. 172-81.
12. Schoenwald, R.D., *Ocular pharmacokinetics and pharmacodynamics*, in *Ophthalmic Drug Delivery Systems*, A.K. Mitra, Editor. 2003, Marcel Deller, New York. p. 135-179.
13. Aukunuru, J.V., et al., *Expression of multidrug resistance-associated protein (MRP) in human retinal pigment epithelial cells and its interaction with BAPSG, a novel aldose reductase inhibitor.* Pharm Res, 2001. **18**(5): p. 565-72.
14. Shen, H., et al., *Impact of genetic knockout of PEPT2 on cefadroxil pharmacokinetics, renal tubular reabsorption, and brain penetration in mice.* Drug Metab Dispos, 2007. **35**(7): p. 1209-16.

Table I.1 List of human genes studied in the analysis

Gene Name	Cornea	Iris-ciliary body	Retina / choroid	Liver	Small intestine	Kidney	Assay I.D.	Accession I.D.
CYP1A2	X	X	X		nd	nd	Hs00167927_m1	NM_000761
CYP3A4			X		nd	nd	Hs00430021_m1	NM_017460
CYP2C8		X			nd	nd	Hs00258314_m1	M17398
CYP2C9		X	X		nd	nd	Hs00426397_m1	NM_000771
CYP2C19		X	X		nd	nd	Hs00426380_m1	NM_000769
CYP2D6					nd	nd	Hs00164385_m1	NM_000106
CYP2A6					nd	nd	Hs00868409_s1	NM_000762
CYP2E1					nd	nd	Hs00559368_m1	NM_000773
CYP3A5		X	X		nd	nd	Hs00241417_m1	NM_000777
CYP2B6	X	X	X		nd	nd	Hs00167937_g1	NM_000767
MDR1							Hs00184500_m1	NM_000927
MRP1							Hs00219905_m1	NM_004996
MRP2							Hs00166123_m1	NM_000392
MRP3							Hs00358656_m1	NM_003786
BCRP							Hs00184979_m1	NM_004827
PEPT1			X				Hs00192639_m1	NM_005073
PEPT2							Hs00221539_m1	NM_021082
HPT1							Hs00184865_m1	NM_004063.2
OATP1A2	X	X			X		Hs00366488_m1	NM_134431
OATP1B1	X	X	X		X	X	Hs00272374_m1	NM_006446
OATP1B3	X	X	X			X	Hs00251986_m1	NM_019844
OATP2B1							Hs00200670_m1	NM_007256
OCT1							Hs00231250_m1	NM_002697
OCT2	X		X		X		Hs00161893_m1	BC039899
OCT3							Hs00222691_m1	NM_021977
OCTN1				X			Hs00268200_m1	NM_003059
OCTN2							Hs00161895_m1	NM_003060
OAT1	X			X	X		Hs00537914_m1	NM_153276.1
OAT2	X	X			X		Hs00198527_m1	NM_153320.2
OAT3	X			X	X		Hs00188599_m1	NM_004254.2
ASBT	X	X	X	X			Hs00166561_m1	NM_000452.1

Table I.2 List of reference and animal genes studied in the analysis

Species	Gene	Accession I.D.	Assay I.D.
Human	β-actin	NM_001101	4333762F
Human	PPIA	NM_002046	4333763F
Human	GAPDH	NM_002046	4333764F
Human	18S	X03205	4333760F
Rabbit	MDR1	NM_001082159	designed
Rabbit	PEPT1	NM_001082337	designed
Rabbit	PEPT2	NM_001082700	designed
Rabbit	GAPDH	DQ403051	designed
Dog	MDR1	NM_001003215	Cf02693309_m1
Dog	PEPT1	NM_001003036	Cf02671917_m1
Dog	PEPT2	XM_545128	Cf02741718_m1
Dog	GAPDH	AB038240	designed
Monkey	MDR1	NM_001032887	Rh01070639_m1
Monkey	PEPT1	NM_001032899	Rh02788451_m1
Monkey	PEPT2	NM_001032953	Rh01113683_m1
Monkey	GAPDH	XM_001105471	Rh02621745_g1

Figure I.1 Relative mRNA expression levels of CYP P450 enzymes in human cornea, iris-ciliary body, and retina/choroid

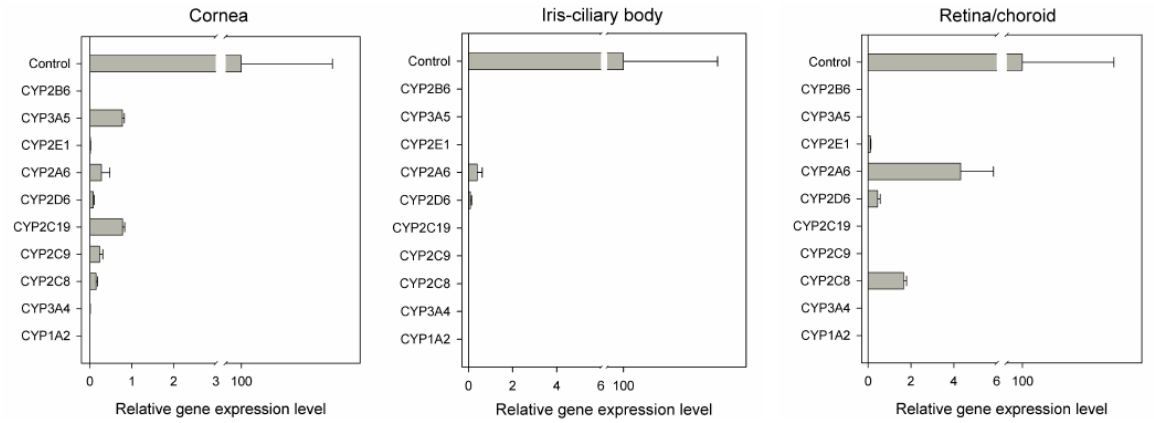

Figure I.2 Relative gene expression levels of ABC transporters in human cornea, irisciliary body, retina/choroid, small intestine, liver and kidney

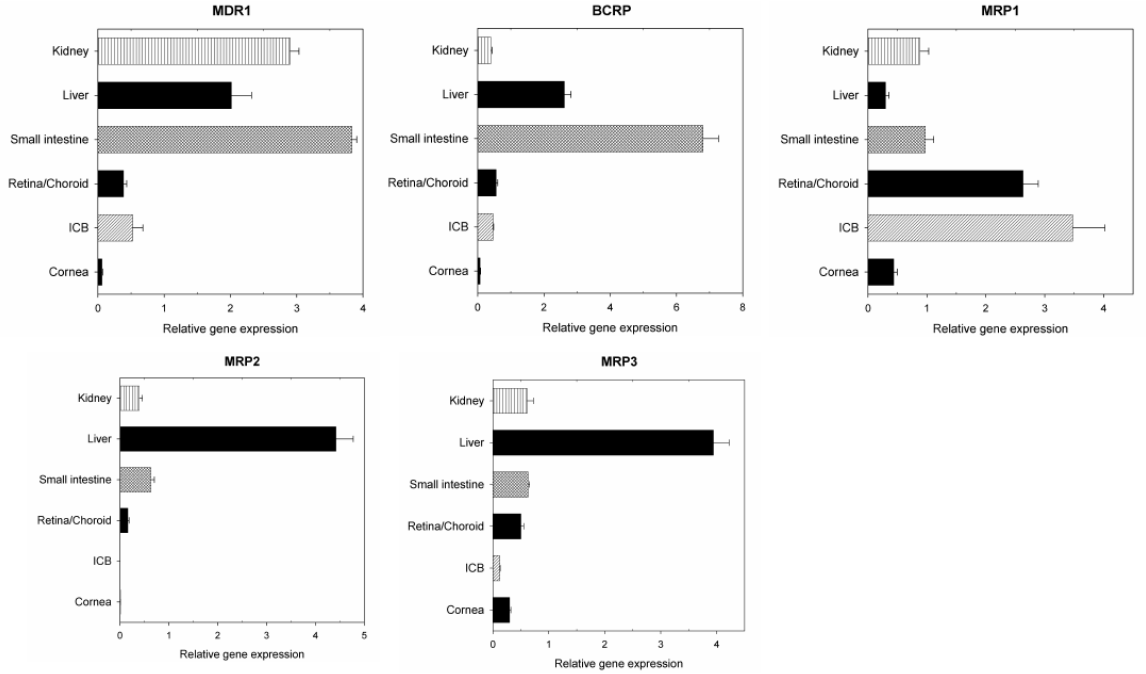

Figure I.3 Relative gene expression levels of SLC transporters in human cornea, irisciliary body, retina/choroid, small intestine, liver and kidney

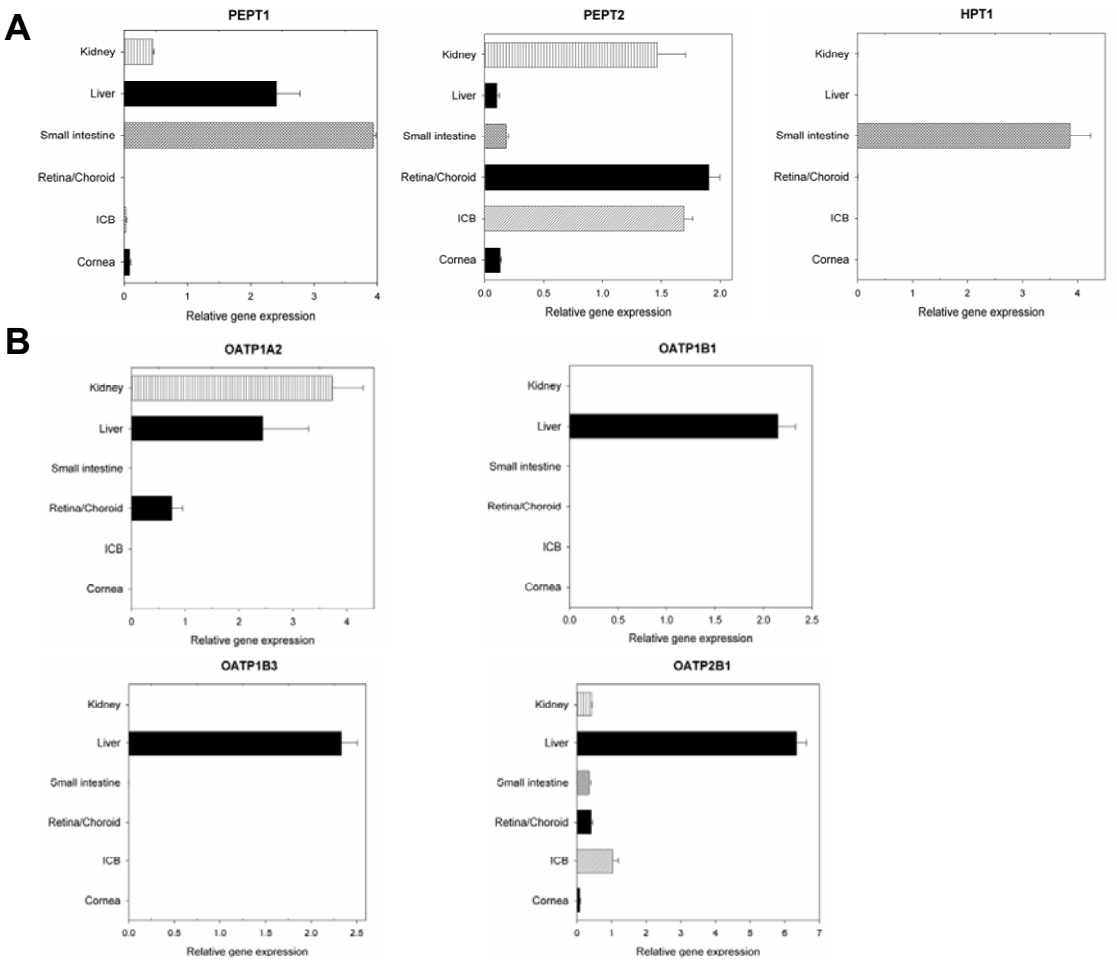

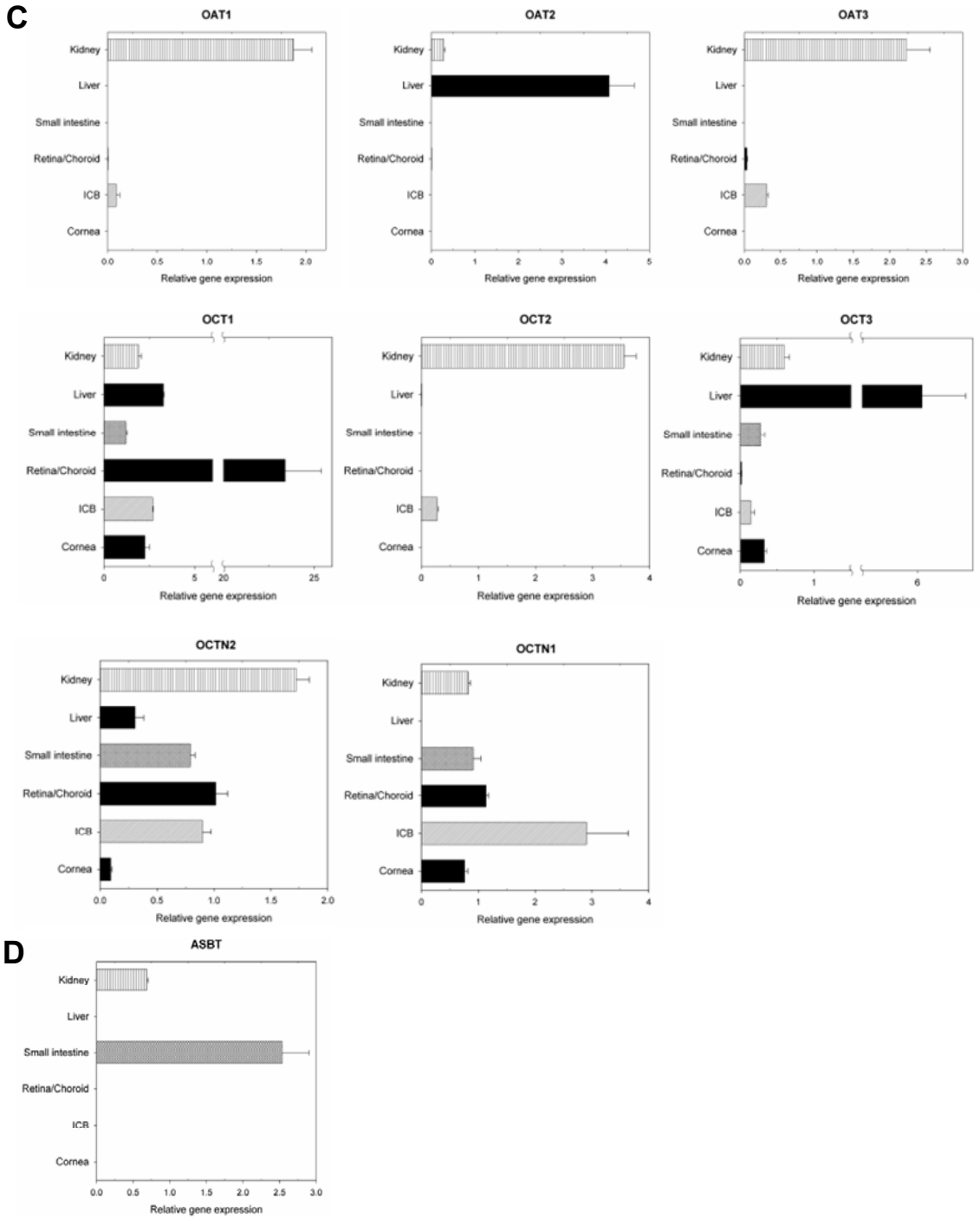
C
OAT1
OAT2
OAT3
OCT1
OCT2
OCT3
OCTN2
OCTN1
D
ASBT
Kidney
Liver
Small intestine
Retina/Choroid
ICB
Cornea
Relative gene expression

Figure I.4 Relative gene expression levels of transporter genes in cornea, iris-ciliary body, retina/choroid of rabbit, dog, monkey and human

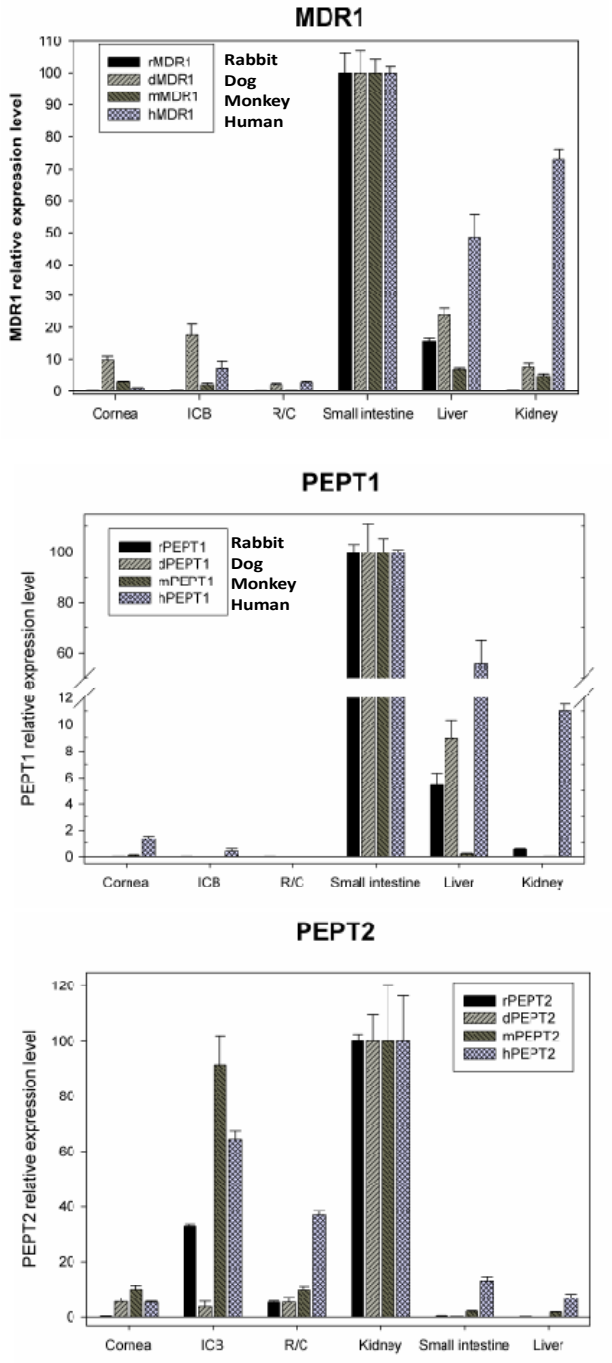

APPENDIX II

(-)-Epigallocatechin-3-gallate Inhibits Hsp90 Function by Impairing Hsp90 Association with Co-chaperones in Pancreatic Cancer Cells

II.1 Abstract

(-)-Epigallocatechin-3-gallate [(-)-EGCG], the most abundant polyphenolic catechin in green tea, showed chemoprevention and anticancer activities. (-)-EGCG was reported to bind to the C-terminal domain of heat shock protein 90 (Hsp90). The purpose of this study is to investigate (-)-EGCG as a novel Hsp90 inhibitor to impair Hsp90 multichaperone complex for simultaneous down-regulation of oncogenic proteins in pancreatic cancer cells. MTS assay showed that (-)-EGCG exhibited anti-proliferative activity against pancreatic cancer cell line Mia Paca-2 *in vitro* with IC50 below 50 μM. (-)-EGCG increased caspase-3 activity up to 3-fold in a time- and concentration-dependent manner. Western blotting analysis demonstrated that (-)-EGCG induced down-regulation of oncogenic Hsp90 client proteins by approximately 70%~95%, including Akt, Cdk4, Raf-1, Her-2, and pERK. Co-immunoprecipitation showed that (-)-EGCG decreased the association of co-chaperones p23 and Hsc70 with Hsp90 by more than 50%, while it had little effect on the ATP binding to Hsp90. Proteolytic fingerprinting assay confirmed direct binding between (-)-EGCG and the Hsp90 C-terminal domain. These data suggest that the binding of (-)-EGCG to Hsp90 impairs the association of Hsp90 with its co-chaperones, thereby inducing degradation of Hsp90 client proteins, resulting anti-proliferating effects in pancreatic cancer cells.

II.2 Introduction

Pancreatic cancer is the fourth leading cause of cancer death in the United States [1]. The overall 5-year survival rate after diagnosis for pancreatic cancer patients is less than 5% [2]. Major therapeutic targets for pancreatic cancer include K-ras pathway downstream signaling (e.g., Raf-MEK ERK pathway), epidermal growth factor receptor (EGFR), ErbB-2 (Her-2), phosphoinositide 3-OH kinase (PI3K)/Akt, and p53 mutant [3-6]. Due to the complexity of the disease, targeting multiple oncogenic pathways would be beneficial for chemoprevention of pancreatic cancer.

Heat shock protein 90 (Hsp90), a highly abundant molecular chaperone actively involved in the stress response, assists maturation of more than 200 proteins, which include transmembrane tyrosine kinases (Her-2, EGFR), metastable signaling proteins (Akt, K-ras, Raf-1), mutated signaling proteins (p53, v-Src), chimeric signaling proteins (Bcr-Abl), cell cycle regulators (Cdk4, Cdk6), and steroid receptors (androgen, estrogen, and progesterone receptors) [7-10] [11]. Many of these client proteins are mutated and/or over-expressed in pancreatic cancer [12, 13]. Based on crystal structure, Hsp90 protein consists of three highly conserved domains: an N-terminal ATP-binding domain, a middle domain and a C-terminal dimerization domain [14]. The N-terminus of Hsp90 contains a specific ATP binding pocket, which has been well characterized [6, 15]. Benzoquinone ansamycins, such as geldanamycin (GA) [16] and its derivatives 17-allylamino-17-desmethoxygeldanamycin (17-AAG) [16, 17], competitively block ATP binding to this N-terminal ATP binding site on Hsp90 [18, 19], resulting in ubiquitination and proteasomal degradation of client proteins.

Hsp90 requires an array of co-chaperones to assemble a super-chaperone complex for its function. These co-chaperones, including p50Cdc37, Hsc70, Hsp40, Hop, Hip, p23, pp5, and immunophilins, bind to and release from the complex at various stages to accomplish the folding and maturation of Hsp90 client proteins [18]. A newly synthesized client protein binds to Hsc70/Hsp40 complex, and then associates with the "open" state Hsp90 via the bridging co-chaperone Hop, which interacts simultaneously with Hsp90 and Hsc70 [12]. Upon ATP binding, Hsp90 then binds to p23 and immunophilins, converting the intermediate chaperone complex into a mature complex [18]. Upon ATP hydrolysis, the correctly-folded client protein is released from Hsp90 [20].

Recently, the C-terminal domain of Hsp90 has been shown to possess a second ATP binding site [21]. Novobiocin, a coumarin antibiotic isolated from *Streptomyces* species, binds Hsp90 at the C-terminal ATP binding site [21]. This binding induced an alteration in Hsp90 conformation [21, 22], interfering Hsp90/Hsc70 and Hsp90/p23 interactions [22]. An allosteric regulation is suggested between the C-terminal and N-terminal domains of Hsp90 such that the interaction of ligands with one site might affect the occupancy of the other site [21].

Green tea is one of the most widely consumed beverages in the world. Epidemiological studies suggest an association between green tea consumption and cancer prevention effects [23]. The various polyphenolic catechins contained in green tea are thought to contribute to its chemoprevention against certain types of cancer. In particular, several studies indicate that (-)-epigallocatechin-3-gallate [(-)-EGCG], the most abundant catechin in green tea, is a potent chemoprevention and anticancer

component [24]. However, the underlying mechanism of (-)-EGCG for its chemoprevention is not well defined. In 2005, Palermo *et al.* reported that (-)-EGCG could inhibit the transcriptional activity of aryl hydrocarbon receptor (AhR) through a mechanism involving direct binding to the C-terminal region of Hsp90 [25]. It remains unclear whether (-)-EGCG could inhibit Hsp90 function through direct binding and how (-)-EGCG affect the chaperone function through this binding. The purpose of this study is to investigate (-)-EGCG as a novel Hsp90 inhibitor to impair Hsp90 super-chaperone complex for inhibiting its chaperoning function, which simultaneously down-regulates oncogenic proteins in pancreatic cancer cell line Mia Paca-2.

II.3 Materials and Methods

II.3.1 Drugs and antibodies

(-)-EGCG was purchased from Calbiochem (EMD Biosciences, Inc., San Diego, CA), and dissolved in DMSO as a stock solution. The following antibodies were used for immunoblotting: Akt, phospho-ERK1/2 (Thr202/Tyr204), ERK1/2 (p44/42 MAPK) (Cell Signaling, Beverly, MA), Hop (Assay Designs, Inc., Ann Arbor, MI), p23 (Abcam, Cambridge, MA), Cdk4, p50Cdc37, Hsp90, Hsp70, Hsc70, Her-2, Raf-1, β-actin (Santa Cruz Biotechnology, Santa Cruz, CA). Purified Hsp90β N-terminus (N-Hsp90β) (amino acids 1-246) was a gift from Dr. Dan Bolon (University of Massachusetts Medical School).

II.3.2 MTS assay

Human pancreatic cancer cells, Mia Paca-2, were seeded in 96-well microplates at a density of 3,000 to 5,000 cells per well. Cells were treated with increasing

concentrations of (-)-EGCG as indicated, and after 24 hr incubation cell viability was assessed by MTS assay (Promega, Madison, WI) according to the manufacturer's instruction. The number of living cells in the culture is directly proportional to the absorbance at 490 nm by a formazan product bioreduced from MTS by living cells. The anti-proliferative effect of (-)-EGCG was also tested on pancreatic cancer cell lines (Panc-1, BxPC-3, and AsPC-1) with similar results, and thus only one cell line (Mia Paca-2) was used for the following mechanistic studies.

II.3.3 Caspase-3 fluorometric assay

Mia Paca-2 cells were treated with (-)-EGCG and collected at different time points as indicated. The following Caspase-3 activity assay was based on the manufacturer's instruction of Caspase-3/CPP32 Fluorometric Assay Kit (Biovision Research Products, Mountain View, CA). Cellular protein was extracted with the supplied lysis buffer, followed by determination of protein concentration using BCA Protein Assay Reagents (Pierce, Rockford, IL). The cleavage of DEVD-AFC, a substrate of caspase-3, was quantified by using a fluorescence microtiter plate reader with a 400 nm excitation filter and a 505 nm emission filter. Results are reported as arbitrary fluorescence units (AFU) normalized to milligram of cellular protein.

II.3.4 Protein expression and purification

The expression plasmids pET15b-hHsp90β, pET28a(+)-hHsp90β (530-724) for human full-length Hsp90β and Hsp90β C-terminus (C-Hsp90β) were kindly provided by Dr. Thomas Ratajczak (University of Western Australia, Australia). The plasmids were transformed into *E.coli* strain Rosetta 2(DE3) (EMD Biosciences, Inc., San Diego, CA) following the protocol provided by manufacturer. Primary cultures of transformed cells

were grown overnight, pelleted by centrifugation, resuspended in fresh culture medium, and grown for 1-2 hr(s) at 37°C until OD_{600} reached 0.6. Protein expression was induced by 0.2 mM IPTG (isopropyl-beta-D-thiogalactopyranoside) (GE Healthcare, Piscataway, NJ) for 2 hrs. His-tagged proteins were purified by affinity chromatography through mixed with HisPurTM Cobalt Resin (Pierce, Rockford, IL), followed by dialysis against PBS. The purity was assessed by SDS-PAGE, and the concentration was determined by BCA assay (Pierce, Rockford, IL). Proteins were stored at -70°C after adding glycerol to 10%.

II.3.5 Western blotting analysis

The procedure for Western blotting analysis was briefly described below. After treated with (-)-EGCG for the indicated time periods, Mia Paca-2 cells were washed twice with ice-cold PBS, collected in RIPA lysis buffer (20 mM Tris-HCl, 150 mM NaCl, 1% NP-40, 5 mM EDTA, 1 mM Na_3VO_4, pH 7.5) supplemented with a protease inhibitor mixture (Sigma-Aldrich, St. Louis, MO), and incubated on ice for 20 min. Afterwards cell lysate was centrifuged at 14,000 x rpm for 10 min, and the supernatant was recovered. Protein concentration was determined with BCA Protein Assay Reagents (Pierce, Rockford, IL). Equal amounts of total protein were subject to SDS-PAGE, transferred to PVDF membrane (BioRad, Richmond, CA), and then probed with appropriate antibodies.

II.3.6 ATP-Sepharose binding assay

Hsp90 Protein (200 μg) was extracted from treated Mia Paca-2 cells and incubated with 25 μl pre-equilibrated γ-phosphate-linked ATP-Sepharose (Jena Bioscience GmbH, Jena, Germany) in 200 μl incubation buffer (10 mM Tris-HCl, 50 mM KCl, 5 mM $MgCl_2$, 2 mM DTT, 0.01% NP-40, pH 7.5) overnight at 4 °C. The beads

were washed four times and bead-bound proteins were subsequently analyzed by SDS-PAGE. For ATP binding assay with purified protein, 5 μg protein was pre-incubated with (-)-EGCG on ice in 200 μl incubation buffer (10 mM Tris-HCl, 50 mM KCl, 5 mM $MgCl_2$, 2 mM DTT, 0.01% NP-40, pH 7.5) for 1 hr. Following incubation, ATP-Sepharose was added and further incubated at 37 °C for 30 min with frequent agitation. The beads were washed and bound proteins were subject to Western blotting.

II.3.7 Co-immunoprecipitation

Mia Paca-2 cells were treated with (-)-EGCG for the indicated time period, and then harvested. Cells were lysed in 20 mM Tris-HCl (pH 7.4), 25 mM NaCl, 2 mM DTT, 20 mM Na_2MoO_4, 0.1% NP-40, and protease inhibitors. After centrifugation, supernatant was recovered and protein concentrations were determined with BCA Protein Assay Reagents (Pierce, Rockford, IL). Protein (500 μg) was first incubated with H9010 antibody (Axxora, San Diego, CA) followed by addition of protein A/G agarose (Santa Cruz Biotechnology, Santa Cruz, CA). The bound proteins were resolved by SDS-PAGE and analyzed by Western blotting.

II.3.8 Trypsinolytic fingerprinting assay

The experiment was performed similarly to previously described [22]. Purified human N-Hsp90β (1-246) and C-Hsp90β (530-724) (0.5 μg) was incubated with DMSO, (-)-EGCG or other compounds in assay buffer (10 mM Tris-HCl, 50 mM KCl, 5 mM $MgCl_2$, 0.1 mM EDTA, pH 7.4) on ice for 1 hr. The samples were digested on ice with different concentrations of trypsin for 6 min. The reactions were terminated by adding SDS sample buffer followed by boiling for 3-5 min. The digested products from N-Hsp90β and C-Hsp90β were analyzed by Western blotting with Hsp90 (N-17) antibody

(Santa Cruz Biotechnology, Santa Cruz, CA) and Hsp90 (AC88) antibody (Assay Designs, Inc., Ann Arbor, MI), respectively.

II.3.9 Statistical analysis

Statistical analysis was performed using student t-test. Data are presented as mean ± SD ($n = 3$, $p < 0.01$).

II.4 Results

II.4.1 (-)-EGCG inhibits cell growth and induces apoptosis in Mia Paca-2 cell

First, we selected a human pancreatic cancer cell line, Mia Paca-2, to evaluate the therapeutic potential of (-)-EGCG. As shown in Figure II.1A, (-)-EGCG exhibited a dose-dependent inhibitory effect on Mia Paca-2 with IC50 less than 50 μM. One of the primary events in apoptosis is activation of caspase-3 [26]. Caspase-3 activity assay showed that (-)-EGCG induced activation of caspase-3 in a time- and dose-dependent manner (Figure II.1B). Markedly, more than a 3-fold increase in caspase-3 activity was observed in Mia Paca-2 cells after incubated with 60 μM (-)-EGCG for 48 hrs in comparison with untreated cells.

II.4.2 (-)-EGCG decreases cellular levels of Hsp90 client proteins

Since the inhibition of Hsp90 will result in simultaneous down-regulation of multiple oncogenic proteins, we examined whether (-)-EGCG could decrease the levels of cancer-associated Hsp90 client proteins in pancreatic cancer cells. Mia Paca-2 cells were treated with either 80 μM (-)-EGCG for 0-24 hrs or 60 μM (-)-EGCG every 24 hrs up to 72 hrs. As shown in Figure II.2A and II.2B, (-)-EGCG caused a progressive decline in the protein levels of Her-2, Akt, Cdk4, Raf-1, and pERK in a time- and dose-

dependent manner. Akt, Raf-1 and pERK were down-regulated by 35%~50% as early as 3 hrs after 80 μM (-)-EGCG incubation (Figure II.2A). All five client proteins were decreased by approximately 70%-80% upon 24 hr incubation with 80 μM (-)-EGCG (Figure II.2A). Moreover, although a 48 hr treatment of Mia Paca-2 cells with 60 μM (-)-EGCG only moderately decreased the cellular levels of Akt, Raf-1, Her-2, Cdk4, and pERK, an additional 24 hr treatment with another dose of 60 μM (-)-EGCG was able to completely abrogate the endogenous levels of Akt, Cdk4, and Her-2 and down-regulate Raf-1 and pERK by about 70% (Figure II.2B). In contrast to ansamycin inhibitors of Hsp90 (e.g., GA, 17-AAG), (-)-EGCG did not induce the protein level of Hsp70 (Figure II.2B).

II.4.3 (-)-EGCG impairs the association of p23 and Hsc70 with Hsp90

We further characterized the effect of (-)-EGCG on the association between co-chaperones and Hsp90. After incubation with different concentrations of (-)-EGCG for various time periods, Mia Paca-2 cells were harvested for extraction of total cellular protein. Hsp90 was immunoprecipitated using its antibody, and the amounts of Hsc70, Hop, Cdc37, and p23 were detected by Western blotting in the precipitated Hsp90 complexes. The result showed that 24 hr treatment with 60 μM (-)-EGCG significantly suppressed the interaction of Hsc70 and p23 with Hsp90 by approximately 60% and 55%, respectively, while this treatment had little effect on the amount of Cdc37 or Hop in the Hsp90 complex (Figure II.3). Higher concentrations of (-)-EGCG further reduced Hsc70/Hsp90 and p23/Hsp90 associations (Figure II.3).

II.4.4 (-)-EGCG directly binds the C-terminal region of Hsp90.

In order to examine how (-)-EGCG impairs the association of p23 and Hsc70 with Hsp90, we utilized proteolytic fingerprinting assay to investigate the region that is involved in the interaction between (-)-EGCG and Hsp90. In the absence of (-)-EGCG, the C-terminal region of Hsp90β (C-Hsp90β, amino acids 530-724) was highly sensitive to proteolytic enzyme digestion. While 30 μg/ml of trypsin yielded a single band close to 6 kD, 150 μg/ml of the enzyme was able to completely hydrolyze the C-Hsp90β (Figure II.4A, lane 1-3). Consistent with the fact that GA does not interact directly with the C-terminal domain of Hsp90β, GA had no effect on the trypsinolytic fingerprint of C-Hsp90β in comparison to control (Figure II.4A, lane 7-9). However, incubation of (-)-EGCG with Hsp90 blocked the trypsin hydrolysis of Hsp90 and produced a band representing complete C-Hsp90β at a lower concentration of trypsin (Figure II.4A, lane 4 & 5). (-)-EGCG protected C-terminus from cleavage by a higher concentration of trypsin (Figure II.4A, lane 4 & 6). As a positive control, binding of ATP to the C-Hsp90β allowed very limited trypsin digestion to occur (Figure II.4B). In addition, the trypsinolytic patterns were different between (-)-EGCG- and ATP-protected C-Hsp90β. This suggests that the binding site of (-)-EGCG on C-Hsp90β may be different from the C-terminal ATP binding site.

In contrast, (-)-EGCG did not change the trypsinolytic fingerprint of N-Hsp90β, either with the cleavage by 30 or 150 μg/ml trypsin compared to control (Figure II.4C, lane 1-6). As expected, Geldanamycin (GA) remarkably protected the enzyme digestion by interacting with the N-terminal nucleotide binding pocket, producing a digest pattern similar to ATP-bound N-Hsp90β (Figure II.4C, lane 7-12).

Next, we examined the effect of (-)-EGCG on ATP binding capacity of cellular Hsp90, recombinant full-length Hsp90β, and purified C-Hsp90β by utilizing ATP-sepharose pull-down assay. The results showed that (-)-EGCG treatment had little effect on the ATP binding to endogenous Hsp90 in pancreatic cancer cells (Figure II.5A). (-)-EGCG did not block the ATP binding to either recombinant full-length Hsp90β or C-Hsp90β (Figure II.5B & Figure II.5C).

II.5 Discussion

In recent years, many studies have shown chemopreventive and chemotherapeutic effect of green tea against skin, lung, breast, colon, liver, stomach, and prostate cancers [27]. Numerous studies have suggested that (-)-EGCG, the most abundant catechin in green tea, is the primary component for these activities [28]. (-)-EGCG induces apoptosis and cell cycle arrest in cancer cells without affecting normal cells [27, 29]. The majority *in vitro* studies have revealed that (-)-EGCG inhibited NF-κB activity, MAPK pathway, activator protein-1 (AP-1) activity, and EGFR-mediated downstream signaling pathways [30]. Clinical trials further verified the cancer preventive effect of (-)-EGCG [24, 31]. The purpose of the current study is to reveal a new chemopreventive mechanism of (-)-EGCG against pancreatic cancer cells.

Hsp90 has emerged as a target in cancer therapeutics based on the Hsp90 super-chaperone complex status in cancer cells. First, Hsp90 is involved in the maturation and stabilization of a wide range of oncogenic client proteins that are crucial for oncogenesis and malignant progression [11, 32]. Second, Hsp90 comprises as much as 4-6% of total protein in tumor cells, in contrast with the 1-2% within normal cells [33]. Finally, Hsp90 predominantly exists as multi-chaperone complex with high affinity for ATP and drug,

whereas in normal cells most Hsp90 is present in an uncomplexed state [33]. Hence, cancer cells are highly dependent on Hsp90 function for their survival and proliferation [33].

The first class of Hsp90 inhibitors, represented by GA, competitively binds to the N-terminal ATP pocket of Hsp90, thus restraining Hsp90 in its ADP-bound conformation and preventing the subsequent "clamping" of Hsp90 around a client protein [19, 33, 34], resulting in proteasome-dependent degradation of the client. Another type of Hsp90 inhibitor, novobiocin, interacts with Hsp90 at the C-terminal ATP binding site with relatively weak activity [21]. Inhibition of Hsp90 by novobiocin was able to induce similar cellular responses as N-terminal inhibitors, i.e., destabilization of a range of Hsp90 client proteins such as Her-2, Raf-1 and p53 mutant [21, 35]. In addition, novobiocin interferes with Hsp90/Hsc70 and Hsp90/p23 association [21, 22]. Furthermore, it was suggested that an allosteric regulation may correlate the C-terminal domain of Hsp90 with the N-terminus, where the interaction of ligands with one site might affect the occupancy of the other site [21, 36].

(-)-EGCG was reported to bind the C-terminus of Hsp90 at the region of amino acids 538-728 on Hsp90; this interaction region was discovered by using affinity chromatography with immobilized (-)-EGCG-sepharose and various purified fragments and truncation mutants of Hsp90 [25]. Because of the similar binding region of novobiocin and (-)-EGCG on Hsp90, in the current study we aim to investigate whether (-)-EGCG: (1) impairs Hsp90 association with its co-chaperones, (2) interferes with Hsp90 chaperoning function, and (3) exerts inhibitory effect on pancreatic cancer cells. Indeed, the data suggest that binding of (-)-EGCG to Hsp90 impairs the association of

Hsp90 with its co-chaperones (Hsc70 and p23), thereby inducing degradation of Hsp90 client proteins, resulting in anti-proliferating effects in pancreatic cancer cells.

Identification of the (-)-EGCG binding site on Hsp90 is the key to understand its effects on Hsp90 function. Proteolytic fingerprinting assay revealed that (-)-EGCG directly bound the purified Hsp90β C-terminus but not N-terminus. Both ATP and (-)-EGCG could prevent C-Hsp90β from trypsin cleavage, although they exhibited different protection patterns. These data suggest that (-)-EGCG may bind to Hsp90 C-terminus differently from ATP binding. A very recent study by using mass spectrometry and chemical detection methods discovered that (-)-EGCG could form covalent adducts with the thiol group of cysteine residues in proteins through autoxidation [37]. Based on the amino acid sequence search (NP 005339), there are three cysteine residues within C-terminal fragment of human Hsp90β (residues 530-724), Cys572, Cys597, and Cys598, all of which do not fall into the C-terminal ATP binding region (residues 663-676). The possible reactions between (-)-EGCG and Hsp90β C-terminus need to be further investigated.

To further validate these assays, we used geldanamycin (GA) as a negative control. Since GA competes with ATP binding to N-terminal pocket of Hsp90 rather than C-terminus, the trypsin digestion of C-terminus of Hsp90 was not affected by GA. On the contrary, ATP and GA shielded the N-terminus of Hsp90β from trypsin cleavage with a similar pattern and high efficiency, while (-)-EGCG did not alter the proteolytic fingerprint of Hsp90N-terminus. These data suggest that (-)-EGCG directly binds to the C-terminal domain of Hsp90β, specifically within the region of amino acids 530-724,

which is supported by the previous study using immobilized (-)-EGCG affinity chromatography [25].

In the current study, co-immunoprecipitation of endogenous Hsp90 from cell lysates demonstrated that (-)-EGCG impaired the association of Hsc70 and p23 with Hsp90. This effect of (-)-EGCG is very similar to that of novobiocin on Hsp90/co-chaperone association as previously reported [21, 22], which provides the biologic significance of (-)-EGCG binding to Hsp90 for its chemoprevention efficacy. Considering the similarity between (-)-EGCG and novobiocn in Hsp90 binding, the influence of (-)-EGCG on association of Hsp90 with the co-chaperones may be expected. First, according to Marcu *et al.* [21], the association region of Hsc70 on Hsp90 overlaps with the C-terminal dimerization domain and contains the novobiocin binding site [38]. In addition, both N- and C-terminal regions of Hsp90 are necessary for interaction with the yeast homolog of p23, SBA1 [39]. Finally, Allan *et al.* [35] suggests that modulation within the Hsp90 C-terminus by novobiocin could significantly impact other regions in Hsp90, probably through allosteric effects [35]. This is consistent with the evidence that an allosteric regulation may influence the conformation of the C-terminus and N-terminus of Hsp90, where the interaction of ligands with one site might affect the occupancy of the other site [21, 35, 36]. Therefore, (-)-EGCG is likely to alter the conformation and/or occupy the necessary residues of Hsp90 by directly binding to its C-terminal domain, subsequently leading to the impairment of Hsp90/Hsc70 and Hsp90/p23 interactions.

In order to assess whether (-)-EGCG affects ATP binding activity of Hsp90, we applied ATP-sepharose binding assay. However, (-)-EGCG treated Mia Paca-2 cells did

not show altered ATP binding to Hsp90. ATP-sepharose pull-down assay with recombinant full-length Hsp90 and C-Hsp90β further confirmed this finding. During the preparation of this manuscript, we located a very recent manuscript by Yin *et al.* [40], which reported that (-)-EGCG inhibited the ATP binding to purified Hsp90 and Hsp90 C-terminus. Presumably, experimental conditions may contribute to this discrenpancy. In ATP-sepharose binding assay, sodium molybdate (Na_2MoO_4) is a common constituent in the incubation buffer, because molybdate can "freeze" Hsp90 complex in the presence of ATP. However, we observed that mixing colorless (-)-EGCG and sodium molybdate together immediately appeared brown, which indicated a reaction occurring between these two compounds. Thus, the incubation buffer of the ATP binding assay used in the current study did not contain sodium molybdate.

As a result of direct binding to Hsp90 and interference with co-chaperone association to Hsp90, (-)-EGCG exhibited a simultaneous down-regulation of oncogenic Hsp90 client proteins in Mia Paca-2 cells. Consequently, the cell growth was inhibited and apoptosis was dramatically induced. Unlike ansamycin inhibitors of Hsp90 (e.g., GA, 17-AAG), (-)-EGCG did not significantly induce the increase of Hsp70 even after a prolonged treatment. This is in contrast to GA, since binding of ansamycin drugs usually induces a heat shock response through the release, activation, nuclear localization and trimerization of heat shock factor-1 (HSF-1) [41]. HSF1 binds to heat shock elements (HSE) to trigger the expression of some stress-responsive proteins such as Hsp70 [41, 42]. This up-regulation of Hsp70 is believed to compromise the Hsp90-targeted drug efficacy by inhibiting apoptosis signaling [41, 42].

In summary, the data presented in this manuscript suggest that (-)-EGCG, a novel Hsp90 inhibitor, impairs the association of Hsp90/Hsc70 and Hsp90/p23 by directly binding to the C-terminal region of Hsp90, inhibits Hsp90 chaperoning function, and simultaneously degrades multiple cancer-related Hsp90 client proteins. This finding provides a new mechanism for chemoprevention efficacy of (-)-EGCG.

II.6 Acknowledgments

This study is partially supported by NIH funding RO1 CA 120023, UM cancer center research grant (Munn), UM cancer center core grant to DS. We thank Dr. Dan Bolon (University of Massachusetts Medical School) and Dr. Thomas Ratajczak (University of Western Australia, Australia) for the generous gifts of the purified N-Hsp90β and expression plasmids, pET15b-hHsp90β and pET28a(+)-hHsp90β (530-724), respectively.

II.7 Reference

1. Jemal, A., et al., *Cancer statistics, 2007.* CA Cancer J Clin, 2007. **57**(1): p. 43-66.
2. Ghaneh, P., E. Costello, and J.P. Neoptolemos, *Biology and management of pancreatic cancer.* Gut, 2007. **56**(8): p. 1134-52.
3. Korc, M., et al., *Overexpression of the epidermal growth factor receptor in human pancreatic cancer is associated with concomitant increases in the levels of epidermal growth factor and transforming growth factor alpha.* J Clin Invest, 1992. **90**(4): p. 1352-60.
4. Yamanaka, Y., et al., *Overexpression of HER2/neu oncogene in human pancreatic carcinoma.* Hum Pathol, 1993. **24**(10): p. 1127-34.
5. Schlieman, M.G., et al., *Incidence, mechanism and prognostic value of activated AKT in pancreas cancer.* Br J Cancer, 2003. **89**(11): p. 2110-5.
6. Prodromou, C., et al., *Identification and structural characterization of the ATP/ADP-binding site in the Hsp90 molecular chaperone.* Cell, 1997. **90**(1): p. 65-75.
7. Westerheide, S.D. and R.I. Morimoto, *Heat shock response modulators as therapeutic tools for diseases of protein conformation.* J Biol Chem, 2005. **280**(39): p. 33097-100.

8. Welch, W.J., *The role of heat-shock proteins as molecular chaperones.* Curr Opin Cell Biol, 1991. **3**(6): p. 1033-8.
9. McClellan, A.J., et al., *Diverse cellular functions of the Hsp90 molecular chaperone uncovered using systems approaches.* Cell, 2007. **131**(1): p. 121-35.
10. Falsone, S.F., et al., *A proteomic snapshot of the human heat shock protein 90 interactome.* FEBS Lett, 2005. **579**(28): p. 6350-4.
11. Kamal, A., M.F. Boehm, and F.J. Burrows, *Therapeutic and diagnostic implications of Hsp90 activation.* Trends Mol Med, 2004. **10**(6): p. 283-90.
12. Pearl, L.H., C. Prodromou, and P. Workman, *The Hsp90 molecular chaperone: an open and shut case for treatment.* Biochem J, 2008. **410**(3): p. 439-53.
13. Didelot, C., et al., *Anti-cancer therapeutic approaches based on intracellular and extracellular heat shock proteins.* Curr Med Chem, 2007. **14**(27): p. 2839-47.
14. Ali, M.M., et al., *Crystal structure of an Hsp90-nucleotide-p23/Sba1 closed chaperone complex.* Nature, 2006. **440**(7087): p. 1013-7.
15. Scheibel, T., et al., *ATP-binding properties of human Hsp90.* J Biol Chem, 1997. **272**(30): p. 18608-13.
16. Workman, P., *Altered states: selectively drugging the Hsp90 cancer chaperone.* Trends Mol Med, 2004. **10**(2): p. 47-51.
17. Solit, D.B. and G. Chiosis, *Development and application of Hsp90 inhibitors.* Drug Discov Today, 2008. **13**(1-2): p. 38-43.
18. Neckers, L., *Development of small molecule Hsp90 Inhibitors: utilizing both forward and reverse chemical genomics for drug identification.* Current Medicinal Chemistry, 2003. **10**(9): p. 733-739.
19. Roe, S.M., et al., *Structural basis for inhibition of the Hsp90 molecular chaperone by the antitumor antibiotics radicicol and geldanamycin.* J Med Chem, 1999. **42**(2): p. 260-6.
20. Terasawa, K., M. Minami, and Y. Minami, *Constantly updated knowledge of Hsp90.* J Biochem, 2005. **137**(4): p. 443-7.
21. Marcu, M.G., et al., *The heat shock protein 90 antagonist novobiocin interacts with a previously unrecognized ATP-binding domain in the carboxyl terminus of the chaperone.* J Biol Chem, 2000. **275**(47): p. 37181-6.
22. Yun, B.G., et al., *Novobiocin induces a distinct conformation of Hsp90 and alters Hsp90-cochaperone-client interactions.* Biochemistry, 2004. **43**(25): p. 8217-29.
23. Landis-Piwowar, K.R., et al., *A novel prodrug of the green tea polyphenol (-)-epigallocatechin-3-gallate as a potential anticancer agent.* Cancer Res, 2007. **67**(9): p. 4303-10.
24. Fujiki, H., *Two stages of cancer prevention with green tea.* J Cancer Res Clin Oncol, 1999. **125**(11): p. 589-97.
25. Palermo, C.M., C.A. Westlake, and T.A. Gasiewicz, *Epigallocatechin gallate inhibits aryl hydrocarbon receptor gene transcription through an indirect mechanism involving binding to a 90 kDa heat shock protein.* Biochemistry, 2005. **44**(13): p. 5041-52.
26. Khan, N., et al., *Targeting multiple signaling pathways by green tea polyphenol (-)-epigallocatechin-3-gallate.* Cancer Res, 2006. **66**(5): p. 2500-5.
27. Yang, C.S., P. Maliakal, and X. Meng, *Inhibition of carcinogenesis by tea.* Annu Rev Pharmacol Toxicol, 2002. **42**: p. 25-54.

28. Nagle, D.G., D. Ferreira, and Y.D. Zhou, *Epigallocatechin-3-gallate (EGCG): chemical and biomedical perspectives.* Phytochemistry, 2006. **67**(17): p. 1849-55.
29. Ahmad, N., et al., *Green tea constituent epigallocatechin-3-gallate and induction of apoptosis and cell cycle arrest in human carcinoma cells.* J Natl Cancer Inst, 1997. **89**(24): p. 1881-6.
30. Shimizu, M., et al., *(-)-Epigallocatechin gallate and polyphenon E inhibit growth and activation of the epidermal growth factor receptor and human epidermal growth factor receptor-2 signaling pathways in human colon cancer cells.* Clin Cancer Res, 2005. **11**(7): p. 2735-46.
31. Jatoi, A., et al., *A phase II trial of green tea in the treatment of patients with androgen independent metastatic prostate carcinoma.* Cancer, 2003. **97**(6): p. 1442-6.
32. Powers, M.V. and P. Workman, *Inhibitors of the heat shock response: biology and pharmacology.* FEBS Lett, 2007. **581**(19): p. 3758-69.
33. Chiosis, G. and L. Neckers, *Tumor selectivity of Hsp90 inhibitors: the explanation remains elusive.* ACS Chem Biol, 2006. **1**(5): p. 279-84.
34. Blagg, B.S. and T.D. Kerr, *Hsp90 inhibitors: small molecules that transform the Hsp90 protein folding machinery into a catalyst for protein degradation.* Med Res Rev, 2006. **26**(3): p. 310-38.
35. Allan, R.K., et al., *Modulation of chaperone function and cochaperone interaction by novobiocin in the C-terminal domain of Hsp90: evidence that coumarin antibiotics disrupt Hsp90 dimerization.* J Biol Chem, 2006. **281**(11): p. 7161-71.
36. Garnier, C., et al., *Binding of ATP to heat shock protein 90: evidence for an ATP-binding site in the C-terminal domain.* J Biol Chem, 2002. **277**(14): p. 12208-14.
37. Ishii, T., et al., *Covalent modification of proteins by green tea polyphenol (-)-epigallocatechin-3-gallate through autoxidation.* Free Radic Biol Med, 2008. **45**(10): p. 1384-94.
38. Young, J.C., W.M. Obermann, and F.U. Hartl, *Specific binding of tetratricopeptide repeat proteins to the C-terminal 12-kDa domain of hsp90.* J Biol Chem, 1998. **273**(29): p. 18007-10.
39. Fang, Y., et al., *SBA1 encodes a yeast hsp90 cochaperone that is homologous to vertebrate p23 proteins.* Mol Cell Biol, 1998. **18**(7): p. 3727-34.
40. Yin, Z., E.C. Henry, and T.A. Gasiewicz, *(-)-Epigallocatechin-3-gallate is a novel Hsp90 inhibitor.* Biochemistry, 2009. **48**(2): p. 336-45.
41. Kaur, J. and R. Ralhan, *Induction of apoptosis by abrogation of HSP70 expression in human oral cancer cells.* Int J Cancer, 2000. **85**(1): p. 1-5.
42. Schmitt, E., et al., *Heat shock protein 70 neutralization exerts potent antitumor effects in animal models of colon cancer and melanoma.* Cancer Res, 2006. **66**(8): p. 4191-7.

Figure II.1 (-)-EGCG inhibited pancreatic cancer proliferation and increased caspase-3 activity

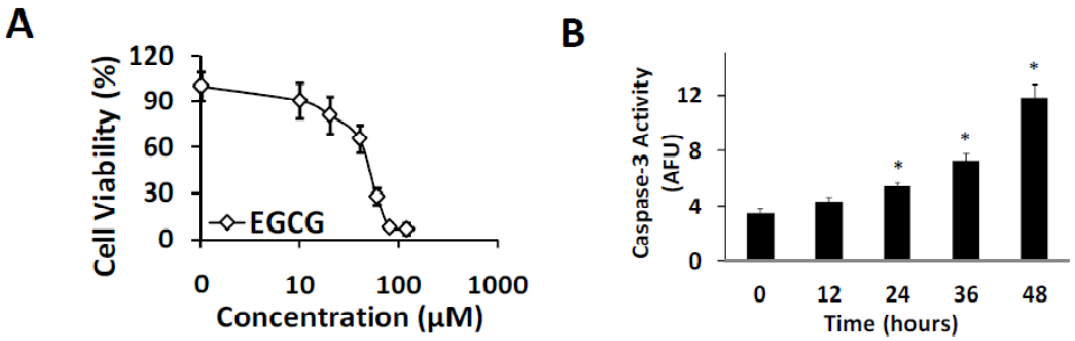

Figure II.2 Effect of (-)-EGCG on Hsp90 client proteins

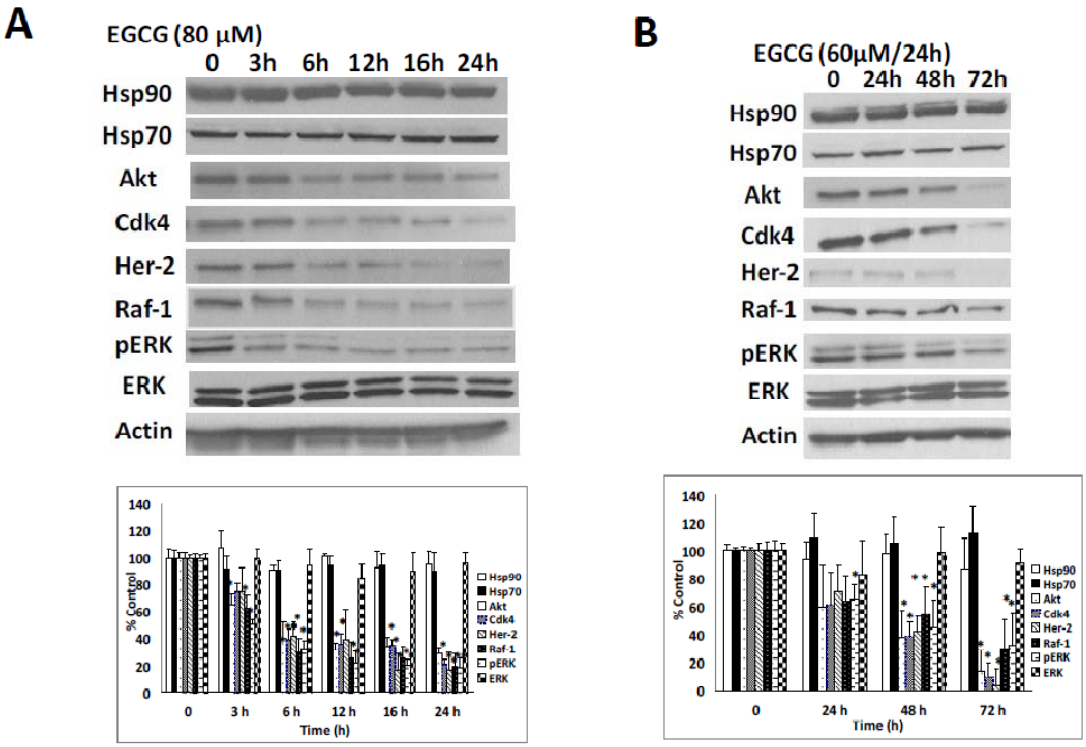

Figure II.3 Influence of (-)-EGCG on Hsp90/co-chaperones association

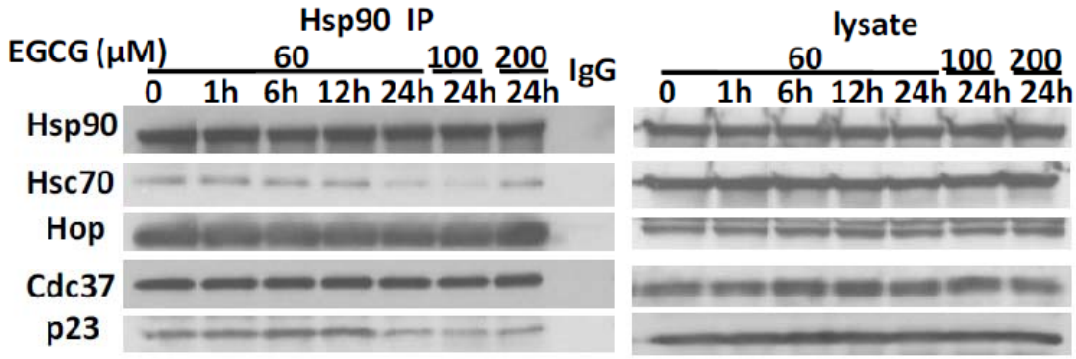

Figure II.4 (-)-EGCG bound to the C-terminus but not N-terminus of Hsp90

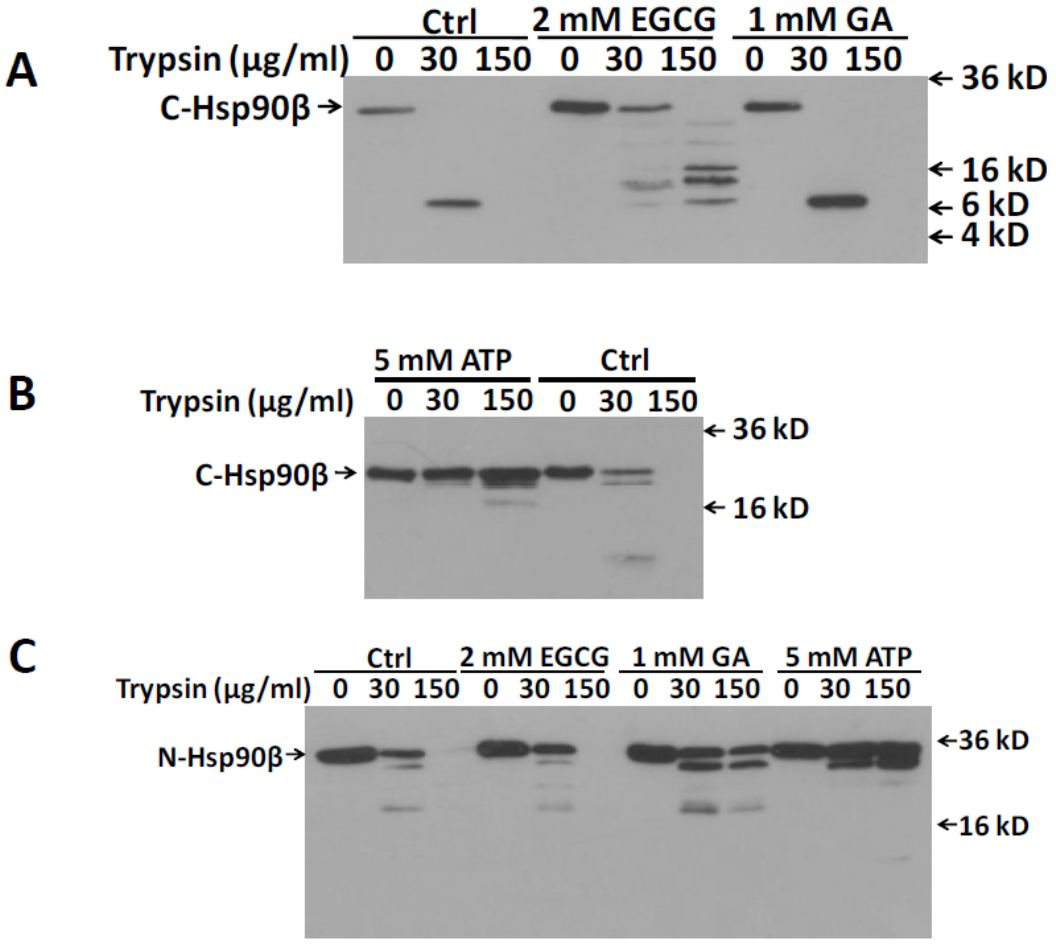

Figure II.5 Effect of (-)-EGCG on ATP binding to Hsp90